

***4D Biofabrication using self-folding  
polymers***

DISSERTATION

zur Erlangung des akademischen Grades eines

Doktors der Naturwissenschaften (Dr. rer. nat.)

in der Bayreuther Graduiertenschule für Mathematik und Naturwissenschaften

(BayNAT)

der Universität Bayreuth

vorgelegt von

***Vladislav Stroganov***

aus *Moskau*

Bayreuth, 2018



The work presented in this dissertation began in September 2012 in TU Dresden and in Leibniz IPF under supervision of Prof. Manfred Stamm and Dr. Leonid Ionov and went until December 2015. It was continued in the University of Georgia (Athens, USA) under supervision of Prof. Leonid Ionov from January 2016 till May 2017. The work was finished in the University of Bayreuth under supervision of Prof. Leonid Ionov between July 2017 and November 2017.

This is a full reprint of the dissertation submitted to obtain the academic degree of Doctor of Natural Sciences (Dr. rer. nat.) and approved by the Bayreuth Graduate School of Mathematical and Natural Sciences (BayNAT) of the University of Bayreuth.

Date of submission: 12.03.2018

Date of defence: 25.07.2018

Acting BayNAT-director: Prof. Dr. Dirk Schüller

Doctoral committee:

Prof. Dr. Leonid Ionov (reviewer)

Prof. Dr. Hans-Werner Schmidt (reviewer)

Prof. Dr. Seema Agarwal (chairman)

Prof. Dr. Markus Retsch



# Table of contents

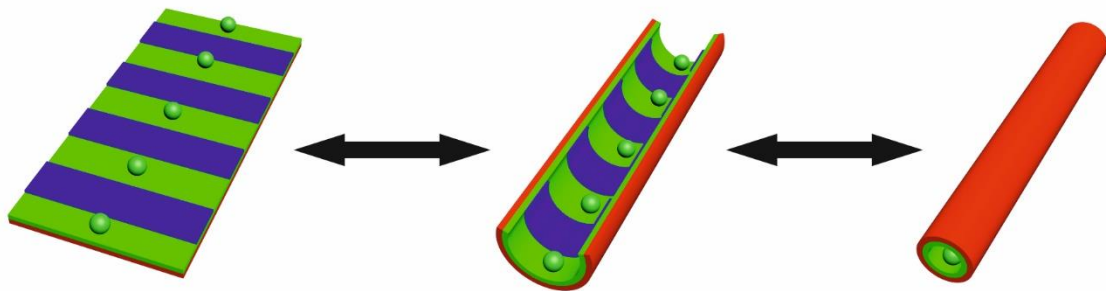
Summary.....	1
Zusammenfassung.....	5
1. Literature overview.....	10
1.1 Biofabrication.....	11
1.1.1 Modular assembly of cell-laden microgels.....	11
1.1.2 3D bioprinting.....	15
1.2 Self-folding materials.....	21
1.2.1 Inorganic self-folding systems.....	22
1.2.2 Polymer self-folding systems.....	23
2. Aims.....	29
3. Synopsis.....	30
4. Literature references.....	35
5. Manuscripts.....	41
Manuscript 1.....	42
Manuscript 2.....	52
Manuscript 3.....	70
6. Conclusions.....	82
7. List of abbreviations.....	88
8. Acknowledgments.....	89
Versicherungen und Erklärungen.....	90



# Summary

Tissue engineering emerged as a field between medicine and science to overcome the mismatch between supply and demand for donor tissues and organs. However, traditional tissue engineering techniques have fallen short of the requirements of such tissue engineered constructs. Therefore, there is a need for new biofabrication technologies. Biofabrication is the production of complex living and non-living biological products from raw biological materials or biochemical molecules. The current challenges of this approach are tissue vascularization and control over cells distribution. To address this, current research work proposes to use stimuli responsive polymers as dynamic scaffolds.

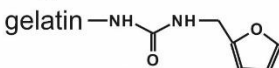
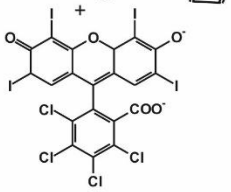
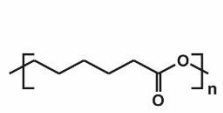
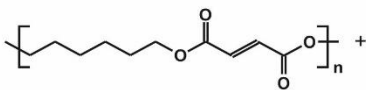
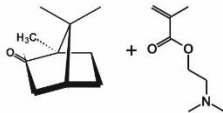
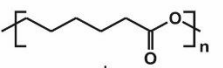
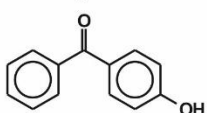
The specific aim of this work was the development of new biocompatible, biodegradable, self-folding, polymer-based systems for cell encapsulation and patterning. Self-folding polymer-based systems are polymeric actuators capable of changing their shape as a response to external stimuli. Here, crosslinked polymer bilayers were used to generate self-rolling tubes, where one layer was hydrophilic, and the other layer was hydrophobic. The hydrophilic polymer swelled in water, but its swelling was restricted by the hydrophobic layer thus creating a bending force (see Figure S1). The advantage to this method compared to creating a tube is that cells can be seeded on the surface of the film before folding and they would be encapsulated in the process. Additionally, it is much simpler to pattern the film surface, which can be useful for directing cell growth and attachment.



**Figure S1.** Schematic illustration of the folding process. Red and green layers are a hydrophilic and hydrophobic, respectively. Blue is protective pattern, which prevents cell adhesion. Spheres represent cells or other encapsulated objects.

## Gelatin-based systems

First, we developed three gelatin-based, biodegradable and biocompatible thermoresponsive systems (Figure S2). Sol-gel transition of gelatin at 36°C was used as a folding/unfolding trigger.

	non-cured films	photocrosslinked films	
hydrophilic	<p>a gelatin</p> <p>pure gelatin</p>	<p>c gelatin-F</p> <p>gelatin </p> <p></p>	<p>e gelatin</p> <p>pure gelatin</p>
hydrophobic	<p>b PCL</p> <p></p>	<p>d PHF-Q</p> <p></p> <p></p>	<p>f PCL-B</p> <p></p> <p></p>

**Figure S2.** Chemical formulas of used polymers.

The first non-cured (Gelatin + PCL) system stood folded at room temperature and irreversibly unfolded at 36°C due to dissolution of gelatin leaving free-floating PCL film. This behaviour was not suitable since the system needed to remain folded under physiological conditions. The second (Gelatin-F + PHF-Q) film was crosslinked by visible light (450 nm) and irreversibly folded at 36°C. The folding occurred when the non-crosslinked gelatin in-between crosslinked bilayers dissolved and released them. The third (Gelatin + PCL-B) system was crosslinked by UV light (256 nm) and as well folded at 36°C. This system was also able to form tubes with different diameters by altering individual layer thicknesses. For further testing of neural cell culture, the second system (Gelatin-F + PHF-Q) was chosen due to its superior mechanical properties compared to the other two systems. It was shown that cells were viable in confined conditions inside tubes. However, the gelatin degraded too rapidly, and tubes lost their shapes after 6 hours of incubation.

### Reversible Gelatin-PCL system

During experiments with the UV-crosslinked Gelatin + PCL-B system it was found that under certain conditions crosslinked bilayers demonstrated reversible folding/unfolding. The folding was induced by decrease of Young's modulus of PCL during its melting at 60°C. This observation was predicted theoretically. Surprisingly, when the temperature was decreased below that point, there was unfolding of the tube back into a flat film. It was found that such reversible behaviour was due to crystallization process of PCL (Figure S3). Crosslinked nature of the polymer layer limited molecular mobility. X-ray scattering on the PCL film showed preferential orientation of polymer molecules parallel to the substrate. The system retained this parallel orientation leading to film unfolding upon melting and crystallization, respectively.

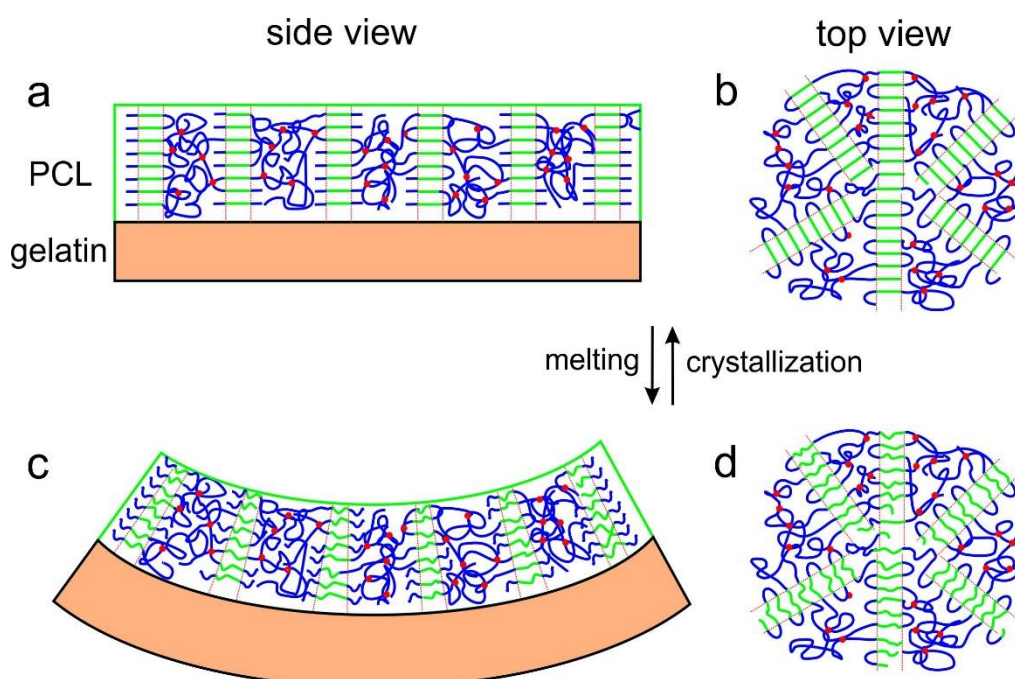


**Figure S3.** Scheme of reversible actuation of gelatin-PCL films.

The reversible gelatin-PCL system showed an alternative way of folding triggering when the hydrophobic polymer played an active role. However, the high actuating temperature of 60°C as well as rapid degradation of gelatin made this system unsuitable for biomedical applications.

### Stable system and cell patterning

Low stability of gelatin-based self-folded structures made them poor candidates for cell encapsulation, and the melting temperature of PCL is too high and could result in cell

destruction. Therefore, gelatin was substituted by the copolymer of N-isopropylacrylamide and acrylic acid (PNIPAM-AA) as the hydrophilic component, and PCL was replaced by polystearylmethacrylate (PSMA) as the hydrophobic component. These polymers are more suitable as the melting point of PSMA is 34°C, and PNIPAM-AA is stable at 37°C in buffer. The new system also included the third polymer – polyethylene glycol (PEG) as the cell patterning agent (Figure S4). All polymers contained photocrosslinking agent either as a comonomer or as an admixture.

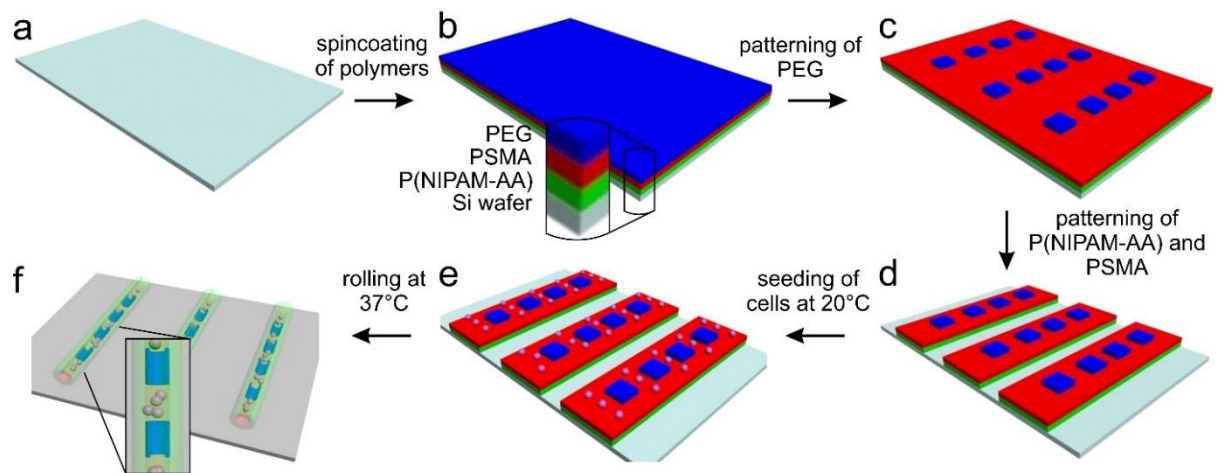


**Figure S4.** Scheme of fabrication of 3D cellular patterns using shape-changing polymer films.

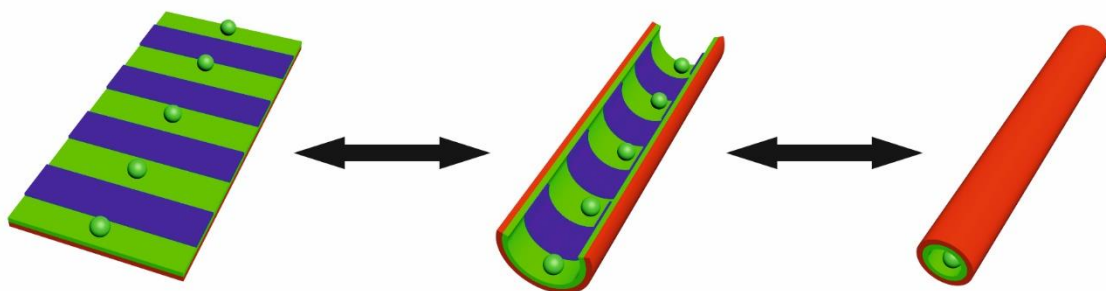
Change of thicknesses of individual layers allowed to get a wide range of diameters – from 30µm up to 300µm. 3T3 mouse fibroblasts were used in cell encapsulation and patterning experiments. It was shown that cells were viable inside tubes even after 2 days of incubations. Cell patterning also was successful – cells adhered only to those areas which weren't covered by PEG.

This work demonstrated a proof-of-concept for bioscaffold fabrication using self-folding polymer films allowing creation of narrow hollow channels with controlled inner cell distribution. Future work will include the development of a fully biodegradable self-folding system and cell patterning will be achieved using 3D bioprinting.

# Zusammenfassung

Das ständige Bedürfnis nach Ersatzorganen und -geweben hat das Gebiet „Tissue Engineering“ zu einem sehr wichtigen Bereich der Wissenschaft und Medizin gemacht. Daher besteht Bedarf an neuen Biofabrikationstechnologien. Biofabrikation ist die Produktion von komplexen lebenden und nicht lebenden biologischen Produkten aus biologischen Rohmaterialien oder biochemischen Molekülen. Die gegenwärtigen Herausforderungen dieses Ansatzes sind die Gewebevaskularisierung und die Kontrolle der Zellverteilung. Um dies anzugehen, wird in aktuellen Forschungsarbeiten vorgeschlagen, Stimuli-reaktive Polymere als dynamische Gerüste zu verwenden.

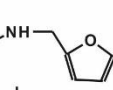
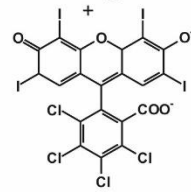
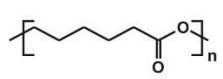
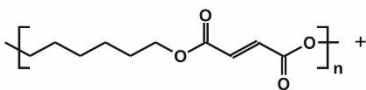
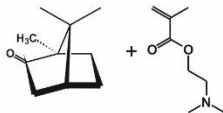
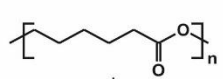
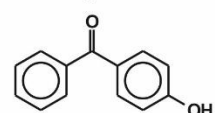
Das spezifische Ziel der vorliegenden Arbeit war die Entwicklung neuer biokompatibler und vorzugsweise biologisch abbaubarer selbstfaltungsfähiger Polymersysteme für die Verkapselung und Strukturierung von Zellen. Selbstfließende Polymersysteme sind polymere Aktoren, die ihre Form als Reaktion auf äußere Reize verändern können. In dieser Arbeit waren Selbstfaltungssysteme vernetzte Polymerdoppelschichten, wobei eine Schicht hydrophil und die andere Schicht hydrophob war. Das hydrophile Polymer quoll in Wasser auf, aber sein Aufquellen wurde durch die hydrophobe Schicht begrenzt, wodurch eine Biegekraft erzeugt wurde (siehe Fig. S1). Vor dem Falten können Zellen auf die Oberfläche des Films ausgesät werden und sie können dabei eingekapselt werden. Zusätzlich kann die Filmoberfläche strukturiert werden, um eine Zelladhäsion an bestimmten Bereichen zu verhindern, die eine Kontrolle über die Zellverteilung herbeiführt.



**Abbildung S1.** Schematische Darstellung des Faltvorgangs. Rote und gelbe Schichten sind hydrophil bzw. hydrophob. Blau ist ein Schutzmuster, das die Zelladhäsion verhindert. Kugeln repräsentieren Zellen oder andere eingekapselte Objekte.

## Gelatine-basierte Systeme

Zunächst entwickelten wir drei biologisch abbaubare und biokompatible thermoresponsive Systeme auf Gelatinebasis (Abbildung S2). Der Lösung-Gel-Übergang bei 36 ° C wurde als Faltungs- bzw. Entfaltungsauslöser verwendet.

	non-cured films	photocrosslinked films	
hydrophilic	<p>a gelatin</p> <p>pure gelatin</p>	<p>c gelatin-F</p> <p>gelatin <math>\text{-NH-CO-NH-}</math> </p> 	<p>e gelatin</p> <p>pure gelatin</p>
hydrophobic	<p>b PCL</p> 	<p>d PHF-Q</p>  	<p>f PCL-B</p>  

**Abbildung S2.** Chemische Formeln von verwendeten Polymeren.

Das erste nicht gehärtete (Gelatine + PCL) System stand gefaltet bei Raumtemperatur und irreversibel entfaltet bei 36 ° C aufgrund der Auflösung von Gelatine unter Freilassung von freischwimmenden PCL-Film. Dieses Verhalten war nicht geeignet, da das System unter physiologischen Bedingungen gefaltet bleiben musste. Der zweite Film (Gelatine-F + PHF-Q) wurde durch sichtbares Licht (450 nm) vernetzt und irreversibel bei 36 ° C gefaltet. Die Faltung trat auf, wenn die nicht vernetzte Gelatine zwischen den vernetzten Doppelschichten gelöst und freigesetzt wurde. Das dritte System (Gelatine + PCL-B) wurde mit UV-Licht (256 nm) vernetzt und bei 36 ° C gefaltet. Es zeigte sich auch die Fähigkeit, Röhre mit unterschiedlichen Durchmessern zu bilden. Das zweite System wurde wegen seiner besseren mechanischen Eigenschaften für die Zellverkapselung am Beispiel neuraler Stammzellen gewählt. Es wurde gezeigt, dass Zellen unter begrenzten Bedingungen innerhalb von Röhren lebensfähig sind, aber unglücklicherweise war die Abbaugeschwindigkeit von Gelatine zu schnell und die Röhren verloren nach sechs Stunden Inkubation ihre Form. Dies führte zu einer weiteren Suche nach einem stabileren System.

### Reversible Gelatine-PCL-System

Bei Experimenten mit dem UV-vernetzten Gelatine + PCL-B-System wurde festgestellt, dass vernetzte Doppelschichten unter bestimmten Bedingungen eine reversible Faltung bzw. Entfaltung zeigten. Die Faltung trat auf, wenn der mechanische Modul von PCL während seines Schmelzprozesses um  $60\text{ }^{\circ}\text{C}$  abnahm. Diese Beobachtung wurde theoretisch vorhergesagt. Die folgende Entfaltung bei Temperaturabnahme war jedoch völlig unerwartet. Es wurde festgestellt, dass ein solches reversibles Verhalten auf den Kristallisationsprozess von PCL zurückzuführen ist (Abbildung S3). Die vernetzte Natur der Polymerschicht begrenzte die molekulare Mobilität. Die Röntgenstreuung auf dem PCL-Film zeigte eine bevorzugte Orientierung der Polymermoleküle parallel zum Substrat. Das System behielt diese parallele Orientierung bei, was zu einer Filmentfaltung beim Schmelzen bzw. Kristallisieren führte.

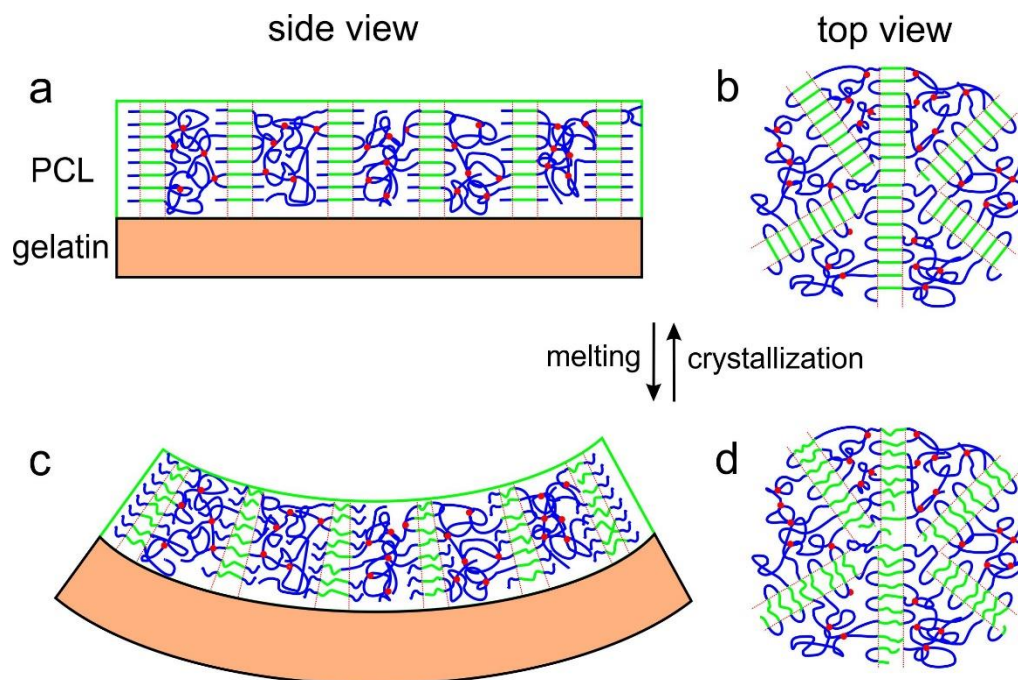


**Abbildung S3.** Schema der reversiblen Aktivierung von Gelatine-PCL-Filmen.

Das reversible Gelatine-PCL-System zeigte eine alternative Art der Faltung, wenn das hydrophobe Polymer eine aktive Rolle spielte. Eine zu hohe Betriebstemperatur von  $60\text{ }^{\circ}\text{C}$  und ein schneller Abbau von Gelatine machen es jedoch für Bioanwendungen ungeeignet.

## Stabile System- und Zellstrukturierung

Eine geringe Stabilität von auf Gelatine basierenden selbstgefalteten Strukturen machte sie zu schlechten Kandidaten für die Zelleinkapselung. Als Ergebnis wurde Gelatine durch das Copolymer von N-Isopropylacrylamid und Acrylsäure (PNIPAM-AA) als die hydrophile Komponente ersetzt. PCL wurde durch Polystearylmethacrylat (PSMA) als hydrophobe Komponente ersetzt. Der Schmelzpunkt von PSMA betrug 34°C, was niedriger als das Schmelzen von PCL war und unter geeigneten physiologischen Bedingungen lag. Das neue System enthielt auch das dritte Polymer - Polyethylenglycol (PEG) als Zellstrukturbildner (Abbildung S4). Alle Polymere enthielten Photovernetzungsmittel entweder als Comonomer oder als Mischung.

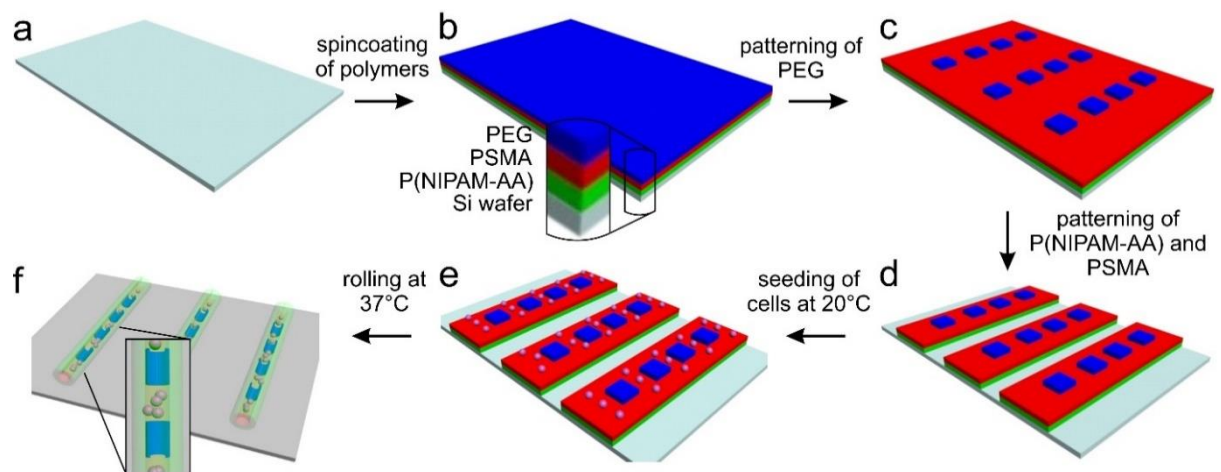


**Abbildung S4.** Schema der Herstellung von 3D-Zellmustern unter Verwendung von formverändernden Polymerfilmen.

Das entwickelte System zeigte die Fähigkeit, Röhre mit einer großen Bandbreite von Durchmessern von 30  $\mu\text{m}$  bis 300  $\mu\text{m}$  herzustellen. 3T3-Mausfibroblasten wurden in Zelleinkapselungs- und Musterbildungsexperimenten verwendet. Es wurde gezeigt, dass Zellen auch nach zwei Tagen Inkubation in Röhren lebensfähig waren. Die Zellstrukturierung war ebenfalls erfolgreich - Zellen hafteten nur an jenen Bereichen, die nicht von PEG bedeckt waren.

Diese Arbeit demonstrierte einen Machbarkeitsnachweis für die Bioscaffold-Herstellung unter Verwendung von selbst faltenden Polymerfilmen, die die Erzeugung enger Hohlkanäle mit kontrollierter innerer Zellverteilung ermöglichen. Zukünftige Arbeiten umfassen die

Entwicklung eines vollständig biologisch abbaubaren Selbstfalzsystems und die Zellstrukturierung wird mittels 3D-Bioprinting erreicht.

# **1. Literature overview**

## **1.1 Biofabrication**

With the development of medicine humanity learned how to transplant organs from one human body to another. Unfortunately, the demand for donor organs is much higher than the supply. Biofabrication is a relatively young field of science which aims to find a way of fabrication of artificial organs and tissues for further transplantation. It can be defined as the fabrication of complex living and non-living biological products from raw materials such as living cells, molecules, extracellular matrices, and biomaterials [1]. This task is not a trivial one since natural organs have complex microarchitectures, dynamic nature and they consist of more than one type of cells. For that reason, scientists constantly develop new bioscaffolds which are supposed to help organise cells in a 3D space in such way that they form a real working tissue.

There are two major approaches of bioscaffold creation. In the first approach a bioscaffold without cells is fabricated first. It is generally made out of biodegradable material. Then cells are seeded on to the scaffold and they are expected to populate it and create the desired microarchitecture. This approach, however, has two major disadvantages which made it less attractive: the resulting cell distribution inside a scaffold is far from homogeneous due to slow and limited cell migration and it is difficult to recreate complex inner microstructural features. In the second approach cells are already present in the processed biomaterial. This allows much greater control over cell distribution in the bulk. Additionally, this method makes it possible to introduce different cell types into the single bioscaffold vastly increasing its potential. Finally, it offers various possibilities to generate inner microarchitectural features such as vascular network or precise positioning of cell clusters. One of promising implementations of the second approach is modular assembly because many natural tissues also consist of repeating units: lobules in liver, muscle myofibers, nephrons in kidneys and so on. In this method it is possible to control cellular distribution, microenvironment and interactions between neighbouring cell clusters.

### **1.1.1 Modular assembly of cell-laden microgels**

#### **Manual manipulation**

One of the basic approaches to create a cell-laden hydrogel was proposed by Khademhosseini and colleagues [2]. Cell suspension in poly(ethylene glycol) diacrylate or in methacrylated hyaluronic acid was deposited on a hydrophilic poly(dimethylsiloxane) (PDMS) stamp and then crosslinked by UV light. The final shape and size of hydrogel units was

determined by shapes of microfeatures on the stamp. These units could be easily detached, cultured and assembled into various constructs with controlled spatial cell distribution. Moreover, using different cell types in different assembly units one can control cell type distribution as well. However, this method is slow and scales hard for large tissue fabrication.

### **Random assembly**

An alternative method to manual assembly was developed by Sefton and colleagues[3]. Sub-millimeter-size collagen rods were coated with endothelial cells. These modules were then assembled into a larger tube. The resulting construct had interconnected channels which could be used for medium perfusion. This work was one of the first examples where vascularization was achieved. Even though this method offers fast and simple assembly, it fails in providing control over the final structure.

### **Microfluidic assembly**

Microfluidic devices offer another way of microgel assembly. Their main advantage is in ability to fabricate very sophisticated architectures. Chung et al. created construct with very precise cell distribution using railed microfluidic device [4]. Special grooves (rails) were created on top of a substrate. Hydrogel microunits moved through these rails and assembled themselves into complex structures with minimal error. It was possible to create multicellular hydrogel assemblies using building units seeded with different cell types. However, the resulted structures were one- or two-dimensional. 3D hydrogel microfluidic assemblies were reported by Whitesides et al. [5]. Collagen rods seeded with cells were assembled in a microchannel. The degree of packing order was determined by ratio between width of the channel and rod dimensions. If the channel width was much bigger than rod diameter random packing took place similar to [3]. The hydrogel units started to become more and more organized when channel width was smaller than their doubled diameter. The greatest degree of order was achieved when channel width was about the same size as rod dimensions. Both examples showed viable ways of bioscaffold fabrication. However, it is worth mentioning that fabrication times were somewhat big which could negatively impact cell viability.

### **Microgel assembly on interfaces**

The possibility to assemble cell-laden microgels on interfaces with different hydrophilicity was investigated by Khademhosseini and co-workers. They proposed an approach which uses tendency of hydrophobic and hydrophilic substances to minimize they contact area with each other. In one work they used microgel particles with different shapes and assembled them at oil-water interface [6]. The hydrogel particles were suspended in oil phase and upon mechanical agitation they started to coalesce together to minimise their surface

tension. The microgel shapes determined the flow of the assembly process. For example, microgels with complementary shapes were able to assemble themselves into highly organized structures. A mathematical model was developed to further enhance this approach [7]. In another work tubular cell-laden hydrogel structures were created out of poly(ethylene glycol) micro rings [8]. It was possible to mimic blood vessels by stacking concentric units where inner rings were seeded with endothelial cells and outer rings contained smooth muscle cells. In another case, microgel assembly happened on the interface between perfluorodecalin and air [9]. The surface tension forces drove hydrophilic hydrogel units together. With this technique it was possible to create centimetre-large sheets which mimicked tissues.

The main problem with the given approaches is that they require hydrophobic organic liquids which could be harmful for sensitive cells. The alternative approach developed by Khademhosseini et al. involved assembly of microgels in PBS solution [10]. They patterned glass substrate with hydrophilic and hydrophobic regions. Then cell-laden microgel dispersion was deposited on top of the patterned substrate and excess liquid was removed. The microgels became trapped in the hydrophilic regions of the slide. During liquid evaporation the microgels assembled together driven by surface tension.

The abovementioned approaches only allowed construction of 2D architectures therefore limiting their use. To address this issue, the process called “Micro-masonry assembly” was developed by Khademhosseini and Fernandez [11]. The produced microgel units were dispersed in a pre-polymer and spread over PDMS cylindrical surface. The excess liquid was removed and microgels started to assemble into a “brick-wall” structure due to capillary forces. Then, the dispersion was irradiated with UV light resulting in mechanically stable construct which could be easily detached and its final shape represented positive replica of the PDMS surface. In the end, hollow tube-like structure was produced. Another way to create 3D structures is to directly stack cell-laden hydrogel sheets [12]. Polyethylene glycol diacrylate was photocrosslinked in a PDMS stencil resulting in an array of microgels. These units were combined into monolayers which were subsequently stacked on top of each other. The final constructs were at least 1cm wide and 3mm thick. Pores could also be generated inside such object if calcium alginate microgel units were introduced and later dissolved.

### **Molecular interactions**

Harada et al. developed a way to create millimeter sized gels using the principle of molecular complementarity [13]. Different microgel particles were functionalized with cyclodextrins (host) or hydrocarbon (guest) groups. By altering the shape and size of initial building units it was possible to get distinct macroscopic objects. Another example is the work

of Elbert et al. where porous scaffolds were fabricated by chemical crosslinking between hydrogel microparticles [14]. Three types of microspheres were produced: microspheres for mechanical support; for delivery of an angiogenesis-promoting molecule and particles containing porogen. All types were functionalized which enabled chemical reactions between them resulting in macroscopic scaffold. Slow dissolution of porogen particles produced porous inner structure. The overall process was proved to be non-cytotoxic.

### **Conclusion**

The given examples of modular assembly allow fabrication of various 2D and 3D hydrogel structures which mimic natural tissues in terms of multicellular composition and microarchitecture. However, disadvantages of these approaches include but are not limited to: the inner pore structure, if it is present, is usually random and doesn't represent real vascular network; It is difficult to produce structures larger than several centimeters in size due to insufficient mechanical stability; many of the approaches utilise potentially not-desired substances or chemically modified natural molecules which may have negative impact on cells in a long run.

### 1.1.2 3D bioprinting

The additive manufacturing or “3D printing” is a very flexible method of object fabrication. It allows easy prototyping and production of parts with almost any geometrical shape without modification of the production equipment. Furthermore, almost any kind of materials can be used in 3D printing including hydrogels. These advantages led to the logical conclusion that scaffolds for tissue engineering could be directly printed on a substrate and it was only a matter of time until bioengineers realized the potential power of 3D bioprinting [15]. In comparison to the assembly methods described above, 3D bioprinting allows much easier production of scaffolds with greater variety of shapes and sizes without usage of additional potentially harmful chemicals. Various bioprinting methods were developed during past 2 decades and this chapter will overview some them.

#### Ink-jet bioprinting

The ink-jet bioprinting technology was the oldest one among other bioprinting techniques. Principles of this approach are very similar to conventional ink-jet printing [16] but instead of regular ink so-called bioink is used. Bioink is usually a cell dispersion in a pre-polymer or in cell culture medium. It is placed in reservoir which is connected to the printing ink-jet device (Figure 1). The ink-jet head produces small droplets of bioink which are propelled towards the substrate. The droplet ejection happens due to small volume changes inside the printhead produced by either thermal or piezo actuators. The deposited droplets can be as small as 20 picolitres in volume [17].

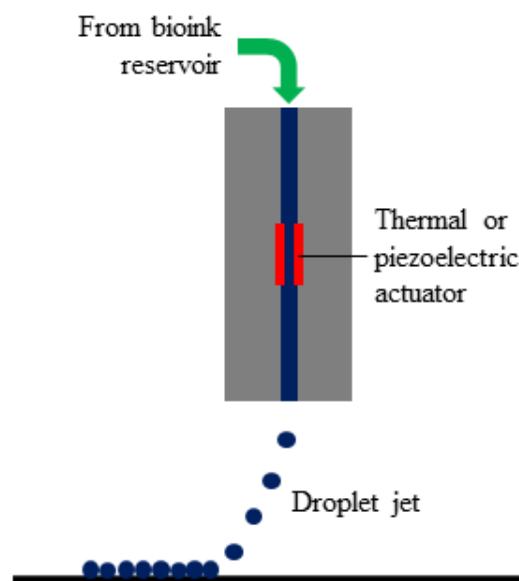


**Figure 1.** Schematic representation of the ink-jet printing process.

When designing the setup for ink-jet printing it is crucial to maintain conditions for viability of printed cells. For example, high shear forces during droplet formation or excessive heat in thermal droplet formation can negatively influence cell behaviour. Cui et al. tested how thermal ink-jet printing influences cell viability [18]. A modified HP Deskjet 500 ink-jet thermal printer was used as a printing platform. Chinese hamster ovary (CHO) cells were printed on glass cover slips and cultures for several days. Overall cell survivability was 89%. It was also found that printing process resulted in pores in cell membranes which disappeared after 2 hours indicating good cell viability. Additional tests showed that permeability of cell membranes was normal as well.

In another work Cui et al. designed a setup to test advantages of controlled cell deposition in comparison to random cell seeding [19]. Mouse myoblasts were printed onto microcantilevers and cultured. It took only 4 days for cells to fuse together and form functional myotubes. In comparison, randomly distributed cells were only able to form myotubes after 14 days.

The main advantages of ink-jet printing are: high cell viability; relatively low effort to assemble a printing setup because the theory of ink-jet printing was already developed by commercial producers and regular ink-jet printers can be modified for bioprinting; Ink-jet printheads can have multiple nozzles working in parallel increasing the total speed of the process. However, there are some disadvantages which are worth mentioning. Due to the nature of droplet formation it is impossible to use ink-jet principle for highly viscous liquids or liquids with high cell density. Also, this method suffers from so-called settling effect [20, 21]. During printing process cells tend to sediment to the bottom of a reservoir increasing bioink viscosity and leading to needle clogging.

### **Laser-assisted bioprinting**

Laser-assisted bioprinting is similar to ink-jet approach in the way that it also produces a constant jet of bioink droplets. Typical setup for laser-assisted printing includes a donor layer which consists of an energy absorbing layer and a layer of bioink underneath it (Figure 2). When a short laser pulse hits the upper layer, the irradiated area almost instantly evaporates. This rapid bubble formation leads to ejection of a bioink droplet. The main difference from the thermal ink-jet printing is that in laser-assisted printing the bioink itself is not heated or evaporated decreasing possibility of cell damage. Another advantage of this approach is the absence of a narrow nozzle meaning that potentially dangerous levels of shear forces are avoided. More types of bioinks can be deposited through this way including ones with high viscosity .



**Figure 2.** Schematic representation of the laser-assisted printing process.

Nahmias et al. have reported a successful attempt to print a hydrogel via laser-assisted direct writing [22]. Human umbilical vein endothelial cells (HUVEC) were printed on a Matrigel with micrometer accuracy. During culturing cells were able to self-assemble themselves into tube-like structures indicating that this is a possible to pattern vascular structures in vitro with high precision. However, these tubes were not real blood vessels and authors stated that more precise control over cellular environment is required to achieve true vascularisation.

Duan et al. printed an alginate/gelatine hydrogel which mimicked heart valve [23]. The hydrogel was filled with aortic root sinus smooth muscle cells (SMC) in the valve root and aortic valve leaflet interstitial cells (VIC) in the leaflets. Cell viability was measured after 7 days of culturing and was high: 81.4% for SMC and 83.2% for VIC. Obtained results demonstrated proof of concept for 3D bioprinting of heart valves.

On the other hand, laser-assisted printing requires powerful diode laser with good resolution which can be quite costly. Furthermore, consequences of laser irradiation on cells are not well understood. For that reason, more researches have focused on investigation of influence of printing parameters on quality of printed patterns and cell viability [24].

### **Direct bioink extrusion**

The direct bioink extrusion (DBE) is probably the simplest bioprinting method in terms of technical implementation. A printing nozzle or needle is connected to a bioink reservoir via tubing. An external pressure is applied to the bioink and it is got extruded from the nozzle and subsequently crosslinked (Figure 3).

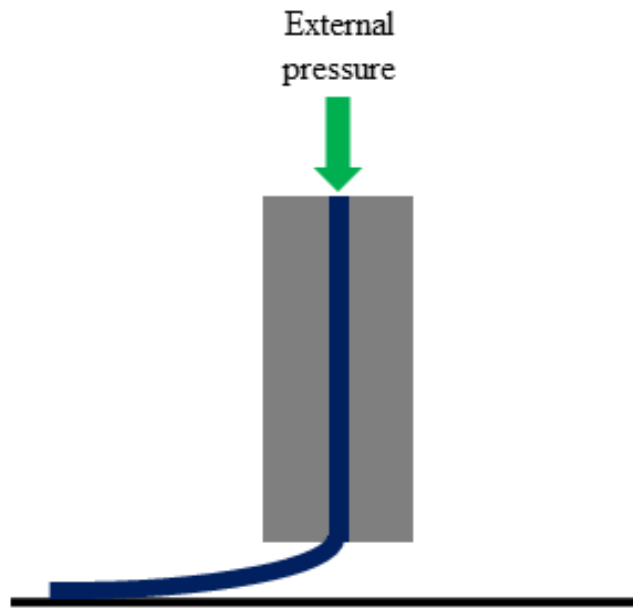


**Figure 3.** Schematic representation of the extrusion-based printing process.

There are three general ways to create the external pressure: screw plunger which rotates and pushes bioink; a piston like the one used in syringes; gas pressure. DBE allows printing of almost all types of bioink including ones with high viscosity. Almost all commercial bioprinters are extrusion-based including Bioplotter (EnvisionTec, Gladbeck, Germany) and NovoGen 3D Bioprinting platform (Organovo, San Diego, USA).

Usually extrusion-based methods produce continuous bioink lines with cylindrical shapes. However, different nozzle types can be used to produce more complicated structures. For example, Gao et al. used coaxial nozzles with 2 independent channels to fabricate a porous hydrogel [25]. 2 different solutions were extruded simultaneously: calcium chloride from the inner nozzle and cell-laden sodium alginate from the outer nozzle. Upon contact between these solutions, calcium ions diffused into alginate phase and crosslinked it resulting in a tube with its walls consisting of crosslinked calcium alginate. The inner area of the tube was filled with calcium/sodium chloride solution. Through the continuous deposition of multiple hydrogel tubes close together it was possible to produce a piece of hydrogel with single continuous inner channel through which a cell culture medium could be pumped. Thus, vascularization was achieved. However, the diameter of inner channel was in range of hundreds of micrometers which is too big for the true vascularization purposes.

Another extrusion bioprinting approach was developed by Lee et al. [26]. Six parallel printing heads were mounted on a XYZ-stage. This allowed printing of a complex multicellular structures with controlled cell distribution. At least 4 nozzles were used in this research: one

nozzle dispensed PEG solution as sacrificial layer, polycaprolactone was deposited through another nozzle and the third and fourth nozzles were used to extrude sodium alginate with encapsulated chondrocytes and adipocytes respectively. Through this approach authors were able to print a 3D structure which resembled a human ear. Cell viability rate in the printed structure was 95%. Levels of chondrogenesis and adipogenesis were high indicating that cells fulfilled their intended roles.

The main disadvantage of the extrusion based printing is potentially high shear forces which are experienced by cells in a narrow nozzle which can limit their viability [27].

### **Other bioprinting approaches**

Several research groups have reported bioprinting approaches which are different from the described above. Miller et al. developed an approach to fabricate complex vascular networks in a prepared hydrogel [28]. Molten sugar glass structure was printed through conventional extrusion. This structure was highly branching with multiple intersections between its parts. A cell dispersion was poured around it and subsequently crosslinked. After certain time of incubation, sugar was dissolved and consumed by cells leaving vast hollow channel network which could be used for nutrient and oxygen delivery.

In another approach a commercial beamer was adopted to project a pattern onto a photocrosslinkable pre-polymer in a layer by layer manner [29-31]. A model of a desired structure was sliced along Z axis to generate a sequence of planes. Then, a projector shined images of these planes onto crosslinkable bioink thus making printing time independent from structure complexity since the whole layer is projected at once. Additionally, such setup required a stage which only moved in Z direction. Cell viability during such approach was on par with other methods – around 95%. Gauvin et al. were able to achieve resolution of 100µm and printing times smaller than 1 hour [29].

A lot of scaffolds were created by crosslinking of a bioink with UV light. Even though it was shown that cells were viable after such treatment, usage of UV light is undesirable due to unpredictable consequences in terms of cell behaviour. A possible solution for this problem have been reported by various research groups [32-36]. It involves so-called two-photon photolithography. Usual photocrosslinking happens when photosensitive molecules absorb a single photon which carries enough energy to excite such molecules. It is possible however under certain circumstances to induce the same chemical reaction when two or more photons are absorbed simultaneously by a single molecule while the energy of each individual photon is not enough to traverse the gap between neighbouring molecular energy levels. One of the conditions to enable the multiphoton process is a high photon density. It was achieved by

focusing a laser beam. The energy density was high enough in the focal point thus allowing multiphoton polymerization only in this spot. Since the energy of each photon can be 2 times smaller for two-photon processes than for usual photochemical reactions it is possible to avoid usage of UV light. The fact that polymerisation happened only in focal point allowed to dramatically increase printing resolution and even traverse diffraction optical limits.

### Conclusion

This chapter have given a brief overview over different bioprinting methods developed so far. The Table 1 shows summary over methods' advantages and disadvantages.

**Table 1.**

	Advantages	Disadvantages
Ink-jet printing	<ul style="list-style-type: none"> <li>• High printing speed;</li> <li>• High cell viability (80%-90%);</li> <li>• Relatively low build cost of a prototype device.</li> </ul>	<ul style="list-style-type: none"> <li>• Only low viscosity, low density bioinks can be printed;</li> <li>• Settling effect.</li> </ul>
Laser-assisted printing	<ul style="list-style-type: none"> <li>• Bioinks with high viscosity can be printed;</li> <li>• No direct contact between a dispenser and a bioink;</li> <li>• Very high cell viability (95%).</li> </ul>	<ul style="list-style-type: none"> <li>• Unknown effects of exposure of cells against laser radiation;</li> <li>• Unknown influence of printing parameters over final printed structure;</li> <li>• High cost.</li> </ul>
Direct extrusion	<ul style="list-style-type: none"> <li>• Suitable for any type of bioink;</li> <li>• Simple technical implementation.</li> </ul>	<ul style="list-style-type: none"> <li>• Potentially high mechanical stresses.</li> </ul>

Despite all the advantages these methods offer, there is one problem that remains generally unsolved. That is the creation of structures with narrow hollow channels while maintaining controlled cell distribution and diameters of individual channels smaller than 100µm. One of the candidate systems which have a potential to solve that problem are self-folding polymer films.

## 1.2 Self-folding materials

The idea of creation of 3D microstructures using controlled folding of thin films emerged nearly 20 years ago [37, 38]. Such approach is often called microorigami due to similarity with ancient Japanese art of paper folding. Nowadays, a great choice of various materials is available which can spontaneously or upon triggering transform from 2D thin films into complex 3D structures. Such process can be either reversible or irreversible. The main advantage of the approach is the ability to create 3D hollow structures with controlled chemical and physical properties of both exterior and interior surfaces.

The first historical evidence of the use of self-folding systems can be tracked to British clockmaker John Harrison who created bimetal strips which bended due to differences of thermal expansion of involved metals. Later, in 1925, Timoshenko conducted first fundamental investigations of folding behaviour of bilayers on the example of bimetal beams[39]. It was found that a strip consisting of two metals welded together and with different thermal expansion coefficients would bend when its temperature was uniformly increased. The final curvature of the strip could be described with the following formula:

$$\frac{1}{\rho} = \frac{6(\alpha_1 - \alpha_2)(t_1 - t_0)(1 + m)^2}{h \left( 3(1 + m)^2 + (1 + mn) \left( m^2 + \frac{1}{mn} \right) \right)}, n = \frac{E_1}{E_2}, m = \frac{a_1}{a_2} \quad 1.1$$

where  $E_x$  is the elasticity modulus,  $a_x$  is the thickness of the metal layer,  $h$  is the total thickness ( $h = a_1 + a_2$ ),  $\alpha_x$  is the thermal expansion coefficient of the layers and  $\rho$  is the radius of curvature. As it comes from the equation 1.1, the greater the difference between thermal expansion coefficients, the smaller will be the radius of curvature. Bending degree also depends on ration between layer thicknesses and relative stiffnesses although the latter has weaker influence. The Timoshenko equation have several limitations: 1) It was derived for small angles of deformations; 2) Doesn't predict folding direction; 3) It is applicable only for reversible elastic deformations.

Folding principle of polymer bilayers is usually similar to that of bimetal trips: Layers have different expansion coefficients. Unlike metals, however, polymers can demonstrate significantly larger volume changes and their folding can be triggered by a broader list of stimuli. The equation 1.1 can be used to qualitatively characterise polymer bilayer folding as well if it is assumed that metal's thermal expansion coefficients are substituted by, for example, swelling degree. In general, polymer self-folding bilayers consist of passive and active components. Active component of a system responds to external stimulus by changing its

physical-chemical properties. Some examples of possible stimuli are: pH, temperature, light, etc. Passive component of the system directs active component's response into bending movement. An example of such system can be a crosslinked polymer bilayer which consists of hydrophilic and hydrophobic polymers [40, 41]. The hydrophilic (active component) polymer swells in water and tries to expand its volume in all directions. The hydrophobic polymer (passive component) restricts such uniform expansion on one side thus creating bending stress.

It is also possible to design a self-folding system out of a single chemically homogeneous material. To achieve that, certain gradients need to be present in the film. For example, a gradient of swelling degree along film's thickness or a gradient of co-monomers concentration inside the pre-polymer will result in a bending behaviour. The work of Hayward et al. is an example of how a crosslinking density gradient induced film curving [42]. The self-folding film was composed out of a lightly crosslinked poly(N-isopropylacrylamide) with highly crosslinked dots embedded into the polymer matrix. Such architecture resulted in a formation of various Gaussian surfaces (spherical caps, saddles and cones) as well as more complex and nearly closed shapes.

Various self-folding inorganic and polymer systems have been reported by a number of research groups. These systems include but are not limited to pH-, temperature- or light-sensitive. They are described in more detail in the following chapters.

### **1.2.1 Inorganic self-folding systems**

The works of Smela [38] and Jager [37] created the foundation for the self-folding systems development. They used patterned polypyrrole-gold bilayers which reversibly folded and unfolded upon electrical triggering. Using this approach, a microgrippers were created capable of capturing and moving microscale objects. Later, several other groups around the globe started the development of various applications for inorganic self-folding systems. For example, approaches of O.G. Schmidt group employed semiconductor and metal oxide self-folding tubes for different applications: energy storage [43-45], lab-on-a-tube concept and nanooptics tools [46-49], a design of an approach to investigate cell behaviour in confinement [50]. Group of D. Gracias focused on the development of metal-based self-folding microdevices with sophisticated 3D shapes. The possible applications of such devices included microsurgery [51], encapsulation and delivery of drugs [52] and cells [53-55] and bioscaffolds production for tissue engineering [56].

Despite this promising demonstration of metal-based systems involvement in bioapplications, this approach is limited due to low biocompatibility and non-biodegradability of inorganic materials. Additionally, they are too rigid to become suitable materials for cell encapsulation and bioscaffolds production.

### **1.2.2 Polymer self-folding systems**

Polymer-based self-folding systems are more suitable for bioapplications since they can avoid all disadvantages of inorganic systems mentioned above. Additionally, polymers possess some traits, which make them even more desirable choice. First, there are polymers which can significantly and reversibly change their volume. This can be used as folding/unfolding driving force. Second, employment of polymers which are sensitive to a specific stimulus allows production of structures, which's folding and unfolding is triggered only by that stimulus such as light, temperature, pH etc. [57]. Polymers can be chosen so that their corresponding stimuli lay in a range of physiological conditions which enables them for cell encapsulation applications. Third, there are polymers that have been already approved for medicinal use [58]. Fourth, there are several already existing techniques which allow easy and precise patterning of polymer films. Photolithography (one- or multistep) is one of such methods allowing creation of almost infinite variety of 2D shapes that can be folded into complex 3D shapes.

#### **Thermoresponsive systems**

Thermoresponsive triggering is usually achieved due to shape-memory effect, melting, sol-gel transitions, or continuous thermal expansion. One example of shape-memory based system was developed by Lendlein et al. [59]. Poly( $\epsilon$ -caprolactone) film was in its temporary shape at low temperature below the melting point of the polymer. The film restored its initial folded shape upon heating creating self-folded cube. Gracias et al. developed self-folding micropatterned polymeric containers based on SU-8 photoresist – polycaprolactone films [60]. Self-folding was driven by a minimization of surface area of the melted polycaprolactone hinges within two-dimensional template. The folding was irreversible and occurred at 58°C. Since the cell encapsulation wasn't possible at that temperature, mammalian cells were loaded into formed structures post-folding using tumbling approach. However, it was demonstrated on the example of glass microspheres that it is possible to encapsulate objects during folding [52, 53].

Even though a variety of thermoresponsive systems had been developed, there was still need in systems with actuation at physiological conditions which was mandatory for cell encapsulation and release. One promising approach was to utilize swelling-induced folding of

thermoreponsive polymers which demonstrated property of Low Critical Solution Temperature (LCST) in water solutions. The poly(N-isopropylacrylamide) (PNIPAM) was a suitable candidate since it has LCST at 33°C for homopolymer. PNIPAM based hydrogels are swollen below that temperature and shrink above it. LCST can be varied by tuning the composition of the polymer, for example increased if hydrophilic comonomers are added or decreased with hydrophobic comonomers. Due to such convenient set of properties of PNIPAM, there were a number of works about PNIPAM based self-folding systems. Peeters et al. developed a bilayer system where swelling of a PNIPAM layer was restricted by a crosslinked mixture of poly(methyl methacrylate), diacrylated triblock copolymer of poly(ethylene glycol) and poly(lactic acid). The bilayers were able to self-fold into shapes with sizes between 0.25mm and 1mm and it was demonstrated that they can be used for encapsulation of cardiomyocytes. Hayward et al. demonstrated a self-folding system based on a random copolymer of N-isopropylacrylamide (NIPAM), acrylamidobenzophenone, acrylic acid and rhodamine B-labelled methacrylate [42]. Via photolithography polymer films were patterned with regions of different crosslinking density which resulted in unequal swelling along the film. The polymer sheets folded into cylindrical structures at 22°C and completely unfolded at 50°C. The process was also reversible.

Another series of notable works about PNIPAM-based systems were made in the group of Dr. L. Ionov. The basics of 2D shape-3D shape dependencies weren't well understood at those times and the work was done to describe how folding behaviour depends on the initial 2D shape of the structures [40, 61, 62]. Self-folding systems were represented by polymer bilayers where one polymer was a copolymer of NIPAM and benzophenone acrylate and the second polymer were either polymethylmethacrylate (PMMA) or PCL. It was shown that rectangular bilayers were able to fold into tubes only when aspect ratio between length and width was at least 1 to 6. Diagonal rolling took place in other cases with multiple pre-tubes formed along bilayer perimeters resulting in an irregular final shape. The folding speed was observed to be dependent on movement speed of the swelling front in the PNIPAM layer. In addition, it was shown that rolling direction was different in cases when self-folding film was on a substrate or free-floating. It was also demonstrated that final 3D shape greatly depended on the radius of curvature which in its turn depended on the ratio between layer thicknesses: it was possible to obtain different final structures out of the same 2D shapes but with different individual layer thicknesses. Finally, possibility to reversibly encapsulate microobjects was shown on the example of silicon oxide particles. The work of Zakharchenko et al. demonstrated the possibility to control the movement and orientation of self-folded tubes [63]. Magnetic

nanoparticles were dispersed in the polymer layers thus providing sensitivity to external magnetic field. It was possible through this approach to encapsulate, move and release microparticles.

The most notable work in terms of the current review was done by Zakharchenko et al. where a scaffold was fabricated consisting of aligned self-folded tubes [64]. The system consisted of N-isopropylacrylamide and acrylic acid copolymer (PNIPAM-AA) as a hydrophilic polymer and PMMA as a hydrophobic one. Tubes self-folded in PBS buffer and had PNIPAM-AA on their outer surfaces. In such conditions PNIPAM-AA was slightly negatively charged. Positively charged silica particles were dispersed along negatively charged tubes leading to tubes agglomeration due to electrostatic attraction. In another experiment, yeast cells were encapsulated inside tubes before agglomeration resulting in a uniaxial tubular homogeneously filled scaffold. This was the first step to create a true scaffold using self-folding materials.

### **pH-responsive systems**

In general, pH-responsive systems contained polyelectrolytes which switched between their uncharged and charged forms. Luchnikov et al. demonstrated several systems which folded at low pH [65-67]. All systems were based on poly(4-vinyl pyridine). Folding occurred when nitrogen atom in pyridine fragment got protonated at sufficiently low pH leading to polymer swelling. Gracias et al. reported a system based on PNIPAM-AA/polyethylene glycol bilayers [68]. The PNIPAM-AA changed its swelling degree as response to pH and ionic strength changes resulting in reversible folding and unfolding of bilayers. Lee et al. developed a poly(methacrylic acid)/poly(2-hydroxyethyl methacrylate) based system which folded at pH 6.5 due to difference in polymer swelling [69]. Authors suggested to use developed self-folding devices as a drug delivery system. The passive layer was preliminary patterned with adhesive patches containing drugs. The proposed approach eliminates drug leakage and improves unidirectional intestinal delivery.

Another system based on poly(2-hydroxyethyl methacrylate-co-acrylic acid) (p(HEMA-co-AA)) and poly(2-hydroxyethyl methacrylate) was developed by Yang et al. [70]. The self-folding bilayers' shapes originally resembled shape of the number 8. At pH 9 they folded and formed spherical microcapsules. Decrease of pH led to gradual opening of the containers due to shrinking of p(HEMA-co-AA). The bilayers completely unfolded into original 8-shape at pH 4. Reversible encapsulation and release of microobjects was demonstrated on the example of 1 $\mu$ m polystyrene particles.

Nasimova et al. developed a hydrogel system with gradient of comonomers concentration [71]. The hydrogel was synthesized by copolymerization of N-isopropylacrylamide and acrylic acid sodium salt between glass and teflon surfaces. Due to unequal distribution of acrylic acid units, the system folded at pH 3 and unfolded at pH 7.

Zakharchenko et al. created a system consisting of polysuccinimide and polycaprolactone [41]. Both polymers were already approved for use in medicine, they are biodegradable, biocompatible and produced in industrial quantities. They are also hydrophobic and water insoluble. Polysuccinimide however hydrolyses in physiological buffer environment yielding water-swelling polyaspartic acid resulting in irreversible folding and tubes formation.

### **Electro-responsive systems**

Most of the electro-responsive systems were metal-based. For example, works of Smela[38] and Jager[37] mentioned above. However, there was an example of polymeric electro-responsive system. Feinberg et al. developed a series of actuators based on polydimethylsiloxane and cardiomyocytes [72, 73]. The cells were aligned on the polymer film surface and folding occurred when an electric current was conducted through the medium. Cardiomyocytes synchronous contraction was the driving force of the folding. As a result, various centimetre-size 3D structures capable of mechanical work were produced.

### **Light responsive systems**

There are several possible approaches of how to convert light energy into self-folding behaviour. One approach involves light-sensitive molecules which undergo conformational changes upon irradiation. Ryabchun et al. developed a system based on crosslinked liquid-crystalline polymer containing azobenzene chromophore [74]. The rectangular polymer film was irradiated with polarized UV-light (364nm). The polarization plane of the light was oriented along the length of the film. Bending of the film was observed during irradiation. The bending behaviour was reversible, and the film started to unfold as soon as the light was turned off. This nature of this photomechanical movement was in change of conformation of the photosensitive molecules. This change occurred due to reversible trans-cis isomerization of the azobenzene fragments.

Another approach developed by Aoyagi et al. involved light-induced pH change as a folding trigger [75]. A photo-initiated proton-releasing agent of *o*-nitrobenzaldehyde (NBA) was integrated into bilayer hydrogels composed of a polyacid layer, poly(*N*-isopropylacrylamide-*co*-2-carboxyisopropylacrylamide) and a polybase layer, poly(*N*-isopropylacrylamide-*co*-*N,N'*-dimethylaminopropylacrylamide). The NBA-integrated bilayer gels demonstrated quick proton

release upon UV irradiation. This led to local decrease of pH below volume phase transition point and bending of the film as a result.

Alternatively, local heat produced by light absorption can be used to power folding behaviour. In the work of Dickey et al. polystyrene film were stretched and frozen below  $T_g$  of the polymer resulting in an internal stress [76]. Black ink was printed on the surface of the polymer. Irradiation by unfocused light led to local heat production inside ink-covered regions and increase of temperature above  $T_g$  of the polymer. These heated hinges relaxed and shrank leading to folding of the whole film into 3D object. The same principle was used by Chen et al. [77]. Pre-stressed nafion films were irradiated by IR laser beam. This led to local temperature increase and relaxation of laser-irradiated regions. The films folded as a result. Both mentioned systems were folding in air conditions. Javey et al. developed a system foldable in water [78]. It was based on PNIPAM composite filled with single-walled carbon nanotubes (CNT) for light absorption. IR laser was used to locally generate heat in the CNT-containing regions which led to shrinkage of PNIPAM and folding of the films. The process was completely reversible since films unfolded after removal of IR radiation. Cube- and flower-like structures were obtained via this method.

## **Conclusion**

Stimuli-responsive self-folding polymer systems have shown a great potential in the field of drug and cell encapsulation. Unlike conventional methods where cells were fixed in a continuous hydrogel matrix, self-folding systems provide certain degree of freedom for cell migration and proliferation. Additionally, nutrients and oxygen can easily diffuse inside self-folded tubes through open ends. The fact that cells can tolerate only limited variations of environmental conditions puts additional restrictions on potential systems for cell encapsulation. Most of the described systems weren't suitable for that purpose since most of the cells can't withstand big pH changes or high temperatures.

In the light of these arguments, temperature-based systems developed by Ionov and co-workers [40, 61-64] have shown the biggest potential towards successful cell encapsulation and scaffold production. However, there are 2 disadvantages that must be overcome before a proper self-folded scaffold can be made. First, these systems were non-biodegradable. Second, at physiological temperature of 37°C these systems were unfolded meaning they can't be used

for cell encapsulation and proper cell incubation. These problems have raised a need for new fully biodegradable systems which keep folded shapes at physiological conditions.

## 2. Aims

The aim of this work was to overcome critical limitations in existing, stimuli-responsive, self-folding systems. In particular, the aims were to improve the biodegradability, the patterning of cells within the tubes, and to find materials that self-fold using cytocompatible stimuli.

The first goal was to develop a biocompatible and biodegradable self-folding system which would be suitable for encapsulation of mammalian cells. The system had to meet the following conditions: remain unfolded at 20°C and fold at 37°C. These conditions were chosen because polymer films needed to be unfolded during cell seeding process, however not perish due to excessive energy exchange 20°C was an ideal temperature to perform cell seeding. After cells have settled, the polymer film should fold in a controlled manner so that it retains shape at human body conditions, thus allowing tissue development. It was decided that gelatin-based self-folding system will meet all the requirements mentioned above. Gelatin was a commonly known biodegradable and biocompatible polymer widely used in food industry. It has a reversible sol-gel transition at 36°C which could be used as folding trigger. To meet the full biodegradability of the self-folding system it was also decided that hydrophobic polymer should be a polyester. Upon successful design and production of self-folding systems, they were meant to be used in cell encapsulation experiments to demonstrate their biocompatibility.

The second main goal was to develop a way to control cell distribution inside self-folded tubes. Therefore, polyethylene oxide (PEO) was used as a third layer of a self-folding system, so that the film surface could be patterned with high cell attachment and low cell attachment materials. This polymer can protect surfaces against protein, bacteria and algae adhesion. Thin patterned layer of PEO on top of self-folding bilayers could therefore prevent cell adhesion on PEO-covered areas. Developed systems were to be used for cell encapsulation to demonstrate their biocompatibility and success of the cell patterning approach.

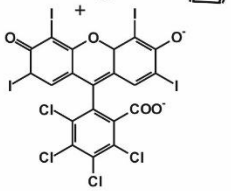
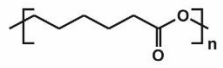
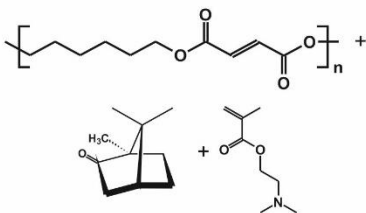
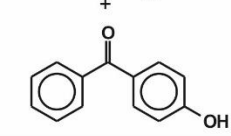
### 3. Synopsis

The current dissertation includes 3 published papers. The aim of the whole work was to develop new biodegradable and biocompatible self-folding systems for cell encapsulation and cell patterning. The results presented in the first and second papers were obtained in Leibniz IPF and in TU Dresden under supervision of Prof. Dr. Manfred Stamm and Dr. Leonid Ionov. The work on the third paper have started in University of Georgia (Athens, USA) under supervision of Prof. Dr. Leonid Ionov and continued in the University of Bayreuth under supervision of Prof. Dr. Leonid Ionov.

#### 3.1 Fully biodegradable and biocompatible systems

The first paper was openly published in *Advanced Functional Materials* under the title: **Biodegradable self-folding polymer films with controlled thermo-triggered folding.**

In this part an attempt was made to create biodegradable self-folding system suitable for cell encapsulation. As a result, three gelatin-based biodegradable and biocompatible thermoresponsive systems were developed (Figure 4). Sol-gel transition of gelatin at 36°C was used as the folding/unfolding trigger.

	non-cured films	photocrosslinked films	
hydrophilic	a gelatin  pure gelatin	c gelatin-F gelatin-NH-CO-NH-  	e gelatin  pure gelatin
hydrophobic	b PCL 	d PHF-Q 	f PCL-B 

**Figure 4.** Chemical formulas of used polymers.

The first (non-cured) system consisted of pure gelatin and PCL. Both polymers were not crosslinked. Such bilayers folded at room temperature due to swelling of the gelatin layer. Gelatin dissolved at 36°C resulting in irreversible unfolding and leaving free-floating PCL film.

Despite this system showed folding/unfolding behaviour, it wasn't suitable since the system needed to stay folded at physiological conditions. The second (Gelatin-F + PHF-Q) bilayer was photolithographically patterned through a photomask by visible light (450 nm) and non-crosslinked PHF-Q was washed away. When this system was immersed in PBS solution both crosslinked and non-crosslinked gelatine swelled but folding didn't occur because bilayers were held in place by non-crosslinked gelatine. The irreversible folding occurred at 36°C when the non-crosslinked gelatin in-between crosslinked bilayers dissolved and released them. The third (Gelatin + PCL-B) system was crosslinked by UV light (256 nm) and had the same folding behaviour as the second system. It also showed the ability to form tubes with different diameters by varying thicknesses of individual layers.

Cell encapsulation experiments showed that neural stem cells could be encapsulated in newly developed self-folded tubes during their formation and they remained alive for a considerable period of time. However, it was observed that tubes lost their shapes after several hours of incubation due to fast degradation rate of gelatin. For that reason, it was decided to develop a new self-folding system which could be stable for a long time. The development of such system is discussed in the third paper.

### **3.2 Reversible folding/unfolding of a gelatine-based system**

During the work on the previous article the Gelatin + PCL-B system showed unusual reversible folding/unfolding behavior. This curiosity drew our attention and its investigation resulted in the second article published in *Nano Letters* under the title: **Reversible thermosensitive biodegradable polymeric actuators based on confined crystallization.**

The UV-crosslinkable gelatin-polycaprolactone system demonstrated a series of interesting properties. It was found that if polycaprolactone was thick enough in comparison to gelatin, the bilayer won't fold even at temperatures slightly above 36 °C. Folding occurred only around 60°C. This temperature was known to be a melting point of PCL and folding took place due to melting and softening of crosslinked PCL which was in complete agreement with the theory. Consequent decrease of the temperature led to unfolding. This observation was in disagreement with theoretical predictions. It was expected that PCL would crystallize in a folded shape upon cooling and no unfolding would occur.

Detailed investigations of this phenomenon showed that reversible folding/unfolding was observed only when PCL thickness was around 500nm and Gelatine was 1.6µm thick. Also, no unfolding was observed with non-crosslinked films. It was found that polymer chains of PCL were parallel to the substrate and this orientation was saved even after melting and

crystallization of the polymer due to low molecular mobility because of crosslinked polymer structure (Figure 5). In other words, it was found that crosslinked Gelatine-PCL bilayers possessed shape-memory property which enabled usage of the system in reversible encapsulation and release of microobjects.

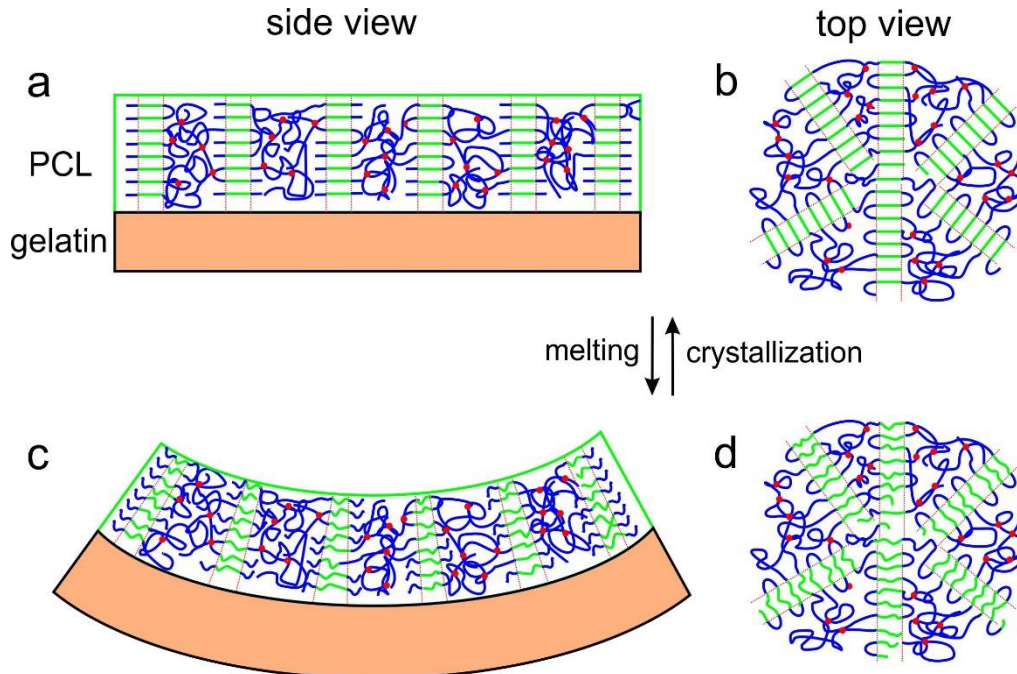


**Figure 5.** Scheme of reversible actuation of gelatin –PCL films.

The possibility to use this system for controlled encapsulation and release was shown on the example of yeast cells. It was stated however that the system can't be directly used for encapsulation of mammalian cells due to high triggering temperature and fast degradation of gelatine. Despite this disadvantage, this system was very important for the whole research because it showed another possible folding trigger – melting of the hydrophobic layer. It was decided to use this principle in the next steps but triggering temperature had to be decreased.

### 3.3 Stable system and cell patterning

The third article focused on the development of a stable biocompatible self-folding system and on achieving cell patterning on the surface of it. The results were published in *Advanced Functional Materials* under the title: 4D biofabrication: **3D cell patterning using shape-changing films.**

The new self-folding system was developed as a solution to the problems stated above: high degradability of gelatine and high folding temperature of gelatin-polycaprolactone system. It was based on two polymers: 1) PNIPAM-AA – Copolymer of N-isopropylacrylamide and acrylic acid as hydrophilic polymer and 2) PSMA –

Polystyrylmethacrylate as hydrophobic one. Both polymers contained 2% of hydroxybenzophenone acrylate comonomer for photocrosslinking purposes. Crosslinked PNIPAM-AA swelled in PBS buffer solution in temperature range 20-37°C while non-crosslinked PNIPAM-AA dissolved. PSMA was a semicrystalline waxy polymer and was inert to water. It also had a melting point around 34°C. The semicrystalline nature of the PSMA allowed it to work as a folding actuator in the same way as polycaprolactone's melting triggered bilayer folding. However, temperature was suitable for cell encapsulation in case of PSMA (Figure 6).

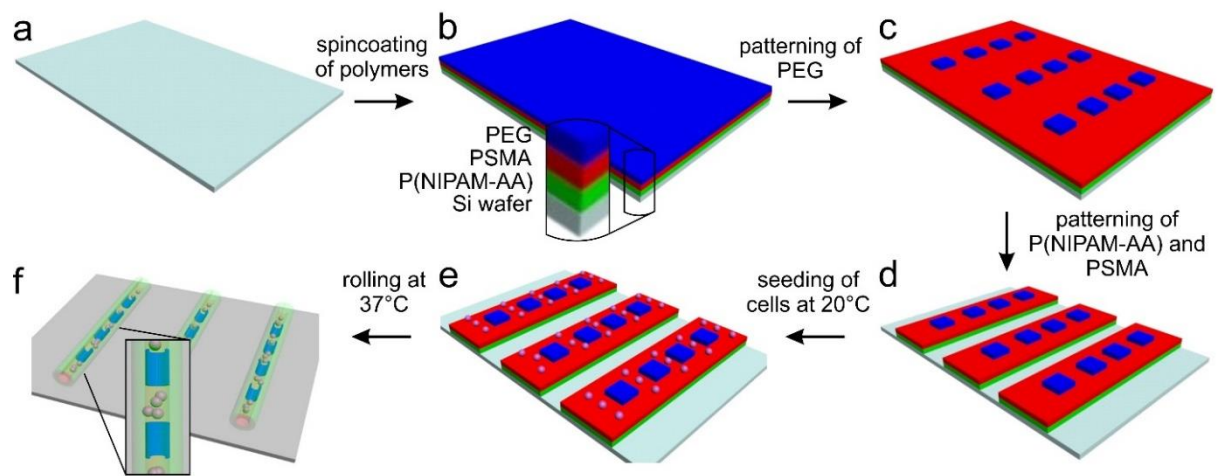


**Figure 6.** Scheme of fabrication of 3D cellular patterns using shape-changing polymer films. a) Silicon wafer or glass were used as a substrate. b) Polymers were sequentially deposited on the substrate via either spin- or deep coating. c) PEG layer was photolithographically patterned during the first photolithography step. d) PNIPAM-AA – PSMA bilayers were patterned through the second photolithography step. e) Cell were seeded on top of flat bilayers at 20°C. f) Bilayers folded at 37°C encapsulating cells inside tubes.

The folding mechanism of the system was similar to that shown in the second paper. The radius of curvature of the system at 20°C was infinite due to high thickness of PSMA resulting in no folding. Upon temperature increase above 34°C PSMA melted and softened which resulted in decrease of the curvature radius and film folding. It was possible to create self-folding tubes with different inner diameters by varying individual polymer thicknesses. Obtained results were in qualitative agreement with theoretical predictions. Self-folded tubes were shown to be stable in water medium for at least 3 months and actuation temperature of 34°C was suitable for the cells. Cell patterning was achieved with the help of the third polymer - Polyethyleneglycol (PEG). Its purpose was to protect certain areas of PNIPAM-AA – PSMA

bilayers from cell adhesion effectively creating a PNIPAM-AA – PSMA – PEG trilayers. PEG-covered areas were formed by photolithographical patterning. 3T3 mouse fibroblasts were used in cell viability and encapsulation experiments. It was shown that system components aren't toxic for the cells and PSMA surface is suitable for cell adherence. Optical observations of folded tubes demonstrated that cells were viable after 2 days of encapsulation and were adhered only to those areas inside tubes which weren't covered with PEG indicating the success of the approach. However, materials used in this research were not biodegradable and therefore the outlook for this work includes further development of self-folding systems and cell patterning approaches.

## 4. Literature references

1. Mironov, V., et al., *Biofabrication: a 21st century manufacturing paradigm*. *Biofabrication*, 2009. **1**(2): p. 022001.
2. Yeh, J., et al., *Micromolding of shape-controlled, harvestable cell-laden hydrogels*. *Biomaterials*, 2006. **27**(31): p. 5391-5398.
3. McGuigan, A.P. and M.V. Sefton, *Vascularized organoid engineered by modular assembly enables blood perfusion*. *Proceedings of the National Academy of Sciences*, 2006. **103**(31): p. 11461-11466.
4. Chung, S.E., et al., *Guided and fluidic self-assembly of microstructures using railed microfluidic channels*. *Nature Materials*, 2008. **7**: p. 581.
5. Bruzewicz, D.A., A.P. McGuigan, and G.M. Whitesides, *Fabrication of a modular tissue construct in a microfluidic chip*. *Lab on a Chip*, 2008. **8**(5): p. 663-671.
6. Du, Y., et al., *Directed assembly of cell-laden microgels for fabrication of 3D tissue constructs*. *Proceedings of the National Academy of Sciences*, 2008. **105**(28): p. 9522-9527.
7. Shi, Z., et al., *Stochastic model of self-assembly of cell-laden hydrogels*. *Physical Review E*, 2009. **80**(6): p. 061901.
8. Du, Y., et al., *Sequential assembly of cell-laden hydrogel constructs to engineer vascular-like microchannels*. *Biotechnology and Bioengineering*, 2011. **108**(7): p. 1693-1703.
9. Zamanian, B., et al., *Interface-Directed Self-Assembly of Cell-Laden Microgels*. *Small*, 2010. **6**(8): p. 937-944.
10. Du, Y., et al., *Surface-directed assembly of cell-laden microgels*. *Biotechnology and Bioengineering*, 2010. **105**(3): p. 655-662.
11. Fernandez, J.G. and A. Khademhosseini, *Micro-Masonry: Construction of 3D Structures by Microscale Self-Assembly*. *Advanced Materials*, 2010. **22**(23): p. 2538-2541.
12. Yanagawa, F., et al., *Directed assembly of cell-laden microgels for building porous three-dimensional tissue constructs*. *Journal of Biomedical Materials Research Part A*, 2011. **97A**(1): p. 93-102.
13. Harada, A., et al., *Macroscopic self-assembly through molecular recognition*. *Nature Chemistry*, 2010. **3**: p. 34.

14. Scott, E.A., et al., *Modular scaffolds assembled around living cells using poly(ethylene glycol) microspheres with macroporation via a non-cytotoxic porogen*. *Acta Biomaterialia*, 2010. **6**(1): p. 29-38.
15. Ahu, A.-Y., et al., *Towards artificial tissue models: past, present, and future of 3D bioprinting*. *Biofabrication*, 2016. **8**(1): p. 014103.
16. Singh, M., et al., *Inkjet Printing—Process and Its Applications*. *Advanced Materials*, 2010. **22**(6): p. 673-685.
17. Nishiyama, Y., et al., *Development of a Three-Dimensional Bioprinter: Construction of Cell Supporting Structures Using Hydrogel and State-Of-The-Art Inkjet Technology*. *Journal of Biomechanical Engineering*, 2008. **131**(3): p. 035001-035001-6.
18. Cui, X., et al., *Cell damage evaluation of thermal inkjet printed Chinese hamster ovary cells*. *Biotechnology and Bioengineering*, 2010. **106**(6): p. 963-969.
19. Cui, X., Gao, G. & Qiu, Y., *Accelerated myotube formation using bioprinting technology for biosensor applications*. *Biotechnol Lett*, 2013. **35**(3): p. 315–321.
20. Pepper, M.E., et al. *Cell settling effects on a thermal inkjet bioprinter*. in *2011 Annual International Conference of the IEEE Engineering in Medicine and Biology Society*. 2011.
21. Pepper, M.E., et al., *Characterizing the effects of cell settling on bioprinter output*. *Biofabrication*, 2012. **4**(1).
22. Nahmias, Y., et al., *Laser-guided direct writing for three-dimensional tissue engineering*. *Biotechnology and Bioengineering*, 2005. **92**(2): p. 129-136.
23. Duan, B., et al., *3D Bioprinting of heterogeneous aortic valve conduits with alginate/gelatin hydrogels*. *Journal of Biomedical Materials Research Part A*, 2013. **101A**(5): p. 1255-1264.
24. Campos, D.F.D., et al., *Three-dimensional printing of stem cell-laden hydrogels submerged in a hydrophobic high-density fluid*. *Biofabrication*, 2012. **5**(1).
25. Gao, Q., et al., *Coaxial nozzle-assisted 3D bioprinting with built-in microchannels for nutrients delivery*. *Biomaterials*, 2015. **61**(Supplement C): p. 203-215.
26. Jung-Seob, L., et al., *3D printing of composite tissue with complex shape applied to ear regeneration*. *Biofabrication*, 2014. **6**(2): p. 024103.
27. Murphy, S.V. and A. Atala, *3D bioprinting of tissues and organs*. *Nature Biotechnology*, 2014. **32**: p. 773.
28. Miller, J.S., et al., *Rapid casting of patterned vascular networks for perfusable engineered three-dimensional tissues*. *Nature Materials*, 2012. **11**: p. 768.

29. Gauvin, R., et al., *Microfabrication of complex porous tissue engineering scaffolds using 3D projection stereolithography*. *Biomaterials*, 2012. **33**(15): p. 3824-3834.
30. Gou, M., et al., *Bio-inspired detoxification using 3D-printed hydrogel nanocomposites*. *Nature Communications*, 2014. **5**: p. 3774.
31. Zongjie, W., et al., *A simple and high-resolution stereolithography-based 3D bioprinting system using visible light crosslinkable bioinks*. *Biofabrication*, 2015. **7**(4): p. 045009.
32. Kufelt, O., et al., *Water-soluble photopolymerizable chitosan hydrogels for biofabrication via two-photon polymerization*. *Acta Biomaterialia*, 2015. **18**: p. 186-195.
33. Nielson, R., B. Kaehr, and J.B. Shear, *Microreplication and Design of Biological Architectures Using Dynamic-Mask Multiphoton Lithography*. *Small*, 2009. **5**(1): p. 120-125.
34. Ovsianikov, A., et al., *Two-photon polymerization technique for microfabrication of CAD-designed 3D scaffolds from commercially available photosensitive materials*. *Journal of Tissue Engineering and Regenerative Medicine*, 2007. **1**(6): p. 443-449.
35. Torgersen, J., et al. *Photo-sensitive hydrogels for three-dimensional laser microfabrication in the presence of whole organisms*. 2012. SPIE.
36. Weiß, T., et al., *Two-Photon Polymerization of Biocompatible Photopolymers for Microstructured 3D Biointerfaces*. *Advanced Engineering Materials*, 2011. **13**(9): p. B264-B273.
37. Jager, E.W.H., O. Inganäs, and I. Lundström, *Microrobots for Micrometer-Size Objects in Aqueous Media: Potential Tools for Single-Cell Manipulation*. *Science*, 2000. **288**(5475): p. 2335-2338.
38. Smela, E., O. Inganäs, and I. Lundström, *Controlled Folding of Micrometer-Size Structures*. *Science*, 1995. **268**(5218): p. 1735-1738.
39. Timoshenko, S., *Analysis of Bi-Metal Thermostats*. *Journal of the Optical Society of America*, 1925. **11**(3): p. 233-255.
40. Stoychev, G., et al., *Shape-Programmed Folding of Stimuli-Responsive Polymer Bilayers*. *ACS Nano*, 2012. **6**(5): p. 3925-3934.
41. Zakharchenko, S., E. Sperling, and L. Ionov, *Fully Biodegradable Self-Rolled Polymer Tubes: A Candidate for Tissue Engineering Scaffolds*. *Biomacromolecules*, 2011. **12**(6): p. 2211-2215.

42. Kim, J., et al., *Designing Responsive Buckled Surfaces by Halftone Gel Lithography*. Science, 2012. **335**(6073): p. 1201-1205.
43. Bof Bufon, C.C., et al., *Self-Assembled Ultra-Compact Energy Storage Elements Based on Hybrid Nanomembranes*. Nano Letters, 2010. **10**(7): p. 2506-2510.
44. Ji, H.-X., et al., *Self-Wound Composite Nanomembranes as Electrode Materials for Lithium Ion Batteries*. Advanced Materials, 2010. **22**(41): p. 4591-4595.
45. Yang, L., et al., *Hierarchical MoS<sub>2</sub>/Polyaniline Nanowires with Excellent Electrochemical Performance for Lithium-Ion Batteries*. Advanced Materials, 2013. **25**(8): p. 1180-1184.
46. Harazim, S.M., et al., *Lab-in-a-tube: on-chip integration of glass optofluidic ring resonators for label-free sensing applications*. Lab on a Chip, 2012. **12**(15): p. 2649-2655.
47. Huang, G.S., et al., *Optical properties of rolled-up tubular microcavities from shaped nanomembranes*. Applied Physics Letters, 2009. **94**(14): p. 141901.
48. Smith, E.J., et al., *Lab-in-a-Tube: Detection of Individual Mouse Cells for Analysis in Flexible Split-Wall Microtube Resonator Sensors*. Nano Letters, 2011. **11**(10): p. 4037-4042.
49. Smith, E.J., et al., *Lab-in-a-tube: ultracompact components for on-chip capture and detection of individual micro-/nanoorganisms*. Lab on a Chip, 2012. **12**(11): p. 1917-1931.
50. Huang, G., et al., *Rolled-up transparent microtubes as two-dimensionally confined culture scaffolds of individual yeast cells*. Lab on a Chip, 2009. **9**(2): p. 263-268.
51. Bassik, N., et al., *Enzymatically Triggered Actuation of Miniaturized Tools*. Journal of the American Chemical Society, 2010. **132**(46): p. 16314-16317.
52. Fernandes, R. and D.H. Gracias, *Self-folding polymeric containers for encapsulation and delivery of drugs*. Advanced Drug Delivery Reviews, 2012. **64**(14): p. 1579-1589.
53. Leong, T.G., et al., *Self-loading lithographically structured microcontainers: 3D patterned, mobile microwells*. Lab on a Chip, 2008. **8**(10): p. 1621-1624.
54. Randall, C.L., et al., *Three-dimensional microwell arrays for cell culture*. Lab on a Chip, 2011. **11**(1): p. 127-131.
55. Randall, C.L., et al., *Self-folding immunoprotective cell encapsulation devices*. Nanomedicine: Nanotechnology, Biology and Medicine, 2011. **7**(6): p. 686-689.
56. Jamal, M., et al., *Directed growth of fibroblasts into three dimensional micropatterned geometries via self-assembling scaffolds*. Biomaterials, 2010. **31**(7): p. 1683-1690.

57. Stuart, M.A.C., et al., *Emerging applications of stimuli-responsive polymer materials*. Nature Materials, 2010. **9**: p. 101.
58. Nair, L.S. and C.T. Laurencin, *Biodegradable polymers as biomaterials*. Progress in Polymer Science, 2007. **32**(8): p. 762-798.
59. Behl, M., M.Y. Razzaq, and A. Lendlein, *Multifunctional Shape-Memory Polymers*. Advanced Materials, 2010. **22**(31): p. 3388-3410.
60. Azam, A., et al., *Self-folding micropatterned polymeric containers*. Biomedical Microdevices, 2011. **13**(1): p. 51-58.
61. Stoychev, G., N. Pureskiy, and L. Ionov, *Self-folding all-polymer thermoresponsive microcapsules*. Soft Matter, 2011. **7**(7): p. 3277-3279.
62. Stoychev, G., et al., *Hierarchical Multi-Step Folding of Polymer Bilayers*. Advanced Functional Materials, 2013. **23**(18): p. 2295-2300.
63. Zakharchenko, S., et al., *Temperature controlled encapsulation and release using partially biodegradable thermo-magneto-sensitive self-rolling tubes*. Soft Matter, 2010. **6**(12): p. 2633-2636.
64. Zakharchenko, S., et al., *Stimuli-responsive hierarchically self-assembled 3D porous polymer-based structures with aligned pores*. Journal of Materials Chemistry B, 2013. **1**(13): p. 1786-1793.
65. Kumar, K., et al., *A Novel Approach for the Fabrication of Silica and Silica/Metal Hybrid Microtubes*. Chemistry of Materials, 2009. **21**(18): p. 4282-4287.
66. Luchnikov, V., K. Kumar, and M. Stamm, *Toroidal hollow-core microcavities produced by self-rolling of strained polymer bilayer films*. Journal of Micromechanics and Microengineering, 2008. **18**(3): p. 035041.
67. Luchnikov, V., O. Sydorenko, and M. Stamm, *Self-Rolled Polymer and Composite Polymer/Metal Micro- and Nanotubes with Patterned Inner Walls*. Advanced Materials, 2005. **17**(9): p. 1177-1182.
68. Bassik, N., et al., *Photolithographically patterned smart hydrogel based bilayer actuators*. Polymer, 2010. **51**(26): p. 6093-6098.
69. He, H., J. Guan, and J.L. Lee, *An oral delivery device based on self-folding hydrogels*. Journal of Controlled Release, 2006. **110**(2): p. 339-346.
70. Shim, T.S., et al., *Controlled Origami Folding of Hydrogel Bilayers with Sustained Reversibility for Robust Microcarriers*. Angewandte Chemie International Edition, 2012. **51**(6): p. 1420-1423.

71. Konotop, I.Y., et al., *Novel pH-responsive hydrogels with gradient charge distribution*. *Soft Matter*, 2010. **6**(8): p. 1632-1634.
72. Alford, P.W., et al., *Biohybrid thin films for measuring contractility in engineered cardiovascular muscle*. *Biomaterials*, 2010. **31**(13): p. 3613-3621.
73. Feinberg, A.W., et al., *Muscular Thin Films for Building Actuators and Powering Devices*. *Science*, 2007. **317**(5843): p. 1366-1370.
74. Ryabchun, A., et al., *Novel Generation of Liquid Crystalline Photo-Actuators Based on Stretched Porous Polyethylene Films*. *Macromolecular Rapid Communications*, 2012. **33**(11): p. 991-997.
75. Techawanitchai, P., et al., *Photo-switchable control of pH-responsive actuators via pH jump reaction*. *Soft Matter*, 2012. **8**(10): p. 2844-2851.
76. Liu, Y., et al., *Self-folding of polymer sheets using local light absorption*. *Soft Matter*, 2012. **8**(6): p. 1764-1769.
77. Chen, T., et al., *A "writing" strategy for shape transition with infinitely adjustable shaping sequences and in situ tunable 3D structures*. *Materials Horizons*, 2016. **3**(6): p. 581-587.
78. Zhang, X., et al., *Optically- and Thermally-Responsive Programmable Materials Based on Carbon Nanotube-Hydrogel Polymer Composites*. *Nano Letters*, 2011. **11**(8): p. 3239-3244.

## **5. Manuscripts**

# Manuscript 1

## Biodegradable self-folding polymer films with controlled thermo-triggered folding

*Vladislav Stroganov, Svetlana Zakharchenko, Evgeni Sperling, Anne Meyer, Oliver G.  
Schmidt and Leonid Ionov*

Advanced Functional Materials

First published: 7 April 2014

**DOI:** 10.1002/adfm.201400176

## Statement of Authors contribution

My personal contribution to that work included:

- Chemical synthesis of polymers;
- Design and production of self-folding bilayers;
- Conduction of experiments with self-folding films. Evaluation of their characteristics such as layer thicknesses, tube diameters and folding conditions;
- Participation in cell encapsulation experiments;
- Participation in writing of the final manuscript.

Degree of my personal contribution to the work is 60%.

Svetlana Zakharchenko provided assistance with evaluation of experimental results in the “self-folding” part. She also participated in cell encapsulation experiments and provided assistance with manuscript writing.

Evgeni Sperling designed the non-crosslinked gelatine-polycaprolactone system and evaluated its properties.

Anne Meyer conducted cell encapsulation experiments.

Oliver G. Schmidt gave valuable advises and shared his experience during active discussions about self-folding systems. He participated in editing of the manuscript.

Leonid Ionov provided supervision, shared his ideas and experience during the whole research process. He wrote the main part of the manuscript.

# Biodegradable Self-Folding Polymer Films with Controlled Thermo-Triggered Folding

Vladislav Stroganov, Svetlana Zakharchenko, Evgeni Sperling, Anne K. Meyer, Oliver G. Schmidt, and Leonid Ionov\*

Self-folding films are a unique kind of thin film. They are able to deform in response to a change in environmental conditions or internal stress and form complex 3D structures. They are very promising candidates for the design of bioscaffolds, which resemble different kinds of biological tissues. In this paper, a very simple and cheap approach for the fabrication of fully biodegradable and biocompatible self-rolled tubes is reported. The tubes' folding can be triggered by temperature. A bilayer approach is used, where one component is active and another one is passive. The passive one can be any biocompatible, biodegradable, hydrophobic polymer. Gelatin is used as an active component: it allows the design of (i) self-folding polymer films, which fold at room temperature (22 °C) and irreversibly unfold at 37 °C, and (ii) films, which are unfolded at room temperature (22 °C), but irreversibly fold at 37 °C. The possibilities of encapsulation of neural stem cells are also demonstrated using self-folded tubes.

as tubes, capsules, cubes, pyramids, etc.<sup>[1]</sup> Self-folding films are films with either vertical (bilayers)<sup>[2]</sup> or lateral (patterned films) inhomogeneities,<sup>[3]</sup> which consist of two or more kinds of components with different volume expansion properties. Such films undergo deformation when the volume of one of the components increases. Self-folding films were demonstrated to be promising candidates for energy harvesting and storage,<sup>[4]</sup> design of porous materials,<sup>[5,6]</sup> sensors,<sup>[7]</sup> cell encapsulation,<sup>[2,8]</sup> microrobotic functionality,<sup>[9]</sup> design of bioscaffolds.<sup>[5,10]</sup> Among the variety of these applications the use of self-folding for biomaterials is especially promising.<sup>[11,12]</sup> In particular, it was shown that self-folded objects are promising candidates for the design of bioscaffolds,

which resemble different kinds of biological tissues.<sup>[5]</sup>

In order to be suitable for biomaterial engineering, the materials which are used for fabrication of self-folding films must fulfill the following requirements: biocompatibility, biodegradability and sensitivity to stimuli in the physiological range. Metals and oxides demonstrate good biocompatibility although they are not biodegradable and their folding is spontaneous and not activated by stimuli in the physiological range. There are examples of polymer-based self-folding films with temperature-controlled folding based on poly(*N*-isopropylacrylamide).<sup>[2,13]</sup> These polymers demonstrate responsive properties in the physiological temperature range (25–37 °C), but are not biodegradable. Recently, we reported for the first time the design of biodegradable/biocompatible self-rolled tubes based on polycaprolactone and polysuccinimide, which roll due to slow hydrolysis of polysuccinimide in a physiological buffer environment.<sup>[12]</sup> The rolling of polysuccinimide-based bilayers is determined by the kinetics of hydrolysis and can hardly be controlled by external signals. Therefore, development of biodegradable/biocompatible self-folding polymer films, whose folding can be triggered by external signals, is strongly desirable. Among all possible signals, which can be used as a trigger, temperature appears to be the most favorable one. Indeed, pH and UV light can cause potential damage to cells, but they can usually tolerate a variation of temperature in the range between 4 °C and 37 °C.

Here, we report a very simple and cheap approach for fabrication of fully biodegradable and biocompatible self-rolled tubes, whose folding can be triggered by temperature. Moreover,

## 1. Introduction

Self-folding films are a unique kind of thin films, which are able to deform in response to a change of environmental conditions or internal stress and form complex 3D structures such

V. Stroganov, S. Zakharchenko, E. Sperling,  
Dr. L. Ionov  
Leibniz Institute of Polymer Research Dresden  
Hohe Str. 6, D-01069, Dresden, Germany  
E-mail: ionov@ipfdd.de

V. Stroganov, S. Zakharchenko, E. Sperling  
Technische Universität Dresden  
Fakultät Mathematik und Naturwissenschaften  
01062, Dresden, Germany

Dr. A. K. Meyer, Prof. O. G. Schmidt  
Institute for Integrative Nanosciences  
IFW Dresden, Helmholtzstr. 20,  
D-01069, Dresden, Germany

Dr. A. K. Meyer  
Division of Neurodegenerative diseases  
Department of Neurology  
University Clinic Carl Gustav Carus Dresden  
Fetscherstr. 74, 01307, Dresden, Germany

Prof. O. G. Schmidt  
Material Systems for Nanoelectronics  
Chemnitz University of Technology  
Reichenhainer Str. 70, D-09107, Chemnitz, Germany



DOI: 10.1002/adfm.201400176

these self-folding films demonstrate different folding behavior depending on the properties of the polymers. We used a bilayer approach where one component is active and another one is passive. The passive one can be any biocompatible, biodegradable hydrophobic polymer. Gelatin was used as an active component. Gelatin forms hydrogels upon cooling from an aqueous solution, due to helix-formation and association of the helices. These physically crosslinked hydrogels have a sol-gel transition temperature.<sup>[14]</sup> Chemically crosslinked gelatin undergoes one-way swelling in aqueous environment, wherein the degree of swelling strongly depends on the temperature. The use of gelatin as a thermoresponsive component is highly attractive since the polymer is cheap and produced in huge quantities by hydrolysis of collagen, which is the main component of connective tissue. The last point is very important because one can expect particularly favorable interactions with cells. Due to biocompatibility and biodegradability gelatin is already offered for application in tissue engineering, therapeutic angiogenesis, gene therapy, and drug delivery.<sup>[15]</sup> Moreover, as we show in this manuscript, gelatin allows the design of (i) self-folding polymer films, which fold at room temperature (22 °C) and irreversibly unfold at 37 °C and (ii) films, which are unfolded at room temperature (22 °C), but irreversibly fold at 37 °C. As a result, gelatin-based self-folding films can be used for both irreversible and reversible encapsulation of cells. Such complex thermoresponsive behavior cannot be achieved by, for example, polymers with LCST behavior, such as poly(N-isopropylacrylamide), which are unfolded and folded at elevated and reduced temperature, respectively.<sup>[2]</sup>

## 2. Results and Discussion

In this paper, we demonstrate two approaches for the design of thermoresponsive gelatin-based self-folding films (Figure 1). For the first one, not-crosslinked biodegradable polycaprolactone

and gelatin were used (Figure 1a,b). In the second approach, we used UV- and VIS- photocrosslinked polymer bilayers. VIS curable system (gelatin-F/PHF-Q) was designed using furfuryl modified gelatin (gelatin-F), which contains a small amount of Rose Bengal as photoinitiator (Figure 1c) and a copolymer of hexanediol and fumaryl chloride (PHF) containing camphorquinone as photoinitiator (Figure 1d). The first UV curable system (gelatin/PHF-Q) was designed using pure gelatin (Figure 1e) and hydrophobic PHF with camphorquinone as photoinitiator (Figure 1d). The second UV curable system was designed using pure gelatin (Figure 1e) and polycaprolactone with 4-hydroxybenzophenone as photoinitiator (Figure 1f). In fact, the use of deep UV irradiation (254 nm) can be considered an advantage: first it allows to minimize the number of modifications required to make polymers photosensitive; second, it allows to avoid water-soluble Rose Bengal as initiator for gelatin; and third, deep UV irradiation is typically used for disinfection of surfaces and allows reduction of biological contamination of materials.

The polymer bilayers, which consist of a bottom gelatin and top hydrophobic polymer, were prepared by sequential dip-coating. All polymers, which were used in this work, are biocompatible and biodegradable: gelatin is a natural polymer, derived from collagen, PCL is a synthetic biocompatible/biodegradable polyester, which is already approved for medical applications,<sup>[16]</sup> PHF, as it is shown below, is also biocompatible. Moreover, since PHF is a linear aliphatic polyester, it is expected to be biodegradable.<sup>[17]</sup> The expected products of the degradation of PHF—hexanediol (used in cosmetics) and fumaric acid<sup>[18]</sup>—are not toxic. The photoinitiators, which are used to induce photocrosslinking of polymers, were already used for bio-related purposes. For example, benzophenone derivatives are used for preparation of photocrosslinked hydrogels, camphorquinone is the photoinitiator for tooth PMMA-based cement, derivative of diazostilbene is antioxidant, Rose

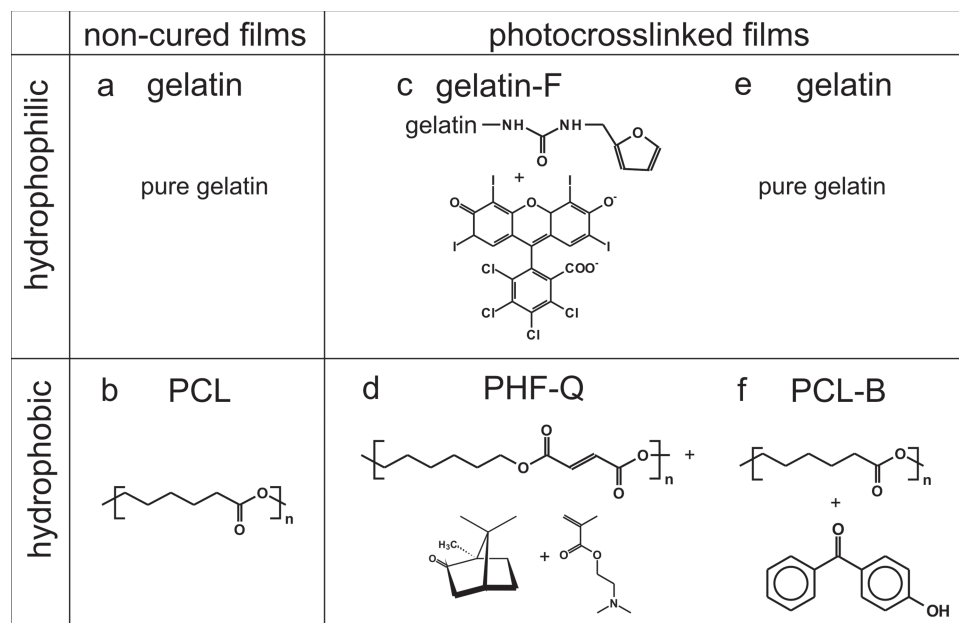
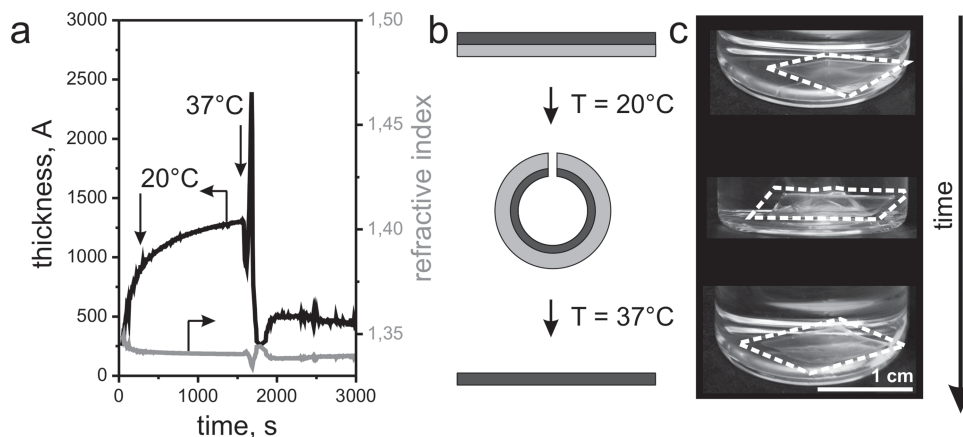


Figure 1. Chemical formulas of polymers which are used for the design of thermoresponsive biodegradable/biocompatible self-folding films.



**Figure 2.** Behavior of non-crosslinked gelatin/polycaprolactone system: (a) Swelling and dissolving of non-crosslinked gelatin film (thickness in a dry state 20 nm) in PBS buffer (0.15 M, pH = 7.4) first at  $T = 22\text{ }^{\circ}\text{C}$  (0–1500 s) and then at  $T = 37\text{ }^{\circ}\text{C}$  (1500–3000 s). Scheme (b) and experimental (c) observation of folding/unfolding of the non-crosslinked gelatin/PCL bilayer in water. The thickness of the gelatin is 200  $\mu\text{m}$ ; the thickness of the PCL is 20  $\mu\text{m}$ .

Bengal is a food dye. The biocompatibility and biodegradability of furfuryl modified gelatin Rose Bengal photoinitiator was previously demonstrated.<sup>[19]</sup> Moreover, furfuryl modified gelatin showed no cytotoxicity, even with more than 20% Rose Bengal. Therefore, we expect that these systems can be applied for bio-applications.

### 2.1. Non-Crosslinked Bilayer

We started from the investigation of the swelling properties of native non-crosslinked gelatin films. Exposure of thin gelatin film to water at room temperature ( $T = 22\text{ }^{\circ}\text{C}$ ) led to its swelling from 20 nm (as measured in a dry state) up to about 120 nm (Figure 2a). Increasing the temperature to body temperature ( $T = 37\text{ }^{\circ}\text{C}$ ) resulted in a sharp increase of the film thickness followed by its abrupt decrease. Obviously, gelatin swells moderately in cold PBS 0.15 M (pH = 7.4) buffer, still staying in a gel form, while further increase of temperature to  $37\text{ }^{\circ}\text{C}$  results in a stronger swelling of the film, accompanied by the polymer dissolution. The residual thickness of gelatin film was 50 nm in a swollen state at  $37\text{ }^{\circ}\text{C}$  and 6 nm after drying, which was found to be independent of the initial thickness of gelatin (either it was 50 nm or 2  $\mu\text{m}$ ). This residual layer most probably originates from adsorption of gelatin on the charged silica wafer. Very thick gelatin films demonstrated similar temperature-dependent swelling behavior. For example, a gelatin film with a thickness of around 200  $\mu\text{m}$  swelled up to 1000% in water at room temperature after 2 h of swelling and up to 1900% after 24 h as measured by the mass change. Heating up to  $37\text{ }^{\circ}\text{C}$  led to the complete dissolution of the swollen gelatin films. Interestingly, dissolution of gelatin occurred exactly at  $37\text{ }^{\circ}\text{C}$  which can be used for temperature controlled release in the human body.

We fabricated a non-crosslinked gelatin-polycaprolactone bilayer by deposition of a 50  $\mu\text{m}$  layer of polycaprolactone on a 220  $\mu\text{m}$  thick layer of gelatin. The sample was annealed at  $60\text{ }^{\circ}\text{C}$  for 30 s in order to melt polycaprolactone, to fuse it to the gelatin layer and to make the bilayer more stable. The film was immersed in cold water. Correspondingly to the swelling

scenario of gelatin, the film slowly deformed and rolled up into a tube (Figure 1b,c). The inner diameter of the tube was around 1–2 mm. An increase of temperature led to the unfolding of the film, which was caused by the dissolution of the gelatin. Finally, an unfolded PCL film was left.

Thus, the non-crosslinked PCL-gelatin system undergoes folding at low temperature and unfolding at higher temperature. Since the polymers are not photocrosslinkable, bilayers with different shape can be prepared by knife cutting or by cutting with an IR heating laser. Both polymers used in this system are biocompatible and biodegradable which allows the non-crosslinked PCL-gelatin system to be employed in bio-related applications.

### 2.2. Crosslinked Films

Next, we investigated folding of four photocrosslinked bilayer, where gelatin is the bottom layer and the hydrophobic polymer is the top layer. Similar to native gelatin, all photocrosslinked gelatin films swelled in cold water ( $T = 24\text{ }^{\circ}\text{C}$ ) up to 1000% of its mass after 2 h of swelling. On the other hand, since the film was crosslinked, heating to  $37\text{ }^{\circ}\text{C}$  did not lead to its dissolution and the swelling degree increased up to 1200%.

The polymer bilayers were prepared by sequential deposition of the respective polymers. The bilayers were photocrosslinked by irradiation through a photomask by using either UV light (254 nm) in the case of gelatin/PHF-Q and gelatin/PCL-B films or blue light (405 nm) in the case of gelatin-F/PHF-Q films. After being photocrosslinked, the bilayer was rinsed in chloroform in order to remove the non-crosslinked hydrophobic polymer leading to the formation of a structured bilayer formed by the bottom layer of the crosslinked and non-crosslinked gelatins and top layer of crosslinked hydrophobic polymers (Figure 3a,d,h).

Immersion of the crosslinked bilayers in cold water ( $24\text{ }^{\circ}\text{C}$ ) led to swelling of both crosslinked and non-crosslinked gelatin (Figure 3a,b) that resulted in slight wrinkling of the bilayer (Figure 3e,i). As it was shown above, non-crosslinked gelatin is not soluble in cold water. Formed gel of non-crosslinked gelatin

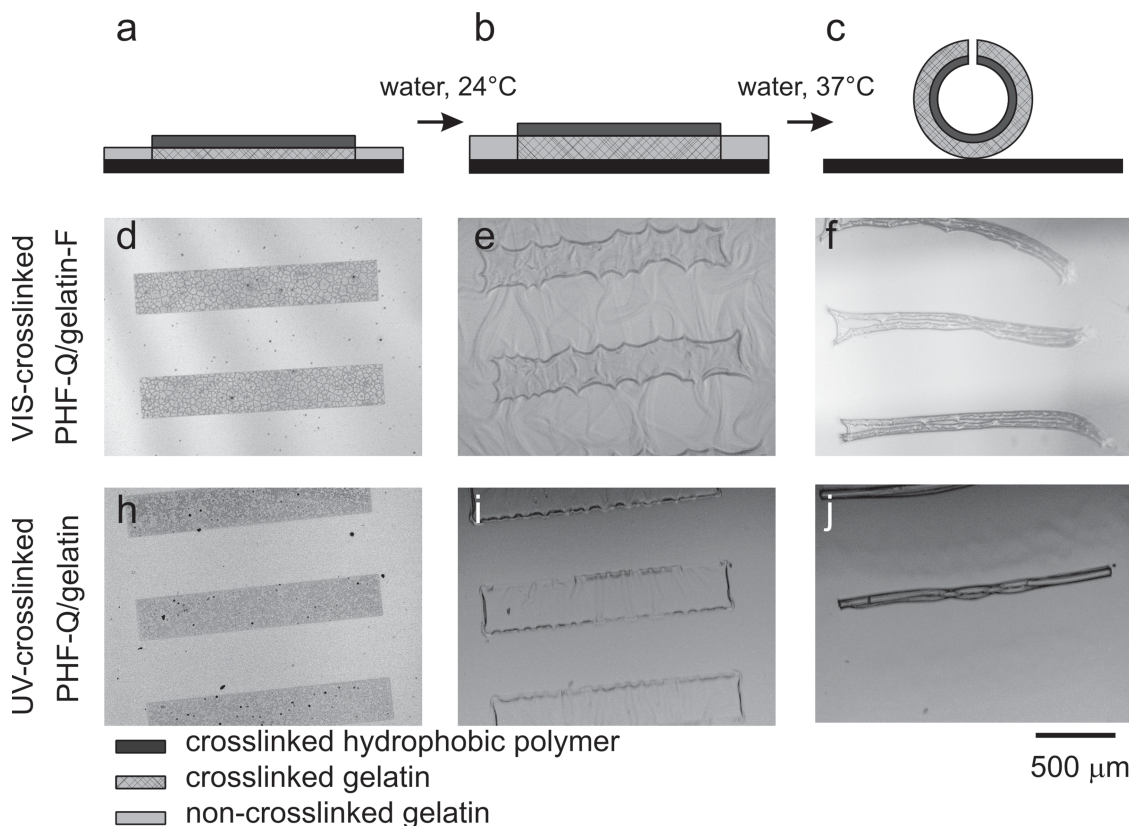


**Figure 3.** Folding of crosslinked bilayers. (a–c) Schematic scenario of temperature-dependent behavior of the bilayer; (d–f) microscopy snapshots of the gelatin-F/PHF-Q bilayer at different temperatures. (h–j) – microscopy snapshots of the gelatin/PCL-Q bilayer at different temperatures. Panels (d) and (h) correspond to panel (a). Panels (e) and (i) correspond to panel (b). Panels (f) and (j) correspond to panel (c). The thickness of the gelatin in both cases is ca 1.7 μm, the thickness of PHF is 100 nm. Gelatin/PCL-Q films demonstrate similar behavior.

merely held photocrosslinked bilayer and prevented its folding. An increase of temperature to  $T = 37\text{ °C}$  led to the dissolution of the non-crosslinked gelatin. As a result, the photocrosslinked bilayer film rolled due to stress produced by swelling of the photocrosslinked gelatin (Figure 3c,f,j).

We investigated the effect of the thickness of each layer on the radius of the formed tubes. It was found that 1.7 μm gelatin and 100 nm PHF-Q layers form tubes with diameters around 10–20 μm. Interestingly, an increase of the thickness of the PHF-Q layer does not lead to an increase of the diameter but results in the inability of the bilayer to fold. The origin of this effect is most probably the high stiffness of the PHF-Q layer. Tubes with different diameters can be however easily prepared using another UV-crosslinkable film gelatin/PCL-Q (Figure 4a,b). The PCL is a relatively soft polymer and the diameter of tubes can easily be adjusted by changing the thickness of each layer. In particular, an increase of the thickness of both polymers results in a diameter increase of the tubes (Figure 4c) which is in qualitative consistence with the Timoshenko equation.<sup>[20]</sup>

### 2.3. Encapsulation of Cells

Finally, we demonstrate possibilities to encapsulate cells using gelatin-based self-folding films and investigate the behavior of

neural stem cells for the example of one of the UV-crosslinked thermoresponsive gelatin-based systems, which contains the minimal number of additives and modifications, namely gelatin/PHF-Q. The behavior of cells was first investigated on individual polymer films: gelatin and PHF (Figure 5). After 66 h the cells were adsorbed on the previously crosslinked polymer films and started to form agglomerates indicating that cells well adhere to both hydrophobic and hydrophilic polymers, as well as that cells are alive and are able to divide. It is interesting to observe that the behavior of cells on both polymers (natural gelatin and synthetic PHF) is almost identical. Next, we adsorbed primary fetal mouse neural stem from their dispersion in serum-free media on the top of unfolded gelatin/PHF-Q bilayer at room temperature and allowed them to settle down for 10 min until a considerable amount was accumulated on the polymer surface. Similar to the previous observations, the increase of the temperature led to rolling of the bilayer and formation of tubes filled with cells (Figure 5).

Finally, we investigated the viability of the cells adsorbed on individual polymers as well as cells encapsulated in the tubes (Figure 6a,b). Polystyrene and fibronectine-coated surfaces were used as negative and positive control, respectively. It was found that cells on gelatin and PHF showed viability close to the positive control – fibronectin. The viability of the cells in the tubes was reduced, possibly due to confinement, but still remained above the values for the negative control. The most important

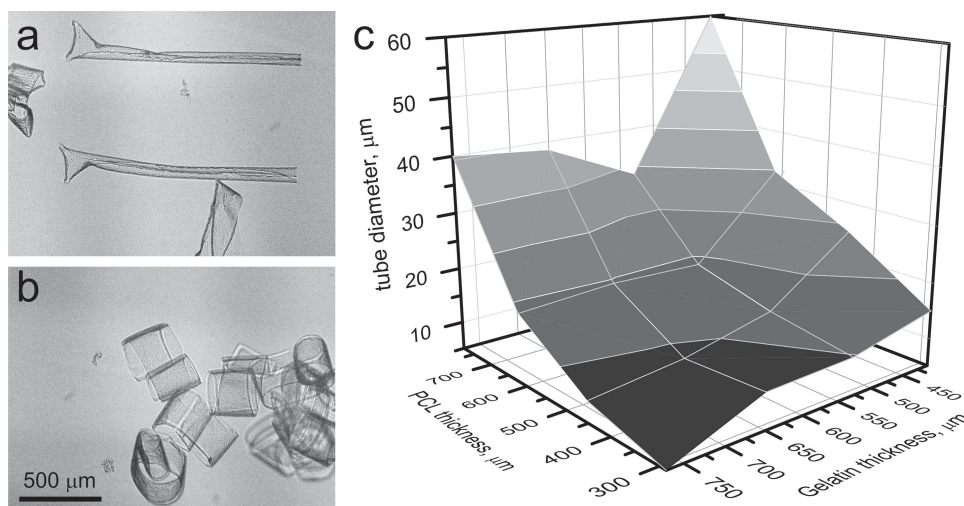


**Figure 4.** Optical microscopy images of tubes (a,b) obtained by folding of gelatin/PCL-Q; Dependence of tube diameter of gelatin/PCL-Q bilayers on the thickness of each layer (c).

aspect was, however, that cells in the tubes remained stable for at least 7 days thus implying that polymers are non-toxic and the tubular environment does not cause apoptosis of the cells.

### 3. Conclusions

In conclusion, we demonstrated two approaches for the design of fully biodegradable and biocompatible self-folding films with temperature-triggered folding. Both approaches are based on gelatin as active component, which can be either native or photocrosslinked. Depending on the properties of gelatin (either crosslinked or not) the films can either fold at room temperature and unfold at 37 °C or remain undeformed at room temperature and fold at 37 °C. Both these scenarios are useful for encapsulation and release of the cells as well as for

the design of bioscaffolds for tissue engineering. We demonstrated that neural stem cells can be encapsulated in rolled-up tubes during their formation and they remain alive for a considerable period of time.

### 4. Experimental Section

**Synthesis of Visible Light Crosslinkable Gelatin:** 1.25 g of gelatin (porcine skin, 300 Bloom) were dissolved in 125 mL of warm (~40 °C) water in 250 mL flask equipped with a magnetic stirrer. Then, 500 μL of furfuryl isocyanate were dissolved in 10 mL of DMSO and added dropwise to the gelatin solution. The reaction lasted 24 h under room temperature and constant stirring. In order to remove DMSO and unreacted furfuryl isocyanate, dialysis of the resulting mixture against distilled water was made. After dialysis, the solution of modified gelatin was reduced to the jelly-state via rotor evaporation. Obtained substance was dried in vacuum under 60 °C temperature for 24 h. 1 g of modified gelatin was

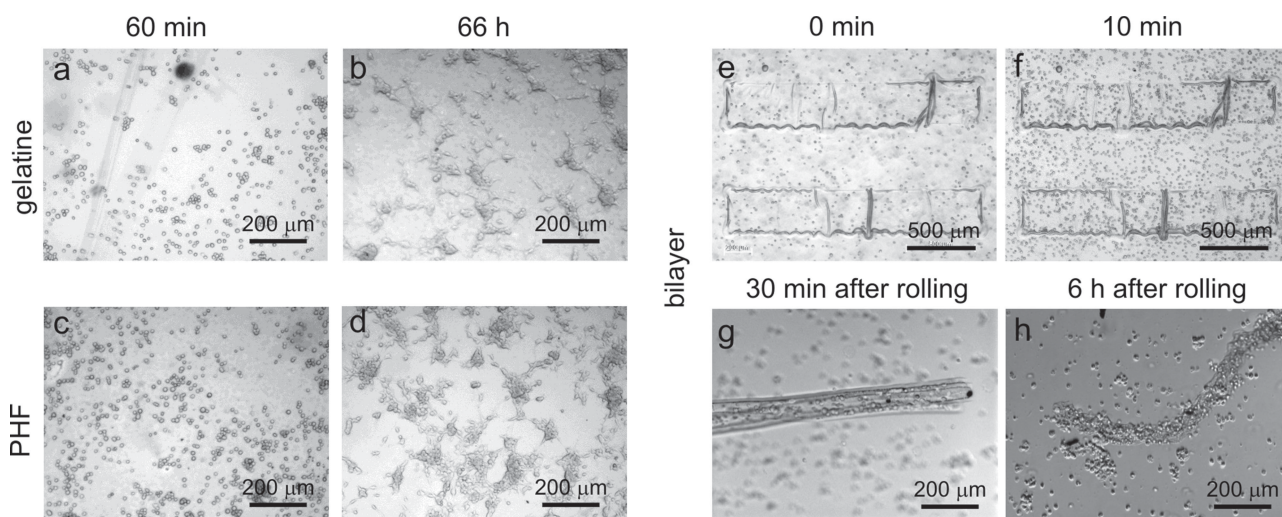


**Figure 5.** Encapsulation of neural stem cells using UV crosslinked gelatin/PHF-Q bilayer. (a,c) – cells on gelatin and PHF directly after seeding; (b,d) – cells on gelatin and PHF after 66 h of incubation. (e,f) – cells on gelatin/PHF-Q bilayer directly after seeding and after 10 min at room temperature (g,h) – cells in the gelatin/PHF-Q.

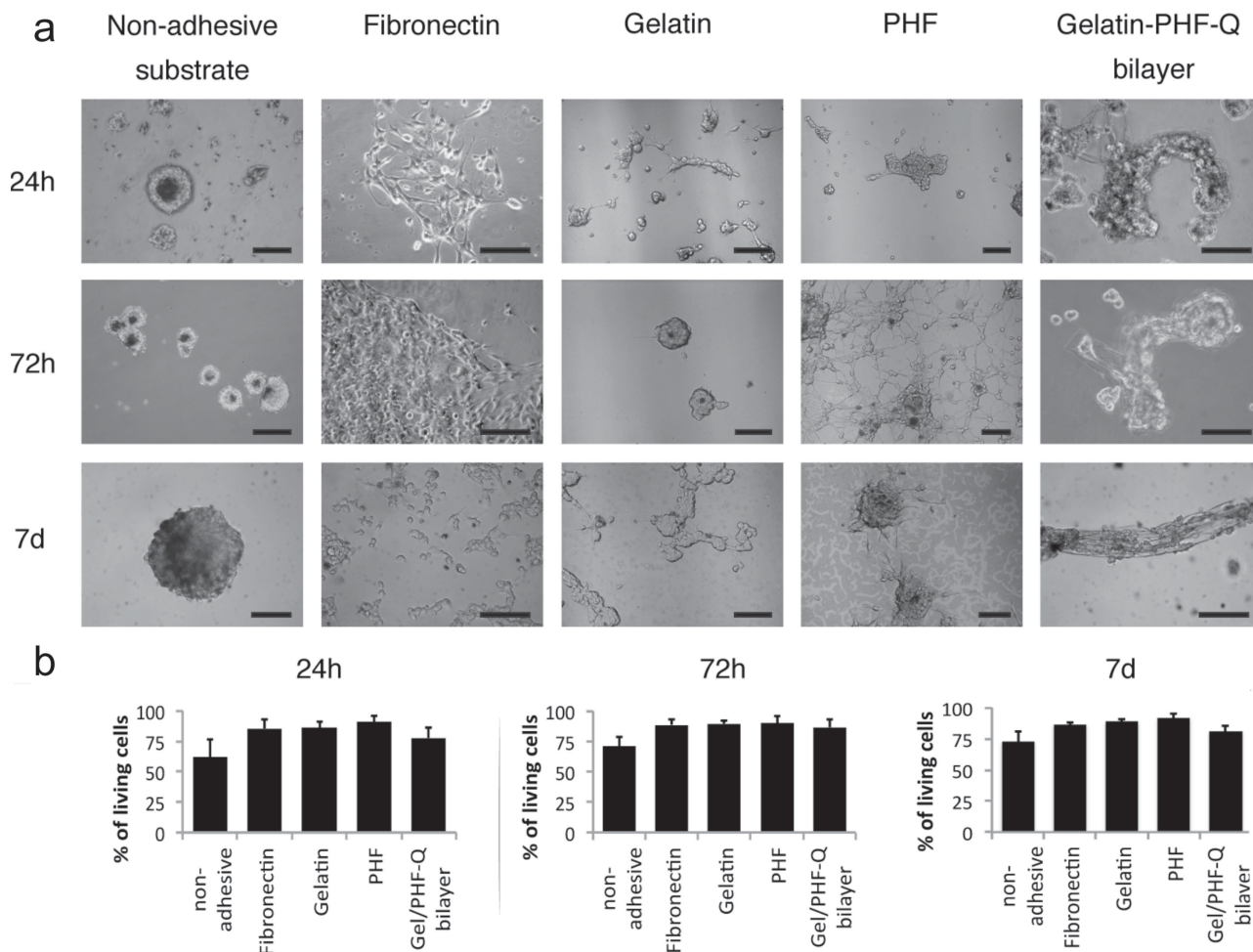


**Figure 6.** Viability of Neural Stem Cells (a) Microscopy images of Neural Stem Cells in gelatin/PHF-Q bilayer tubes, on gelatin, PHF, fibronectin functionalized substrate (positive control) and negative control (non-adhesive substrate). Trypan blue staining shows dead cells. Scale bar = 100  $\mu$ m; (b) Cell counts of trypan-blue stained Neural Stem Cell cultures demonstrate high biocompatibility of gelatin and PHF).

dissolved in 10 mL of warm water. Then, 50 mg of Rose Bengal were added to the gelatin solution. We also added 100 U/mL of penicillin and 100  $\mu$ g/mL of streptomycin to gelatin solution.

**Synthesis of Biodegradable Hydrophobic Visible Light Crosslinkable Polymer – PHF:** PHF were synthesized by the reaction of polycondensation between 1,6-hexanediol and fumaryl chloride. Before the reaction 1,6-hexanediol was dried in vacuum under 60  $^{\circ}$ C temperature for 24 h. Fumaryl chloride was distilled in vacuum in order to remove fumaric acid.

2.615 g of dried 1,6-hexanediol were dissolved in 20 mL of dehydrated THF in dry two-necked 50 mL flask equipped with a magnetic stirrer and CaCl<sub>2</sub> tube. Then 2.4 mL of distilled fumaryl chloride were dissolved in 5 mL of dehydrated THF and added dropwise to the solution of 1,6-hexanediol. After reagents were mixed, the temperature was raised up to 80  $^{\circ}$ C and all THF was evaporated from the mixture. The reaction lasted until the mixture became solid. Then 20 mL of CH<sub>2</sub>Cl<sub>2</sub> were added to dissolve it. The final polymer was obtained by precipitation in 1 L of petroleum ether. <sup>1</sup>H NMR (CDCl<sub>3</sub>, 500 MHz): 6.84 (s, 2H), 4.20 (s, 4H), 1.71 (s, 4H), 1.42 (s, 4H).

Solution of the polymer was prepared as follows: 350 mg of PHF were dissolved in 10 mL of CHCl<sub>3</sub>. Then 50  $\mu$ L of DMAEMA and 50 mg of Camphorquinone were added to the solution.

**Fabrication of Self-Rolled Tubes:** For the preparation of gelatin-based bilayers, polymers were sequentially deposited on a cleaned silicon

wafer substrates with a typical size of 11 mm  $\times$  25 mm using dip-coating. First, gelatin layer was deposited from its warm (37–40  $^{\circ}$ C) water solution. Passive polymer was then deposited from the selective solvent on the top of the first layer. In the case of crosslinkable systems, resulting bilayers were illuminated either with UV- or with VIS-light through a photomask. Then, uncrosslinked polymers were fully or partially developed using corresponding solvents. For non-crosslinkable gelatin-based system bilayer patterning was achieved by cutting.

**Neural Stem Cell Culture and Encapsulation:** Primary fetal mouse neural stem cells were a gift of A. Storch (University Clinic Carl Gustav Carus Dresden) Stem cell culture was done as described previously.<sup>[21]</sup> In short, neural stem cells were maintained in serum-free media comprising a DMEM (high glucose)/F-12 mixture (2:1), supplemented with 20 ng/mL of Egf and Fgf-2 (Sigma) and 2% B-27 supplement (Gibco/Invitrogen, Carlsbad, CA, USA).

**Cell Survival of Neural Stem Cells:** Trypan blue cell survival method is based on the principle that live (viable) cells do not take up trypan blue, whereas dead (non-viable) cells do. Neural stem cells were cultivated on a substrate functionalized with fibronectin as a positive control, non-adhesive substrate as a negative control, PHF, gelatin and in bilayer tubes. After 24 h, 72 h and 7 d medium was aspirated from cultures and replaced by phosphate buffered saline (pH 7.4). The same amount of 0.4% Trypan Blue solution (w/v) was added, and the sample

was allowed to stand for 5 to 15 min. Viable and non-viable cells were counted separately.

## Supporting Information

Supporting Information is available from the Wiley Online Library or from the author.

## Acknowledgements

Georgi Stoychev is acknowledged for SEM experiments. V.S., S.Z. and L.I. thank the DFG (IO68/1-1) for financial support. O.G.S. and A.M. acknowledge financial support by the Volkswagen Foundation (contract no. 86 362).

Received: January 17, 2014

Revised: February 17, 2014

Published online: April 7, 2014

- 
- [1] a) J. S. Randhawa, K. E. Laflin, N. Seelam, D. H. Gracias, *Adv. Funct. Mater.* **2011**, *21*, 2395; b) L. Ionov, *Soft Matter* **2011**, *7*, 6786.
- [2] S. Zakharchenko, N. Pureskiy, G. Stoychev, M. Stamm, L. Ionov, *Soft Matter* **2010**, *6*, 2633.
- [3] a) H. Thérien-Aubin, Z. L. Wu, Z. Nie, E. Kumacheva, *J. Am. Chem. Soc.* **2013**, *135*(12), 4834; b) J. Kim, J. A. Hanna, M. Byun, C. D. Santangelo, R. C. Hayward, *Science* **2012**, *335*, 1201.
- [4] a) X. Y. Guo, H. Li, B. Y. Ahn, E. B. Duoss, K. J. Hsia, J. A. Lewis, R. G. Nuzzo, *Proc. Natl. Acad. Sci. U.S.A.* **2009**, *106*, 20149; b) J. Deng, H. Ji, C. Yan, J. Zhang, W. Si, S. Baunack, S. Oswald, Y. Mei, O. G. Schmidt, *Angew. Chem. Int. Ed.* **2013**, *52*, 2326.
- [5] S. Zakharchenko, N. Pureskiy, G. Stoychev, C. Waurisch, S. G. Hickey, A. Eychmuller, J.-U. Sommer, L. Ionov, *J. Mater. Chem. B* **2013**, *1*, 1786.
- [6] Y. Mei, D. J. Thurmer, C. Deneke, S. Kiravittaya, Y.-F. Chen, A. Dadgar, F. Bertram, B. Bastek, A. Krost, J. r. Christen, T. Reindl, M. Stoffel, E. Coric, O. G. Schmidt, *ACS Nano* **2009**, *3*, 1663.
- [7] E. J. Smith, S. Schulze, S. Kiravittaya, Y. Mei, S. Sanchez, O. G. Schmidt, *Nano Lett.* **2010**, *11*, 4037.
- [8] a) G. S. Huang, Y. F. Mei, D. J. Thurmer, E. Coric, O. G. Schmidt, *Lab Chip* **2009**, *9*, 263; b) S. Schulze, G. Huang, M. Krause, D. Aubyn, V. A. B. Quiñones, C. K. Schmidt, Y. Mei, O. G. Schmidt, *Adv. Eng. Mater.* **2010**, *12*, B558.
- [9] a) A. A. Solovev, W. Xi, D. H. Gracias, S. M. Harazim, C. Deneke, S. Sanchez, O. G. Schmidt, *ACS Nano* **2012**, *6*, 1751; b) W. Xi, A. A. Solovev, A. N. Ananth, D. H. Gracias, S. Sanchez, O. G. Schmidt, *Nanoscale* **2013**, *5*, 1294.
- [10] a) E. Gultepe, J. S. Randhawa, S. Kadam, S. Yamanaka, F. M. Selaru, E. J. Shin, A. N. Kalloo, D. H. Gracias, *Adv. Mater.* **2012**, *25*, 514; b) C. L. Randall, Y. V. Kalinin, M. Jamal, A. Shah, D. H. Gracias, *Nanomed.-Nanotechnol.* **2011**, *7*, 686.
- [11] a) M. Jamal, S. S. Kadam, R. Xiao, F. Jivan, T.-M. Onn, R. Fernandes, T. D. Nguyen, D. H. Gracias, *Adv. Healthcare Mater.* **2013**, *2*, 1142; b) M. Jamal, N. Bassik, J. H. Cho, C. L. Randall, D. H. Gracias, *Biomaterials* **2010**, *31*, 1683.
- [12] S. Zakharchenko, E. Sperling, L. Ionov, *Biomacromolecules* **2011**, *12*, 2211.
- [13] G. Stoychev, N. Pureskiy, L. Ionov, *Soft Matter* **2011**, *7*, 3277.
- [14] E. H. Schacht, *J. Phys: Conference Series* **2004**, *3*, 22.
- [15] a) X. Wu, Y. Liu, X. Li, P. Wen, Y. Zhang, Y. Long, X. Wang, Y. Guo, F. Xing, J. Gao, *Acta Biomater.* **2010**, *6*, 1167; b) S. Young, M. Wong, Y. Tabata, A. G. Mikos, *J. Control. Release* **2005**, *109*, 256.
- [16] a) C. Chiari, U. Koller, R. Dorotka, C. Eder, R. Plasenzotti, S. Lang, L. Ambrosio, E. Tognana, E. Kon, D. Salter, S. Nehrer, *Osteoarthritis Cartilage* **2006**, *14*, 1056; b) J. M. Williams, A. Adewunmi, R. M. Schek, C. L. Flanagan, P. H. Krebsbach, S. E. Feinberg, S. J. Hollister, S. Das, *Biomaterials* **2005**, *26*, 4817.
- [17] M. A. Rice, J. Sanchez-Adams, K. S. Anseth, *Biomacromolecules* **2006**, *7*, 1968.
- [18] S. Wang, L. Lu, M. J. Yaszemski, *Biomacromolecules* **2006**, *7*, 1976.
- [19] T. I. Son, M. Sakuragi, S. Takahashi, S. Obuse, J. Kang, M. Fujishiro, H. Matsushita, J. Gong, S. Shimizu, Y. Tajima, Y. Yoshida, K. Suzuki, T. Yamamoto, M. Nakamura, Y. Ito, *Acta Biomater.* **2010**, *6*, 4005.
- [20] S. Timoshenko, *J. Opt. Soc. Am. Rev. Sci. Instrum.* **1925**, *11*, 233.
- [21] A. K. Meyer, A. Jarosch, K. Schurig, I. Nuesslein, S. Kissenkoetter, A. Storch, *Brain Res.* **2012**, *1474*, 8.



## Manuscript 2

# Reversible thermosensitive biodegradable polymeric actuators based on confined crystallization

*Vladislav Stroganov, Mahmoud Al-Hussein, Jens-Uwe Sommer, Andreas Janke, Svetlana  
Zakharchenko, and Leonid Ionov*

Nano Letters

First published: 4 February 2015

**DOI:** 10.1021/nl5045023

## Statement of Authors contribution

My personal contribution to that work included:

- Design and production of self-folding bilayers;
- Conduction of experiments with self-folding films. Evaluation of their characteristics such as layer thicknesses, tube diameters and folding conditions;
- Participation in X-ray scattering experiments;
- Participation in AFM imaging;
- Participation in writing of the final manuscript.

Degree of my personal contribution to the work is 50%.

Mahmoud Al-Hussein conducted X-ray scattering experiments and evaluated the obtained results.

Jens-Uwe Sommer provided facilities and equipment for X-ray scattering experiments as well as shared his knowledge and experience.

Andreas Janke and measured mechanical moduli of polycaprolactone at different conditions.

Svetlana Zakharchenko conducted AFM imaging of thin polycaprolactone films.

Leonid Ionov provided supervision, shared his ideas and experience during the whole research process. He wrote the main part of the manuscript.

## Reversible Thermosensitive Biodegradable Polymeric Actuators Based on Confined Crystallization

Vladislav Stroganov,<sup>†,‡</sup> Mahmoud Al-Hussein,<sup>§</sup> Jens-Uwe Sommer,<sup>†,‡</sup> Andreas Janke,<sup>†</sup> Svetlana Zakharchenko,<sup>†,‡</sup> and Leonid Ionov<sup>\*,†</sup>

<sup>†</sup>Leibniz-Institut für Polymerforschung Dresden e.V., Hohe Strasse 6, 01069 Dresden, Germany

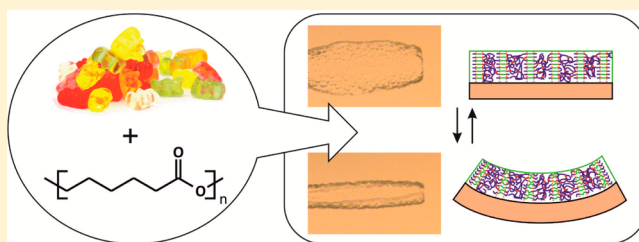
<sup>‡</sup>Technische Universität Dresden, 01062 Dresden, Germany

<sup>§</sup>Department of Physics, The University of Jordan, Amman 11942, Jordan

### S Supporting Information

**ABSTRACT:** We discovered a new and unexpected effect of reversible actuation of ultrathin semicrystalline polymer films. The principle was demonstrated on the example of thin polycaprolactone-gelatin bilayer films. These films are unfolded at room temperature, fold at temperature above polycaprolactone melting point, and unfold again at room temperature. The actuation is based on reversible switching of the structure of the hydrophobic polymer (polycaprolactone) upon melting and crystallization. We hypothesize that the origin of this unexpected behavior is the orientation of polycaprolactone chains parallel to the surface of the film, which is retained even after melting and crystallization of the polymer or the “crystallization memory effect”. In this way, the crystallization generates a directed force, which causes bending of the film. We used this effect for the design of new generation of fully biodegradable thermoresponsive polymeric actuators, which are highly desirable for bionano-technological applications such as reversible encapsulation of cells and design of swimmers.

**KEYWORDS:** Reversible actuators, thermoresponsive, polycaprolactone, confined crystallization, stimuli-responsive



Polymer actuators are materials capable of changing their shape in response to variation of environmental conditions, thus performing mechanical work. There are many kinds of polymer actuators such as liquid crystals, where actuation is achieved by cooperative reorganization of mesogen groups,<sup>1</sup> hydrogels based on reversible swelling,<sup>2</sup> shape memory polymers based on temperature-induced relaxation,<sup>3</sup> as well as actuators where the driving force is surface tension.<sup>4</sup> Polymer actuators have been used for many applications such as controlling the liquid flow in microfluidical devices actuators,<sup>5–9</sup> designing of swimmers,<sup>10,11</sup> walkers,<sup>12</sup> sensors,<sup>13,14</sup> imaging devices,<sup>15,16</sup> and 3D microfabrication.<sup>17</sup> One of the promising fields of applications of polymeric actuators is the design of biomaterials such as stents,<sup>18</sup> sutures,<sup>19</sup> as well as bioscaffolds.<sup>20–22</sup> For such kind of applications, polymeric actuators must be both biocompatible and biodegradable. Moreover, the set of stimuli, which can be used in living systems, is substantially limited. While UV light harms the cells and can cause DNA damage, changes in pH in a broad range is also not possible. Nonetheless, the cells can survive in a broad temperature range between 4 and 37 °C and therefore the temperature can be used as a signal to trigger actuation.

Examples of biocompatible/biodegradable thermoresponsive polymers with LCST behavior, which can be used for the design of actuators, have been reported in the literature.<sup>23</sup> However, these polymers are sensitive to pH and ionic strength

that strongly affect their switching temperatures. Other examples of temperature-sensitive biodegradable shape memory polymers, which undergo one way transition only have been also demonstrated.<sup>24</sup> In contrast, very recently Lendlein reported macroscopic shape memory polymers with reversible actuation.<sup>25,26</sup> They are based on two cross-linked crystalline polymers with different melting points. The polymer is deformed at a temperature above the melting points of both polymers and then cooled down to room temperature. During cooling, the polymer with the higher melting point crystallizes first and forms a framework/scaffold, which restricts the mobility of the second polymer chains. Heating above the melting point of the polymer with the lower melting point results in partial relaxation of shape of the polymer. Cooling down leads to the recrystallization of this polymer, which is guided by the framework of the first polymer that recovers the deformed shape.

In this paper we report biodegradable thermoresponsive polymeric films with reversible actuation based on polycaprolactone-gelatin bilayers. In a previous work, we demonstrated that this system can be used for one-way folding or one-way folding and unfolding.<sup>27</sup> The actuation was based on switching

**Received:** November 24, 2014

**Revised:** January 26, 2015

**Published:** February 4, 2015

of the swelling properties of the gelatin layer. Gelatin swelled in water and caused bending of the bilayer. In contrast, the reversible actuator we demonstrate here is based on switching of the properties of the hydrophobic polymer (PCL) that is guided by confined crystallization of the polymer chains in thin films.

**Results and Discussions.** We fabricated gelatin-PCL films by sequential dip coating of pure gelatin and PCL containing 4-hydroxybenzophenone. The thickness of gelatin and PCL layers were 1.6  $\mu\text{m}$  and 500 nm, respectively. The film was irradiated by UV light (254 nm) through a photomask to cross-link the polymers. The film was rinsed in organic solvent in order to remove non-cross-linked PCL. The obtained film was exposed to water (Figure 1a). Similar to the previously described

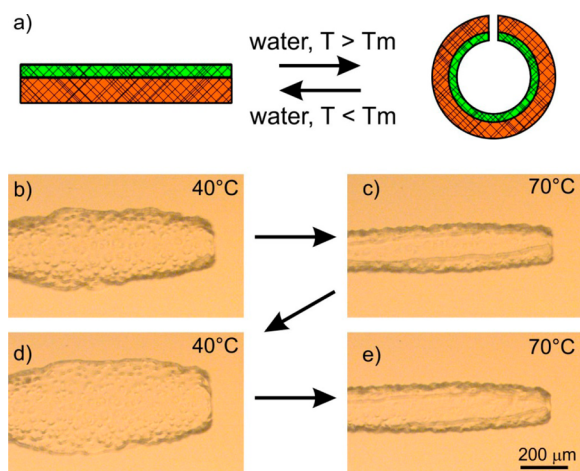


**Figure 1.** Thermoresponsive actuation of thin gelatin-PCL films (see Video\_S1\_actuation, Supporting Information); (a) scheme of actuation of (red is gelatin, green is PCL); (b–e) microscopy snapshots of gelatin-PCL bilayer at different temperatures.

approach<sup>27</sup> both cross-linked and non-cross-linked gelatin swelled in water. Increase of the temperature led to the dissolution of non-cross-linked gelatin at  $\sim 40$  °C. On the other hand, contrary to the experiments described in our previous paper, dissolution of gelatin did not result in folding of the bilayer film and it remained undeformed at 40 °C (Figure 1b). However, further heating above 60 °C led to the rolling of the films and the formation of tubes (Figure 1c). Subsequent cooling to room temperature led to the recovery of the initial shape (unfolding, Figure 1d). The folding and unfolding was exhibited by the same bilayer film many times upon successive heating–cooling cycles indicating the reversibility of the actuation process (Figure 1e).

In order to explain the observed folding/unfolding, we investigated the responsive properties of the gelatin and PCL layers. Cross-linked gelatin films were swollen up to 1000–1200 vol % in water. The swelling degree was found to be independent of temperature within a range of 20–80 °C. Moreover, repetitive cooling and heating did not influence the swelling degree. The PCL layer demonstrated on the other hand responsive properties. Heating resulted in a volume expansion and a substantial decrease in the elastic modulus. We found that the volume of the PCL layer increased by  $\sim 10\%$  upon heating to 65 °C. The change of the elastic modulus was more considerable ( $E_{\text{PCL},23\text{ }^\circ\text{C}} = 524 \pm 78$  MPa,  $E_{\text{PCL},65\text{ }^\circ\text{C}} = 0.617 \pm 0.032$  MPa). Cooling down to room temperature led

to the recovery of the initial volume and elastic modulus. Therefore, we conclude that heating the bilayer film in the range 20–80 °C results in switching the properties of the PCL layer solely, whereas the gelatin layer remains swollen in the entire temperature range.

We modeled the radius of curvature of the folded bilayer in the states when the PCL layer is hard (low temperatures) and when it is soft (high temperatures) using Timoshenko equation (for details see Supporting Information).<sup>28</sup> The results of the modeling are shown in Figure 2. As can be seen, increasing the

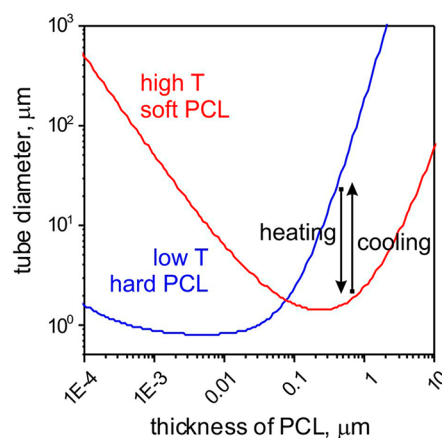


**Figure 2.** Estimated dependence of diameter of gelatin-PCL tubes on thickness of PCL layer obtained using Timoshenko eq 1; see Supporting Information.

thickness of the PCL layer leads first to a decrease in the radius of curvature. It then reaches a certain minimum value and further increase of the thickness of the PCL layer leads to an increase in the radius of curvature. The position of the curve minimum depends on the elastic modulus of the PCL layer. Decreasing  $E_{\text{PCL}}$  leads to a shift in the position of the curve minimum to higher values of the thickness of the PCL layer. The left region of the curve corresponds to very thin films. Such bilayer must roll and form tubes at low temperatures. In our experiments, the thickness of the PCL layer is  $\sim 500$  nm, which corresponds to the minimum on the red curve (soft PCL, Figure 2) and upward slope in blue curve (hard PCL). The values predicted by Timoshenko equation appear to be lower in comparison with the experimentally observed diameter of the tube, although it is able to qualitatively explain why the bilayer is undeformed at room temperature and folds when the PCL layer becomes soft at temperatures  $>60$  °C. Indeed, contrary to previous experiments,<sup>27</sup> we used thicker PCL layer, which is stiffer and does not allow rolling of the bilayer at room temperature even if the gelatin is swollen.

To elucidate the origin of the unfolding, which occurs upon cooling, we performed a set of experiments. In the first experiment, we found that folded gelatin-PCL bilayers with non-cross-linked PCL folded upon heating but were unable to unfold during subsequent cooling. In the second experiment, the same behavior was found for tubes with 5  $\mu\text{m}$  thick cross-linked PCL layer. They folded upon heating but no unfolding was observed upon cooling. Apparently, in the first case we observe a plastic (irreversible) deformation of the PCL chains that is intrinsic to non-cross-linked polymers. These experiments show that cross-linking and the thickness of the PCL

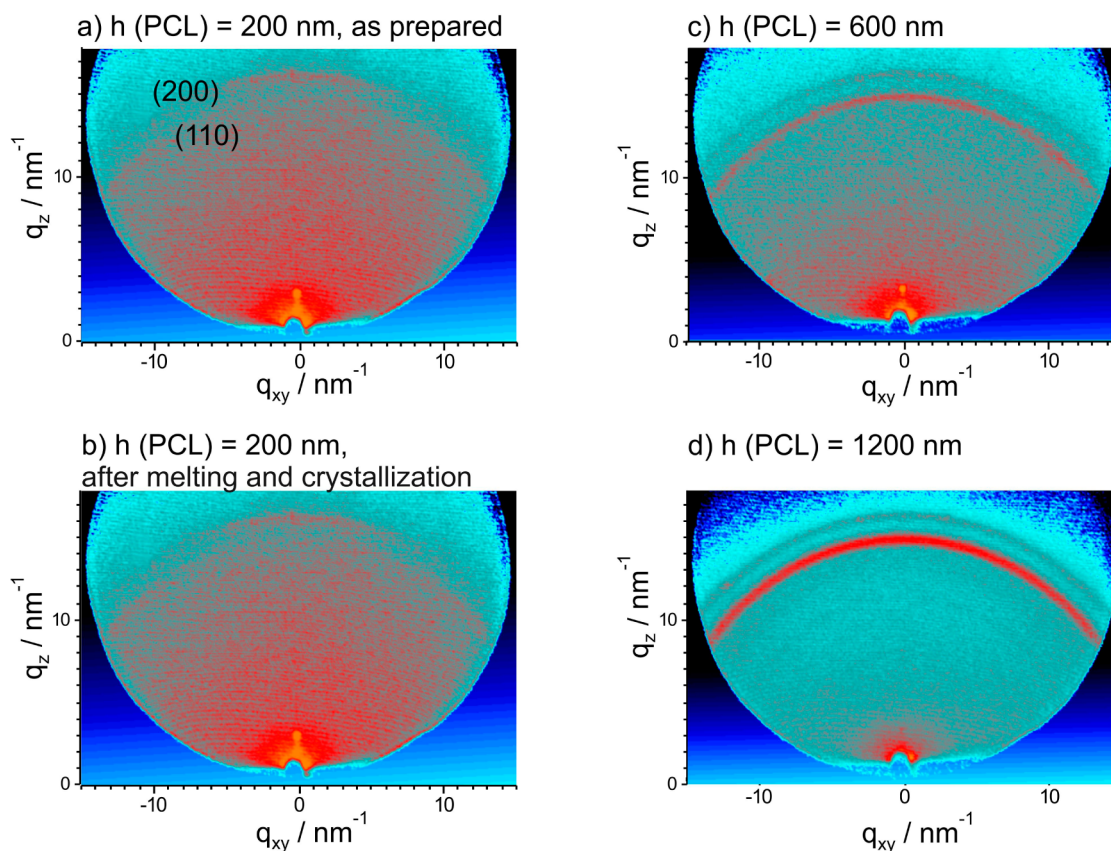


**Figure 3.** Two-dimensional grazing incidence X-ray scattering patterns of PCL films deposited on gelatin on silicon substrates of thicknesses: (a) 200 nm before melting and (b) after melting and recrystallization of the film of (a); (c) 600 nm, (d) 1200 nm.

layer play a crucial role in attaining reversible folding/unfolding bilayer films.

In order to determine the effect of the thickness of the PCL layer we investigated the morphology and structure of 200 nm, 500 nm, and 5  $\mu\text{m}$  thick PCL layers. All films exhibit spherulites typical of semicrystalline polymers. The size of the spherulites depends on thickness of the PCL layer (Supporting Information Figure S1). Smaller spherulites are observed in the case of 5  $\mu\text{m}$  thick PCL film and very large spherulites are observed in the case of the very thin films because of reduction of number of primary nucleation sites.

The crystalline structure of the PCL films with different thicknesses was investigated using GIWAXS (scattering geometry of the experiment is illustrated in Supporting Information Figure S2). We found that all PCL films are semicrystalline as evidenced by the typical (110) and (200) reflections of the PCL crystals. It is known that PCL crystallizes in an orthorhombic structure with unit cell dimensions:  $a = 7.496 \text{ \AA}$ ,  $b = 4.974 \text{ \AA}$ , and  $c = 17.297 \text{ \AA}$  (chain axis).<sup>29</sup> The films with different thicknesses have nearly the same degree of crystallinity  $\sim 40\%$  (Supporting Information Figure S3). Temperature-dependent GIWAXS measurements showed that the melting points of the thin films are 3–5° lower than the melting point of the thick film (see Supporting Information, Figure S4). This indicates a poorer crystalline organization in thin films. More importantly, detailed XRD investigation showed a preferential orientation of the chains in the crystalline regions of the PCL layer parallel to the surface in thin films and no preferred orientation in thick films (for details see Supporting Information). The preferential orientation of the

polymer chains is retained after melting of the film and its second crystallization (Figure 3b). In light of these results, we can conclude that the formation of the edge-on lamellae is significantly affected by the PCL film thickness.

In fact, the dependence of lamellae orientation on thin film thickness has already been observed for many semicrystalline polymers, including PCL.<sup>30–35</sup> However, in contrast to the edge-on orientation of our system for most of these polymers the lamellae were oriented flat-on to the substrate, that is, with the polymer chain axis perpendicular to the substrate. Upon decreasing the film thickness, the crystalline lamellae can have a preferential orientation relative to the substrate influenced by polymer–substrate (gelatin) interactions. In contrast, thicker polycrystalline films tend to have more overlapped crystalline domains leading to bulklike randomly distributed lamellae. We propose that the gelatin layer plays a role in determining the edge-on orientation. The defects on the gelatin layer surface (roughness, dust particle, scratches) serve as nucleation sites that initiate the growth of the crystalline lamellae. However, as the film thickness increases, the gelatin layer effect becomes limited only to adjacent layers of the PCL film and a bulklike behavior dominates in the rest of the film.

In light of these results, we can suggest the following scenario of reversible folding/unfolding of the gelatin-PCL bilayers. The PCL layer is partially crystalline with preferential orientation of chains parallel to the surface of the film (Figure 4a,b). This parallel orientation is caused by confinement effect—small thickness of the PCL film and the influence of the gelatin underlayer. The amorphous phase of the PCL layer is soft ( $T_g = -50 \text{ }^\circ\text{C}$ ) and cross-linked. In contrast, the crystalline phase is

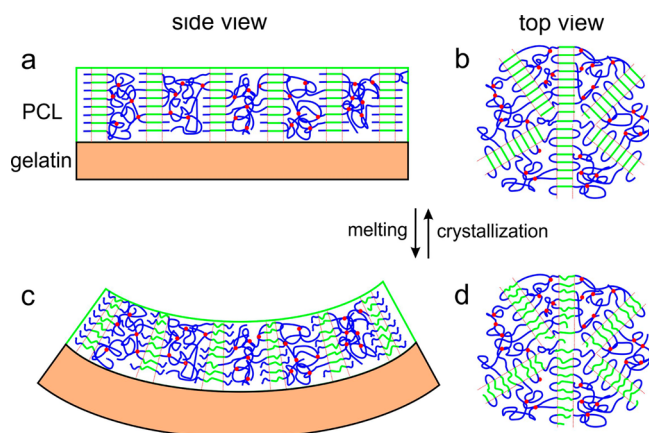


**Figure 4.** Scheme of reversible actuation of gelatin-PCL films. PCL film consists of amorphous part (blue chains) and crystalline part (green chains). Amorphous part is cross-links (cross-linking points are red). (a,b) Structure of the gelatin-PCL at low temperature (a, side view; b, top view); (c,d) structure of the gelatin-PCL at elevated temperature (c, side view; d, top view).

not cross-linked (cross-linking leads to amorphization of polymer because of the size of photoinitiator molecules) and hard ( $T_m = 55\text{--}60\text{ }^\circ\text{C}$ ). Swelling of the gelatin layer in water generates compressive stresses against the PCL layer. Apparently, the rigid crystalline regions of the PCL layer can withstand such compressive stresses and no bending is observed at room temperature. As demonstrated by the temperature-dependent GIWAXS measurements, heating above  $55\text{ }^\circ\text{C}$  leads to the melting of the crystalline phase of the PCL layer making it softer. Because of the substantial loss in the rigidity, the PCL layer can no longer resist the compressive stresses of the gelatin layer causing bending. Since the amorphous part is cross-linked the mobility of polymer chains is substantially restricted. We believe that part of the chains forming the crystalline phase maintain their locations and just undergo transition to disordered state upon melting (Figure 4c,d). Subsequent cooling to room temperature leads to crystallization of the same regions of PCL layer under confinement inducing the chains to assume a parallel orientation to the surface of the film again. The change in conformation of polymer chains generates counter stresses working against the compressive stresses of the gelatin layer. Apparently, recrystallization stresses outweigh the gelatin compressive stresses and the bilayer unfolds upon recrystallization. (Figure 4a,b).

It is worth noting that the mechanism of reversible deformation of PCL-gelatin actuators, which we observed, is different from the mechanisms of reversible deformation described by Lendlein, which involves hard scaffold formed by one of the two polymers.<sup>25,26</sup> In our case, there is no hard scaffold and the cross-linked amorphous phase of the PCL layer is in a soft rubbery state at room temperature ( $T_g = -50\text{ }^\circ\text{C}$ ). Only this soft part cannot influence the direction of crystallization or its preferential orientation. Therefore, we believe that confinement plays the role of such hard scaffold which guides crystallization. There are other reports of macroscopic two-way shape memory polymers.<sup>36,37</sup> In one approach,<sup>36</sup> the reversibility of actuation is achieved by incomplete melting of polymers. In fact, the part of polymer that is not molten plays a role of rigid scaffold. The part of polymer with low melting point melts and crystallizes during

temperature cycling that leads to change of volume. Irreversible deformation is observed when the polymer is completely melted. We observe reversible actuation even if we go well above melting point of PCL ( $T_m(\text{PCL}) = 60\text{ }^\circ\text{C}$ ), that is, we heat up to more than  $70\text{ }^\circ\text{C}$ . In another report,<sup>37</sup> the cross-linked samples were stretched in molten state to introduce anisotropy, which is required for directed crystallization of polymer chains. In our approach, the anisotropy is generated already during preparation of film by confined crystallization.

In order to estimate the force balance between bending driven by swelling and crystallization (i.e., to estimate if the energy of crystallization is sufficient to cause the deformation of the bilayer), we apply a mean-field approach to the gel-component (the details are given in Supporting Information). If we assume that the shape memory is caused by crystallization of otherwise geometrically blocked parts of the semicrystalline PCL-layer, we should compare the value for energy gain per unit volume ( $\sigma$ ) with the free energy gain per volume unit,  $h$ , obtained by crystallization. This can be considered as the tension due to crystallization if the film has the freedom to expand against bending to restore the original crystalline domains (Figure 4). Let us estimate the latter by the latent heat of crystallization which is given by  $H \cong 142\text{ J/g}$ . Given a degree of crystallinity of about 0.5 and the density given by  $\rho_{\text{PCL}} \cong 1.2\text{ g/cm}^3$ , we obtain  $h \cong 8 \times 10^7\text{ Pa}$ . From this we can conclude that

$$h \cong 100\sigma$$

In other words, energy gain from crystallization of PCL considerably exceeds the energy gain of swelling of gelatin.

Finally, we demonstrated some applications of the reversibly folding PCL-gelatin thin film. In the first example, we demonstrate a reversible encapsulation and release of bakery yeast cells (Video\_S2\_Cell\_encapsulation, Supporting Information). The cells were adsorbed on the polymer film at room temperature when it was unfolded (Figure 5a). Heating led to

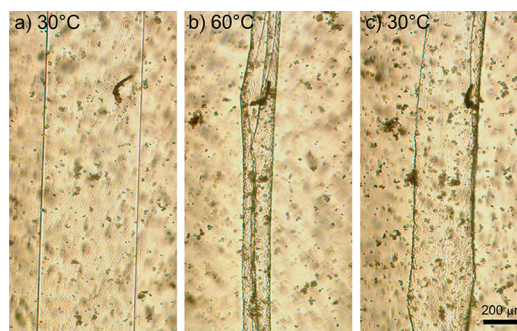


**Figure 5.** Reversible encapsulation and release of yeast cells inside PCL-gelatin tubes: (a) original state at  $30\text{ }^\circ\text{C}$ ; (b) rolled tube with cells at  $60\text{ }^\circ\text{C}$ ; (c) unrolled bilayer with cells at  $30\text{ }^\circ\text{C}$ .

rolling of the film and encapsulation of cells inside the tube (Figure 5b). Cooling down unfolded the tube that made the cells accessible (Figure 5c). We also observed that rolling causes movement of the films (Video\_S3\_actuation, Supporting Information) that can, for example, be used for the design of biodegradable microswimmers.

**Conclusions.** In this work, we demonstrated and investigated unusual reversible thermoactuation of thin cross-linked polycaprolactone-gelatin films. The films are unfolded at room temperature, fold at temperature above polycaprolactone

melting point, and unfold again at room temperature. We hypothesize that the origin of this unexpected behavior is the orientation of polycaprolactone chains parallel to the surface of the film, which is retained even after melting and crystallization of the polymer. We also demonstrated potential application of such reversible biodegradable thermosensitive actuators for encapsulation of cells. The material that we demonstrated actuates around the melting temperature of polycaprolactone (55–60 °C). We foresee that this temperature can readily be reduced to body temperature, which is more appropriate for experiments with cells, by proper choice of hydrophobic polymer and its composition. We foresee a great potential of the developed approach for cell encapsulation and release, design of scaffolds, and externally controlled microswimmers.

## ■ ASSOCIATED CONTENT

### Supporting Information

Experimental details, details of modeling of bending radius, morphology of PCL films, details of XRD analysis, detailed expiation of mean-field approach as well as videos of actuation of gelatin-PCL films. This material is available free of charge via the Internet at <http://pubs.acs.org>.

## ■ AUTHOR INFORMATION

### Corresponding Author

\*E-mail: [ionov@ipfdd.de](mailto:ionov@ipfdd.de).

### Funding

DFG IO68/1–3. M.A.H. thanks The University of Jordan and Leibniz-Institut für Polymerforschung, Dresden (IPF) for financial support.

### Notes

The authors declare no competing financial interest.

## ■ REFERENCES

- (1) Ohm, C.; Brehmer, M.; Zentel, R. *Adv. Mater.* **2010**, *22*, 3366–3387.
- (2) Ionov, L. *Adv. Funct. Mater.* **2013**, *23*, 4555–4570.
- (3) Behl, M.; Razzaq, M. Y.; Lendlein, A. *Adv. Mater.* **2010**, *22*, 3388–3410.
- (4) Azam, A.; Laffin, K. E.; Jamal, M.; Fernandes, R.; Gracias, D. H. *Biomed. Microdevices* **2011**, *13*, 51–58.
- (5) Yu, Q.; Bauer, J. M.; Moore, J. S.; Beebe, D. J. *Appl. Phys. Lett.* **2001**, *78*, 2589–2591.
- (6) Arndt, K.-F.; Kuckling, D.; Richter, A. *Polym. Adv. Technol.* **2000**, *11*, 496–505.
- (7) Dong, L.; Jiang, H. *Soft Matter* **2007**, *3*, 1223–1230.
- (8) Beebe, D. J.; Moore, J. S.; Yu, Q.; Liu, R. H.; Kraft, M. L.; Jo, B.-H.; Devadoss, C. *Proc. Natl. Acad. Sci. U.S.A.* **2000**, *97*, 13488–13493.
- (9) Eddington, D. T.; Beebe, D. J. *Adv. Drug Delivery Rev.* **2004**, *56*, 199–210.
- (10) Kwon, G. H.; Park, J. Y.; Kim, J. Y.; Frisk, M. L.; Beebe, D. J.; Lee, S. H. *Small* **2008**, *4*, 2148–2153.
- (11) Magdanz, V.; Stoychev, G.; Ionov, L.; Sanchez, S.; Schmidt, O. *Angew. Chem., Int. Ed.* **2014**, *126*, 2711–2715.
- (12) Osada, Y.; Okuzaki, H.; Hori, H. *Nature* **1992**, *355*, 242–244.
- (13) Bashir, R.; Hilt, J. Z.; Elibol, O.; Gupta, A.; Peppas, N. A. *Appl. Phys. Lett.* **2002**, *81*, 3091–3093.
- (14) Hilt, J. Z.; Gupta, A. K.; Bashir, R.; Peppas, N. A. *Biomed. Microdevices* **2003**, *5*, 177–184.
- (15) Dong, L.; Agarwal, A. K.; Beebe, D. J.; Jiang, H. *Nature* **2006**, *442*, 551.
- (16) Richter, A.; Paschew, G. *Adv. Mater.* **2009**, *21*, 979–983.
- (17) Ionov, L. *Soft Matter* **2011**, *7*, 6786–6791.
- (18) Yakacki, C. M.; Shandas, R.; Lanning, C.; Rech, B.; Eckstein, A.; Gall, K. *Biomaterials* **2007**, *28*, 2255–2263.
- (19) Lendlein, A.; Langer, R. *Science* **2002**, *296*, 1673–1676.
- (20) Zakharchenko, S.; Pureskiy, N.; Stoychev, G.; Waurisch, C.; Hickey, S. G.; Eychmuller, A.; Sommer, J.-U.; Ionov, L. *J. Mater. Chem. B* **2013**, *1*, 1786–1793.
- (21) Zakharchenko, S.; Sperling, E.; Ionov, L. *Biomacromolecules* **2011**, *12*, 2211–2215.
- (22) Jamal, M.; Kadam, S. S.; Xiao, R.; Jivan, F.; Onn, T.-M.; Fernandes, R.; Nguyen, T. D.; Gracias, D. H. *Adv. Healthcare Mater.* **2013**, *2*, 1142–1150.
- (23) Seuring, J.; Agarwal, S. *ACS Macro Lett.* **2013**, *2*, 597–600.
- (24) Lendlein, A.; Schmidt, A. M.; Langer, R. *Proc. Natl. Acad. Sci. U.S.A.* **2001**, *98*, 842–847.
- (25) Behl, M.; Kratz, K.; Zotzmann, J.; Nochel, U.; Lendlein, A. *Adv. Mater.* **2013**, *25*, 4466–9.
- (26) Behl, M.; Kratz, K.; Nochel, U.; Sauter, T.; Lendlein, A. *Proc. Natl. Acad. Sci. U.S.A.* **2013**, *110*, 12555–12559.
- (27) Stroganov, V.; Zakharchenko, S.; Sperling, E.; Meyer, A. K.; Schmidt, O. G.; Ionov, L. *Adv. Funct. Mater.* **2014**, *24*, 4357–4363.
- (28) Timoshenko, S. *J. Opt. Soc. Am.* **1925**, *11*, 233–255.
- (29) Bittiger, H.; Marchessault, R. H.; Niegisch, W. D. *Acta Crystallogr., Sect. B: Struct. Crystallogr. Cryst. Chem.* **1970**, *26*, 1923–1927.
- (30) Taguchi, K.; Miyaji, H.; Izumi, K.; Hoshino, A.; Miyamoto, Y.; Kokawa, R. *Polymer* **2001**, *42*, 7443–7447.
- (31) Grozev, N.; Botiz, I.; Reiter, G. *Eur. Phys. J. E* **2008**, *27*, 63–71.
- (32) Reiter, G.; Sommer, J.-U. *J. Chem. Phys.* **2000**, *112*, 4376–4383.
- (33) Zhou, W.; Cheng, S. Z. D.; Putthananat, S.; Eby, R. K.; Reneker, D. H.; Lotz, B.; Magonov, S.; Hsieh, E. T.; Geerts, R. G.; Palackal, S. J.; Hawley, G. R.; Welch, M. B. *Macromolecules* **2000**, *33*, 6861–6868.
- (34) Taguchi, K.; Miyamoto, Y.; Miyaji, H.; Izumi, K. *Macromolecules* **2003**, *36*, 5208–5213.
- (35) Sutton, S. J.; Izumi, K.; Miyaji, H.; Miyamoto, Y.; Miyashita, S. *J. Mater. Sci.* **1997**, *32*, 5621–5627.
- (36) Zhou, J.; Turner, S. A.; Brosnan, S. M.; Li, Q.; Carrillo, J.-M. Y.; Nykypanchuk, D.; Gang, O.; Ashby, V. S.; Dobrynin, A. V.; Sheiko, S. S. *Macromolecules* **2014**, *47*, 1768–1776.
- (37) Chung, T.; Romo-Uribe, A.; Mather, P. T. *Macromolecules* **2007**, *41*, 184–192.

# Supporting Information

## Reversible thermosensitive biodegradable polymeric actuators based on confined crystallization

*Vladislav Stroganov<sup>1,2</sup>, Mahmoud Al-Hussein<sup>3</sup>, Jens-Uwe Sommer<sup>1,2</sup>, Andreas Janke<sup>1</sup>,  
Svetlana Zakharchenko<sup>1,2</sup>, and Leonid Ionov<sup>1\*</sup>*

<sup>1</sup>Leibniz-Institut für Polymerforschung Dresden e.V., Hohe Str. 6, 01069 Dresden, Germany

<sup>2</sup>Technische Universität Dresden, 01062 Dresden, Germany

<sup>3</sup>Department of Physics, The University of Jordan, Amman 11942, Jordan

AUTHOR INFORMATION

**Corresponding Author**

\* Leonid Ionov, [ionov@ipfdd.de](mailto:ionov@ipfdd.de)

## Experimental Section.

Preparation of samples. For the preparation of gelatin-polycaprolactone bilayers, polymers were sequentially deposited on a cleaned silicon wafer substrates with a typical size of 11 mm x 25 mm using dip-coating. First, gelatin layer was deposited from its warm (37-40 °C) water solution. Polycaprolactone (PCL) with 4-hydroxybenzophenone (2.5 mass % with respect to mass of PCL) was then deposited from the toluene solution on the top of the gelatin layer by dipcoating. The bilayer was irradiated by UV light (254 nm) through the photomask. Finally, the uncrosslinked PCL was removed by rinsing in toluene. Non-crosslinked gelatin was dissolved during folding experiments.

Null-ellipsometry. The thickness of the polymer layers on the smooth substrates in the dry state was measured at  $\lambda=632.8$  nm and an angle of incidence of  $70^\circ$  with a null-ellipsometer (Multiscope, Optrel Berlin, Germany) in a polarizer-compensator-sample-analyzer configuration.

AFM. For topography images the Dimension V AFM (Veeco Instruments, Inc., USA) was used. The measurements were made in Tapping Mode both in dry and aqueous media (with a Fluid Tip Holder) with silicon tip Tap300 (BudgetSensors, Bulgaria; resonant frequency 200-400kHz)

XRD. Grazing incidence wide-angle X-ray measurements (GIWAXS) were performed using a Bruker D8 Discover diffractometer operating at 1.6 kW. The diffractometer is equipped with a Cu Twist tube, Ni filter ( $\lambda = 1.5418$  Å), point focusing PolyCap™ system for parallel beam generation, and 0.3 mm PinHole collimator for the incident beam. The sample was mounted on an Eulerian Cradle with automatic controlled X–Y–Z stage. An Anton Parr DCS350 heating stage (with accuracy 0.1 °C) equipped with a graphite dome was used as a temperature-controlled sample stage. The GIWAXS patterns were recorded with a VÅNTEC-

500 area detector using a sample-to-detector distance of 165 mm and an incident angle of 1.5°. To extract quantitative information, the intensity is integrated over arc slices taken from the 2D GIWAXS pattern using Bruker LEPTOS software.

Further texture examination was done by recording diffraction curves in both grazing and specular geometries using a 2-circle diffractometer (XRD 3003 T-T, Seifert-FPM) and a point detector. By employing a parabolic multilayer mirror, a highly parallel beam of a monochromatic Cu-K $\alpha$  radiation ( $\lambda = 1.5418 \text{ \AA}$ ) was obtained. For grazing incidence geometry, the incident angle was 4°.

### Modeling of folding behavior.

We modelled the radius of curvature of the folded bilayer in the states when the PCL layer is hard (low temperatures) and when it is soft (high temperatures) using Timoshenko equation<sup>1</sup> (equation 1).

$$\frac{1}{\rho} = \frac{6(\varepsilon_{gelatin} - \varepsilon_{PCL})(1+m)^2}{h \left( 3(1+m)^2 + (1+mn) \left( m^2 + \frac{1}{mn} \right) \right)} \quad (1)$$

$$\frac{E_{PCL}}{E_{gelatine}} = n \quad (2)$$

$$\frac{a_{PCL}}{a_{gelatin}} = m \quad (3)$$

where E is the elasticity modulus,  $\alpha$  is the layer thickness, h is the total thickness ( $h = \alpha_{PCL} + \alpha_{gelatin}$ ),  $\rho$  is the radius of curvature, and  $\varepsilon$  is the strain. For simplicity, we kept the thickness of the gelatin layer constant and varied the thickness of the PCL layer. The elastic moduli and strains of both layers were found to be:  $E_{PCL} = 524 \pm 78$  MPa at 23°C,  $E_{PCL} = 0,617 \pm 0,032$  MPa at 65°C,  $E_{gelatin} = 100$  kPa,  $\varepsilon_{PCL} = 1$ ,  $\varepsilon_{gelatin} = 2.2$ .

## Morphology of PCL films

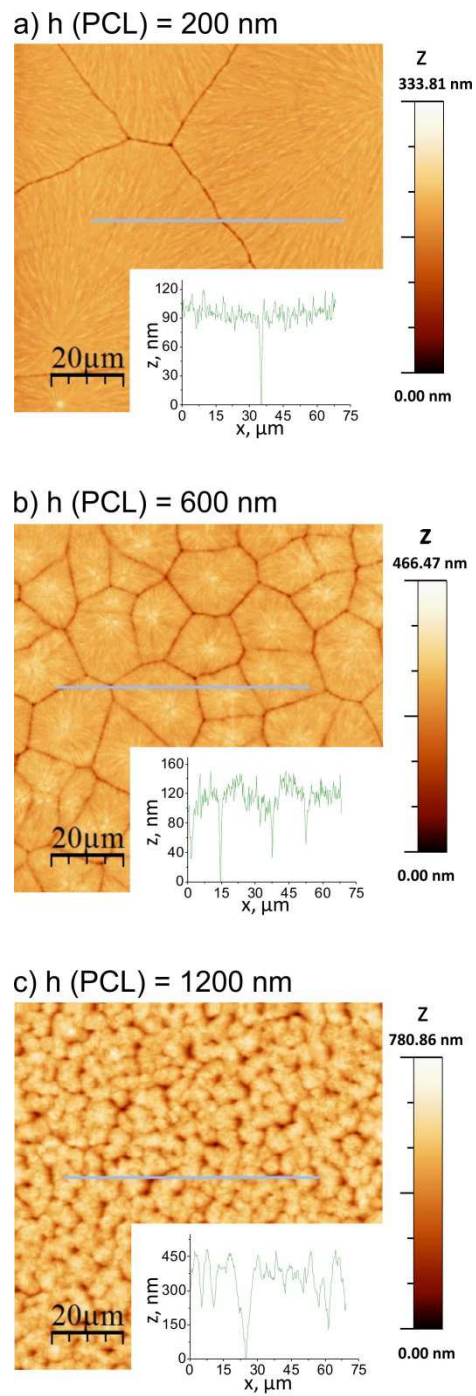


Figure S1. AFM images of surface morphology of PCL films with different thickness 200 nm

(a), 600 nm (b) and 1200 nm (c).

## XRD Analysis

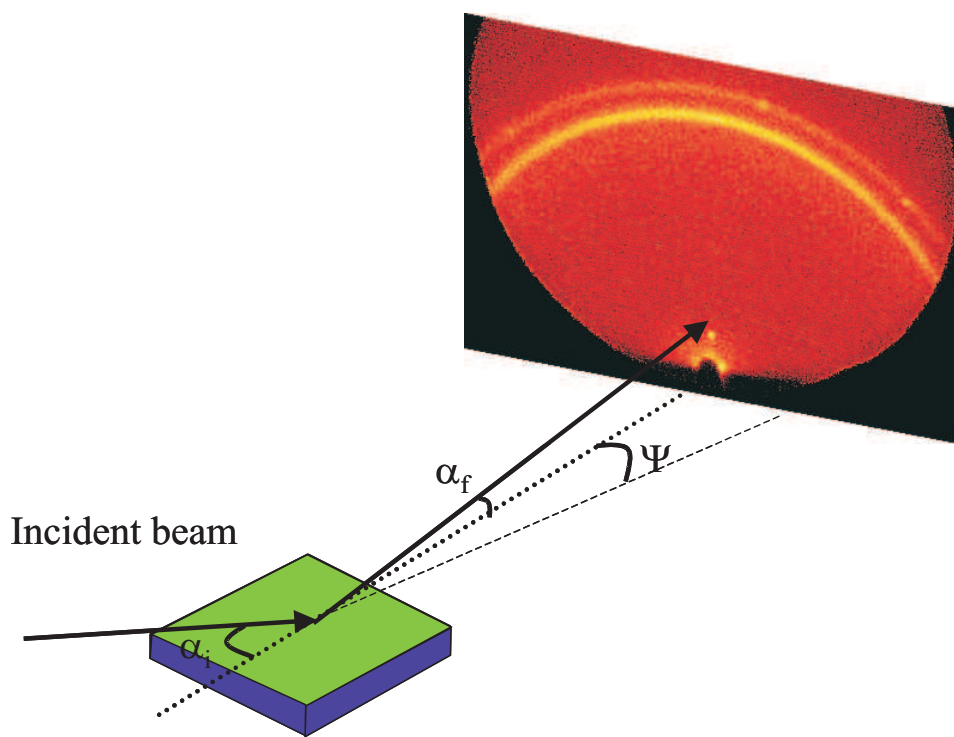


Figure S2. Schematic drawing of the GIWAXS experimental geometry. The sample is placed horizontally (xy plane), and the X-ray beam impinging at a fixed incident angle  $\alpha_i$  with the sample surface.

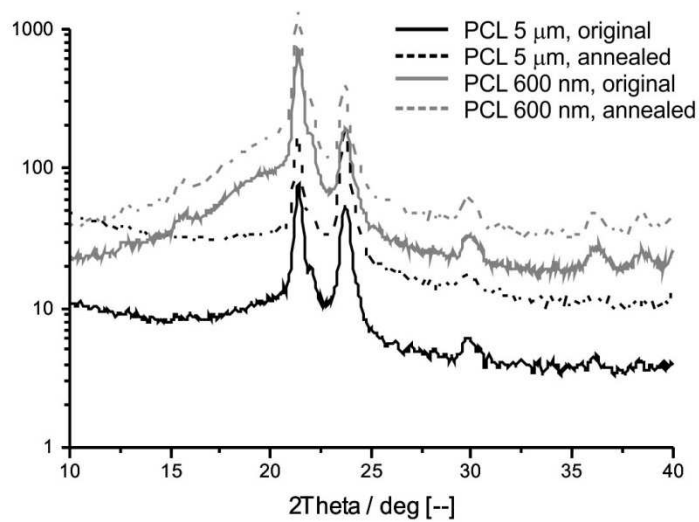


Figure S3. 1D XRD of PCL films with different thickness

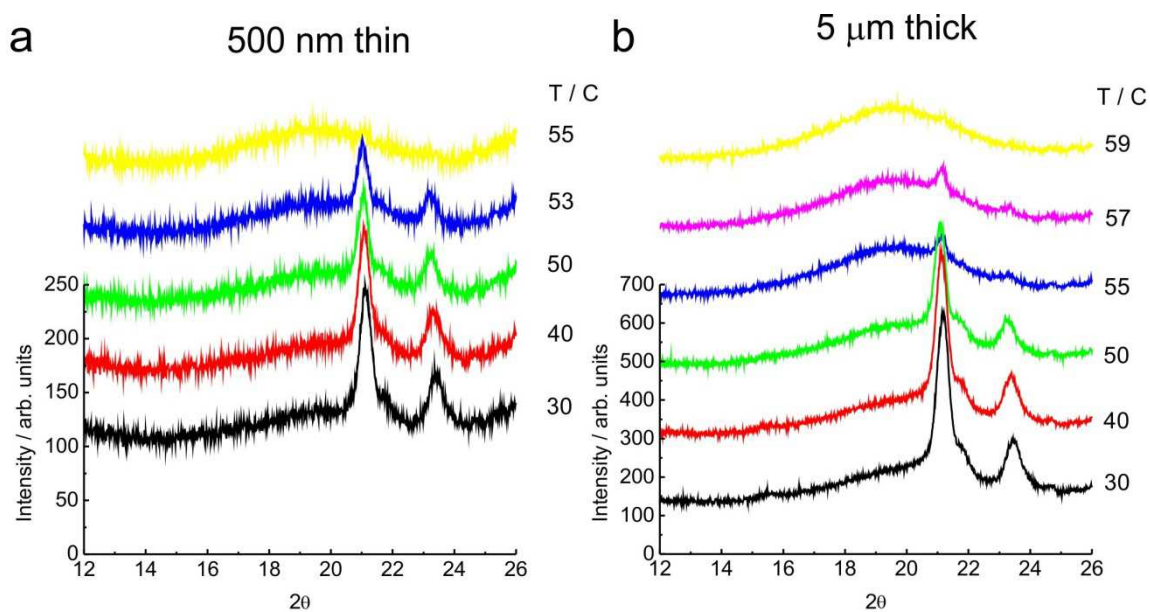


Figure S4. Figure S1. X-ray diffraction curves during heating to the melt of PCL films of thicknesses (a) 500 nm and (b) 5 μm.

### **Detailed explanation of GIWAXS experiments.**

The GIWAXS investigation showed a preferential orientation of the chains in the crystalline regions of the PCL layer parallel to the surface in thin films and no preferred orientation in thick films. The thickest film exhibits isotropic diffraction rings (Figure 3d), which indicates a random distribution of the crystalline domains with no preferable orientation. Meanwhile, the (200) reflection exhibits a slightly higher intensity in the qz direction of the intermediate thickness film (Figure 3c) indicating the presence of more crystalline lamellae having their lamellar planes oriented normal to the substrate (z-direction). By contrast, the thinnest film exhibits the strongest orientation (Figure 3a). The appearance of both sharp (200) arc reflection at the meridian and a four-point (110) arc pattern indicate that the c-axis of the lamellae is oriented parallel to the substrate thus forming edge-on crystalline lamellae with the chains parallel to the substrate. Further proof of the edge-on orientation is provided by monitoring the (110) reflection intensity in the grazing and specular geometries of the thinnest film as shown in Figure S5. As can be seen, while both (110) and (200) reflections can be seen in the grazing incidence diffraction (GID) curve, only the (200) reflection and is observed in the specular curve. This implies that the a-axis is oriented along the film normal confirming the edge-on orientation of the crystalline lamellae of the 200 nm film.

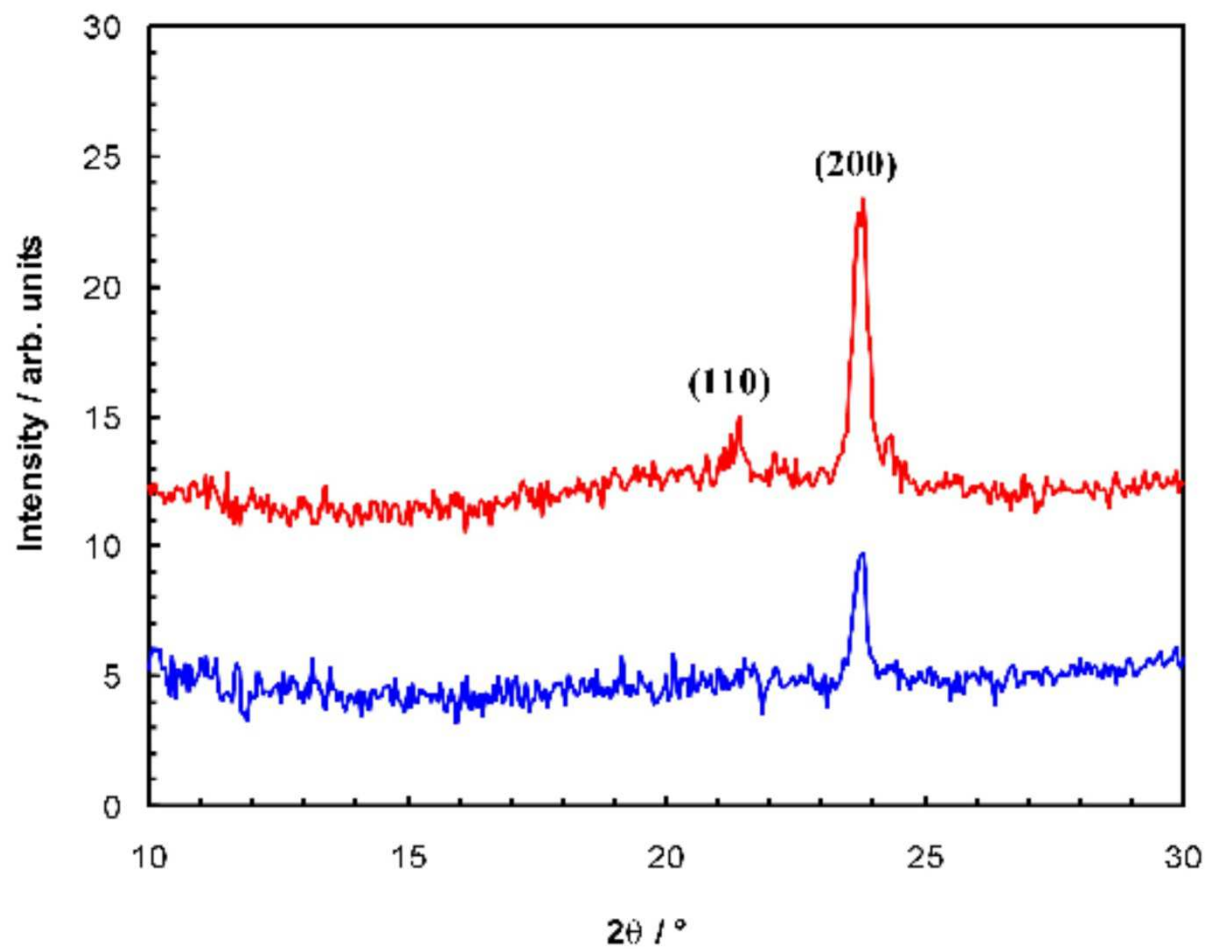


Figure S5. Diffraction curves of a 200 nm PCL film deposited on gelatin on silicon substrate obtained under grating (top) and specular (bottom) geometries.

## Detailed expiation of mean-field approach

The corresponding free energy per monomer can be written as

$$F = G_0 \cdot \text{Tr}\Lambda^2 + \frac{\nu}{Q}$$

Here, we use  $k_B T = 1$  as the unit for the energy and the volume of a Kuhn segment,  $\nu_0 = 1$ , as the unit volume. The volume degree of swelling is denoted by  $Q = V_0/V$  ( $V$ ,  $V_0$ -volume in the swollen, dry state), and the shear modulus in the dry state is given by  $G_0$ . The deformation matrix is given by  $\Lambda$ , and  $\nu$  denotes the strength of binary monomer interactions (excluded volume). According to this model the shear modulus in the swollen state is  $G_Q = G_0/Q^{1/3}$ . The driving force for bending is given by the change in free energy in the uniaxially swollen state by extension in one direction perpendicular to swelling. For this case we consider  $\Lambda = \text{diag}(\lambda_x, 1, \lambda_z)$ , where the swelling perpendicular to the film surface is given by  $\lambda_z$  and the extension in the direction of bending is given by  $\lambda_x$  (Figure 4). Equation (2) yields the uniaxial swelling equilibrium according to  $Q_x = \left(\frac{\nu}{G_0}\right)^{1/3} \cdot \lambda_x^{2/3}$ , and free energy gain per unit volume ( $\sigma$ ) under (small) expansion in x-direction ( $\lambda \cong 1$ ) is given by

$$\sigma = Q_x \cdot G_0 = Q^{8/9} G_0$$

The latter relation uses the degree of swelling in the isotropically swollen state of the gel,  $Q = Q_x^{9/5}$ , which can be obtained by standard measurements in the swollen state. The gelatin materials used in this work can be characterized by  $Q = 10$  and  $G_Q = 7 \times 10^4$  Pa, which leads to  $\sigma \cong 5 \times 10^5$  Pa.

## References

1. Timoshenko, S. *J. Opt. Soc. Am.* **1925**, *11*, 233-255.



# Manuscript 3

## 4D biofabrication: 3D cell patterning using shape-changing films

*Vladislav Stroganov, Jitendra Pant, Georgi Stoychev, Andreas Janke, Dieter Jehnichen, Hitesh Handa and Leonid Ionov*

Advanced Functional Materials

First published: 18 January 2018

**DOI:** 10.1002/adfm.201706248

## Statement of Authors contribution

My personal contribution to that work included:

- Proposed the original idea of how to achieve cell patterning on self-folding bilayers;
- Chemical synthesis of polymers;
- Design and production of self-folding bilayers;
- Conduction of experiments with self-folding films. Evaluation of their characteristics such as layer thicknesses, tube diameters and folding conditions;
- Participation in cell encapsulation experiments;
- Writing of the final manuscript.

Degree of my personal contribution to the work is 60%.

Jitendra Pant conducted cell encapsulation experiments and participated in writing the of the manuscript.

Georgi Stoychev gave critical advices and participated in editing of the final manuscript. He also checked quality of written English in the final version of the paper.

Andreas Janke measured mechanical moduli of polystearylmethacrylate at different conditions.

Dieter Jehnichen conducted X-ray scattering experiments and calculated degree of crystallinity of polystearylmethacrylate.

Hitesh Handa provided equipment and facilities for cell encapsulation experiments as well as gave valuable advises and shared his experience. He participated in the editing of the manuscript.

Leonid Ionov provided supervision, shared his ideas and experience during the whole research process. He participated in the writing of the manuscript.

# 4D Biofabrication: 3D Cell Patterning Using Shape-Changing Films

Vladislav Stroganov, Jitendra Pant, Georgi Stoychev, Andreas Janke, Dieter Jehnichen, Andreas Fery, Hitesh Handa, and Leonid Ionov\*

A novel approach for fabrication of 3D cellular structures using new thermo-sensitive shape-changing polymer films with photolithographically patterned surface—4D biofabrication is reported. The surface of shape-changing polymer films is patterned to selectively adsorb cells in specific regions. The 2D cell pattern is converted to the 3D cell structure after temperature-induced folding of the polymer films. This approach has a great potential in the field of tissue engineering and bioscaffolds fabrication.

## 1. Introduction

Fabrication of 3D cellular structures with controlled architectures is of increasing importance in the field of tissue engineering and pharmacy.<sup>[1]</sup> Indeed, 3D cellular structures can be used in vivo for regeneration of tissues and organs<sup>[2,3]</sup> as well as for ex vivo testing of drugs on tissues.<sup>[4]</sup> There are two general approaches for designing 3D cellular structures. First, cells are mixed with hydrogel precursor and then this mixture is deposited by variation of 3D printing on a substrate and crosslinked.<sup>[5]</sup> According to the second one, the porous scaffold is prepared first by 3D printing or porogen leaching and then filled with cells.<sup>[3]</sup> Each of these approaches has own advantages and disadvantages. For instance, filling of the preliminarily fabricated scaffold with cells allows a broad choice of materials, but is complicated by difficulties to homogeneously distribute cells inside the porous material and to deposit cells of different sorts in a programmed way. On the other hand, the encapsulation of cells inside hydrogel does not allow reconstructing of both

microporosity needed for cell migration and the proper mechanical environment.

Spontaneous deformation of polymer films<sup>[6,7]</sup> offers an excellent alternative to existing approaches for 3D biofabrication. It provides a combination of homogenous distribution of cells, intrinsic to hydrogel-based approach, and microporosity, intrinsic to scaffolds.<sup>[8]</sup> Usually, these shape-changing films are formed by two kinds of polymers with different volume expansion coef-

ficients (swelling). They can fold and form different 3D shapes that depend on their shape, anisotropy, and pattern.<sup>[9,10]</sup> There are many kinds of shape-changing films made from biodegradable or non-biodegradable polymer, which are sensitive to different stimuli including temperature, light, and pH.<sup>[3,6,9]</sup> Shape-changing films can be used for fabrication of a variety of different 3D shapes, which can be filled with cells<sup>[11,12]</sup> and assembled together to form even more complex 3D cellular structures.<sup>[8]</sup> In all these approaches, cells of one sort were seeded on the whole surface of shape-changing films and they are homogeneously distributed inside the folded object. There is very promising attempt to create complex cellular 3D structures by patterning of cells on the surface of stretched rubbery polydimethylsiloxane (PDMS) shape-changing film using microfluidic device.<sup>[13]</sup> Folding of the film with patterned cells of different sorts on it allows fabrication of 3D multicellular structures. This approach has one considerable limitation. The shape-changing films are made by cutting, which limits fabrication of millimeter and submillimeter range large shape-changing films with arbitrary shapes.

Use of photolithography to pattern both shape of shape-changing films and adhesion behavior of cells on their surface is more favorable than use of microfluidic systems because: (i) photolithography allows fabrication of arbitrary shapes and patterns, (ii) it has excellent spatial resolution, and (iii) large-scale manufacturing is possible. Moreover, use of thermoresponsive shape-changing films is more suitable than the use of stretched rubbery films because folding is triggered by changing temperature, and no holding of stretched films is required. This is particularly inconvenient when many small films are required to be fabricated simultaneously. There are several reports about preparation of thermoresponsive shape-changing films by photolithography.<sup>[12,14–16]</sup> One of them is based on poly(*N*-isopropylacrylamide).<sup>[15]</sup> This system folds at room temperature and unfolds at physiological temperature,<sup>[15]</sup> which is not suitable for encapsulation of cells at 37 °C. The folding at elevated temperature can be achieved if the polymer film is fabricated by polymerization of monomers and crosslinker in a solution that is technically more complicated than photo-crosslinking of dry

V. Stroganov, J. Pant, Dr. G. Stoychev, Prof. H. Handa, Prof. L. Ionov  
College of Engineering  
University of Georgia  
Athens GA 30602, USA  
E-mail: leonid.ionov@uni-bayreuth.de

V. Stroganov, Dr. G. Stoychev, Prof. L. Ionov  
College of Family and Consumer Sciences  
University of Georgia  
Athens GA 30602, USA

A. Janke, Dr. D. Jehnichen, Prof. A. Fery  
Leibniz-Institut für Polymerforschung Dresden e.V.  
Hohe Str. 6, 01069 Dresden, Germany

V. Stroganov, Prof. L. Ionov  
Faculty of Engineering Science  
University of Bayreuth  
Universitätsstr. 30, 95440 Bayreuth, Germany

 The ORCID identification number(s) for the author(s) of this article can be found under <https://doi.org/10.1002/adfm.201706248>.

DOI: 10.1002/adfm.201706248

solid films.<sup>[17]</sup> Upper critical solution temperature systems demonstrate folding at physiological temperature, but the folding is smooth and is completed at a temperature higher than 60 °C, which does not allow their use for encapsulation of cells.<sup>[18]</sup> Polycaprolactone–gelatin bilayer<sup>[12,16]</sup> is also able to fold upon heating and its folding was completed already at 33 °C, which made this system almost ideal for encapsulation of cells. The disadvantage was very rapid degradation of gelatin within 24 h, which substantially restricts the applicability of this system. Thus, until now no one has reported that thermoresponsive shape-changing films are suitable for experiments with cells and 3D patterning cells on their surface.

In this paper, a novel approach for 3D patterning of cells using photopatterning of the surface of the new thermoresponsive shape-changing system (4D biofabrication) is reported. The approach is based on the use of polymer trilayers where bottom layer is photo-crosslinkable hydrophilic copolymer of *N*-isopropylacrylamide with a small addition of acrylic acid and benzophenone acrylate (P(*N*-isopropylacrylamide (NIPAM)-acrylic acid (AA))), and the middle layer is a photo-crosslinkable hydrophobic copolymer of stearyl methacrylate and benzophenone acrylate (PSMA). The top layer is a thin-patterned layer of photo-crosslinkable poly(ethylene glycol) (PEG) (Figure 1). Due to the presence of large fractions of acrylic acid groups in P(NIPAM-AA) layer, it does not demonstrate thermoresponsive behavior in the physiological temperature range and easily detaches from a substrate (silicon wafer or glass). It simply swells and the folding behavior is provided by melting of PSMA. When cells are seeded on top of such films, they adhere only to those areas which are not covered by PEG. This system allows to overcome many problems of other thermoresponsive systems as well as stretched rubbery films and offers the combination of the following practical benefits: (i) folding at 33 °C, (ii) chemical and mechanical stability, (iii) fabrication using photolithography, (iv) crosslinking in dry state, (v) possibility of surface patterning using photolithography, and (iv) possibility of fabrication of 3D cellular patterns.

## 2. Results and Discussions

First, polymer bilayers were prepared by sequential deposition of P(NIPAM-AA) (bottom layer) and PSMA (top layer). These bilayers exhibit shape-changing behavior when immersed in water due to swelling of P(NIPAM-AA) layer. The composition of P(NIPAM-AA) was chosen in the way that it demonstrates no thermoresponsive behavior in a temperature range between 0 and 40 °C in the buffer, and its swelling degree is  $\approx 10$  that corresponds to 1000 vol% (ratio between volume of swollen and dry polymers) in this temperature range. The cloud point of the polymer with 3% in cell culture media is around 90 °C. The storage modulus of photo-crosslinked and water-swollen P(NIPAM-AA) polymer ( $E_{\text{storage}} = 146$  Pa at 25 °C) was much higher than loss modulus ( $E_{\text{loss}} = 31$  Pa at 25 °C). P(NIPAM-AA) copolymer was used because it can be deposited from organic solvents such as ethanol, it forms solid smooth surface, and it is not soluble in toluene, which is used for deposition of PSMA. The responsive properties of the polymer bilayer are provided by PSMA, which was deposited on the top of P(NIPAM-AA) layer. PSMA is a fusible polymer with a melting point of 34 °C and degree of crystallinity around 10–30%, as it was obtained from X-ray diffraction (XRD) and differential scanning calorimetry (DSC, Figures S1, S2, Supporting Information). PSMA is stiff below its melting point ( $E = 394$  MPa at 20 °C) and substantially restricts the folding of the bilayer. The increase of temperature leads to its softening ( $E = 1.25$  MPa at 40 °C). Melting of polymer is also accompanied with volume change that is intrinsic to all first-order phase transitions. Its magnitude is however much smaller ( $\approx 10\%$ ) than swelling degree of hydrogel. As a result of rolling, the tubes are formed. P(NIPAM-AA) forms outer layer because it has higher volume expansion coefficient.

The folding occurs when several conditions are fulfilled. First, stress in the film must be generated that is achieved by swelling hydrogel. One can expect that generated stress is proportional to the thickness of hydrogel and its elastic modulus. Second, this stress must be sufficient to bend PSMA layer and

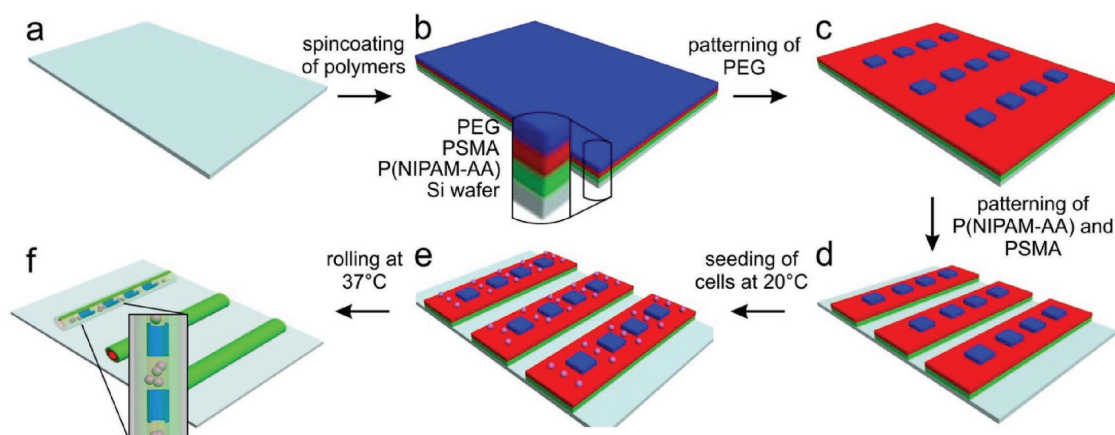


**Figure 1.** Scheme of fabrication of 3D cellular patterns using shape-changing polymer films: a,b) polymers are sequentially deposited on the surface of a substrate (Si wafer) by deep coating leading to formation of P(NIPAM-AA)–PSMA–PEG trilayer; c) PEG is crosslinked by illumination with UV light through a photomask, and PEG pattern on the surface of P(NIPAM-AA)–PSMA bilayer is fabricated; d) P(NIPAM-AA)–PSMA bilayer with PEG pattern on it is crosslinked by illumination with UV light through a photomask, and array of shape-changing P(NIPAM-AA)–PSMA bilayers with PEG pattern on them is fabricated; e) cells are seeded on the surface of the bilayer with PEG pattern on it at room temperature and they adhere to the areas with no PEG; f) increase of temperature to 37 °C results in the rolling of the bilayer and formation of 3D object with patterned cells inside.

detach the bilayer from substrate. Since both polymer and substrate are negatively charged and hydrated, the adhesion between them is weak. Thus, the stress generated by swollen hydrogel must be sufficient to deform hydrophobic polymer. Since hydrophobic polymer is considerably softer in molten state than in solid state, we can expect that folding of bilayer with molten PSMA must occur at smaller thickness of hydrogel layer. Solid PSMA layer could be bent by thick hydrogel layer.

In order to test this hypothesis, we investigated effects of thickness of the layers as well as temperature on the folding (Figure 2a). In order to address this point, we prepared two sets of samples with thin (0.7  $\mu\text{m}$ ) and thick (1.2  $\mu\text{m}$ ) P(NIPAM-AA) layers. The thickness of PSMA was varied in the range between 2 and 8  $\mu\text{m}$ . No folding of bilayers with thin P(NIPAM-AA) layer was observed at room temperature independent of the thickness of PSMA. However, bilayers with thick P(NIPAM-AA)

layer fold at room temperature, albeit very slowly (60 min). It was observed that an increase of the thickness of PSMA increases the diameter of tubes (Figure 2b). The increase of the temperature resulted in the folding of all films. The diameter of the tubes, which could roll at room temperature, decreased at 33  $^{\circ}\text{C}$ .

In order to qualitatively explain observed folding behavior, Timoshenko equation<sup>[19]</sup> was used (Equation (1))

$$\frac{1}{\rho} = \frac{6(\varepsilon_2 - \varepsilon_1)(1+m)^2}{h \left( 3(1+m)^2 + (1+mn) \left( m^2 + \frac{1}{mn} \right) \right)} \quad (1)$$

where  $n = E_1/E_2$ ,  $m = a_1/a_2$ ,  $E_x$  is the elasticity modulus,  $a_x$  is the thickness of the metal layers,  $h$  is the total thickness ( $h = a_1 + a_2$ ),  $\varepsilon$  is the thermal expansion coefficient of the layers, and  $\rho$  is

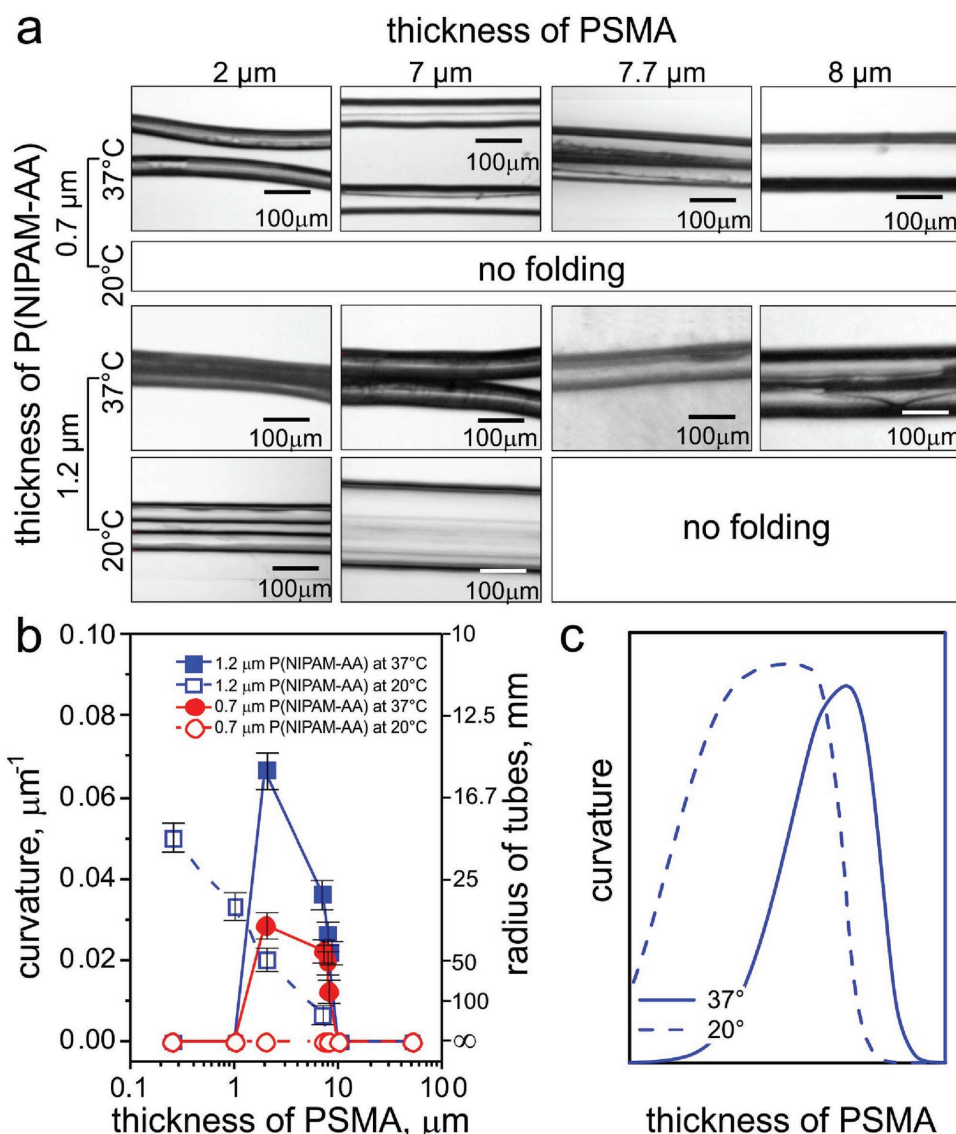


**Figure 2.** Folding of P(NIPAM-AA)–PSMA bilayer: a) microscopy snapshots of formed tubes; b) experimental values of curvature and radius of formed tubes; c) qualitative dependence of curvature of the folded film on the thickness of PSMA layer at 20 and 37  $^{\circ}\text{C}$ , dashed rectangle shows area corresponding to experimental results in (b).

the radius of curvature. Originally, this equation was derived to explain the bending of bimetal beams upon change of temperature. This equation was transferred into the field of shape-changing polymer films by assuming that thermal expansion coefficient can be replaced by swelling degrees of both polymers: component 1 as PSMA and component 2 as PNIPAM. The values  $m$ ,  $h$ , and  $\varepsilon$  can be taken out from experimental values. Note, Timoshenko equation was developed for small deformations and is able to provide qualitative not quantitative dependence of curvature on thickness of layers in the case of large deformations.<sup>[20]</sup>

According to Equation (2), increase of the thickness of the upper layer (component 1) and a decrease of the thickness of the bottom layer (component 2) would lead to increase of radius of curvature and vice versa. The similar results were observed experimentally (Figure 2b,c). As shown in Figure 2a, PSMA layer gets thicker, diameter gets bigger, and when P(NIPAM-AA) layer's thickness increases, diameter decreases. The second prediction made by Timoshenko equation says that mechanical properties influence radius as well: increase of stiffness of upper polymer will lead to increase of tubes' diameter. This effect was observed experimentally when film folded at room temperature when PSMA was stiff which produced bigger diameter than that at increased temperature when PSMA was molten and soft (Figure 2). Thus, experimental results and predictions made by Timoshenko equation are in qualitative agreement.

Thus, the behavior of P(NIPAM-AA)–PSMA bilayer is similar to that shown in our previous paper (gelatin–PCL),<sup>[12]</sup> but it has a big advantage over the previous system: since current polymers being used are not biodegradable, the system shows indefinite mechanical and chemical stability. Non-biodegradability of scaffold is relevant if the cellular construct is used *ex vivo* as microtissue for testing of effects of drugs. For comparison, previously reported shape-changing films were able to hold their shape only for several hours, which is not enough for scaffolding. Thus, P(NIPAM-AA)–PSMA layer is able to irreversibly fold when the temperature is above 30 °C that makes it promising for encapsulation of cells.

The folding of this particular bilayer is irreversible at the conditions that allow manipulation with cells. On the other hand, at other conditions, for example, at different pH = 8 (tris-buffered saline), further increase of temperature to 35 °C results in

unfolding of the bilayer that is due to shrinking of thermoresponsive P(NIPAM-AA) layer (Figure 3). The same effect can also be achieved by using thermoresponsive PNIPAM-based layer without acrylic acid.<sup>[21]</sup>

We explored the possibilities to encapsulate pattern cells inside P(NIPAM-AA)–PSMA tubes. The preliminary experiments showed that F3T3 cells readily adhere to native and oxidized PSMA layers (Figure S4, Supporting Information). The next step was to test if cells can be encapsulated inside the tubes. To achieve that, F3T3 cell dispersion was dispensed on top of P(NIPAM-AA)–PSMA bilayers at room temperature. Thicknesses of both layers were chosen in a way that polymer films remained unfolded at that temperature: 1.2  $\mu\text{m}$  for P(NIPAM-AA) and 8  $\mu\text{m}$  for PSMA (Figure 2a). About 30 min were given for cells to precipitate to the polymer surface. Then the temperature was increased to 37 °C. At that temperature, PSMA layer became molten, its mechanical modulus decreased, and films were able to fold while encapsulating cells that were on their surfaces (Figure 4a). Cells can be seen to hold their special star-like shapes inside tubes for 24 h, meaning that this confinement is not harmful to them. It is worth mentioning that it was possible to fabricate single-walled tubes with cells, doubled tubes with cells, and multiwalled tubes with cells (Figure 4a). The number of walls depends on the diameter of the tube in equilibrium state and the size of the film—the larger is the film, the more walls are formed. This can be useful for making tubes with different permeability and resistance to internal pressure. For example, if they are used for blood vessel reconstruction.

The next step involved testing of cells' adhesion to PSMA surface with patterned PEG which were deposited on the top of PSMA layer. It was found that PEG solution in ethanol–water mixture dewetted instantly on hydrophobic PSMA surface prohibiting deposition of a thin layer. To solve that problem, the surface of PSMA was oxidized with piranha mixture (see Experimental Section) to hydrophilize it: water contact angle was reduced from 115° to 95° (Figure S3, Supporting Information). PEG with high molecular weight ( $M_w = 200$  kDa) was used because it forms a stable layer, which does not dewet and is not washed away after crosslinking. PEG was deposited from the ethanol–water mixture (95:5) because it has lower surface tension than water does and PEG is soluble in it.<sup>[22]</sup> PEG layer was crosslinked by illumination with UV light through a

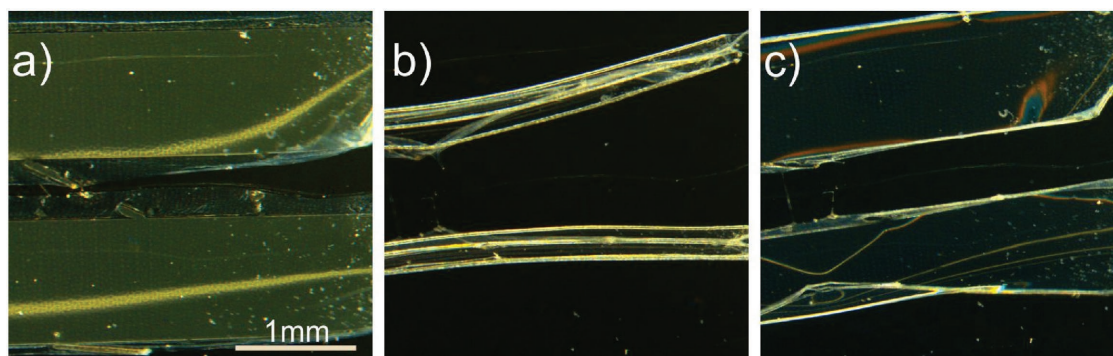


**Figure 3.** Shape of P(NIPAM-AA)–PSMA bilayer in tris-buffered saline (pH = 8) solution at different temperatures: a)  $T = 20$  °C—flat; b)  $T = 30$  °C—folded; c)  $T = 35$  °C—flat.

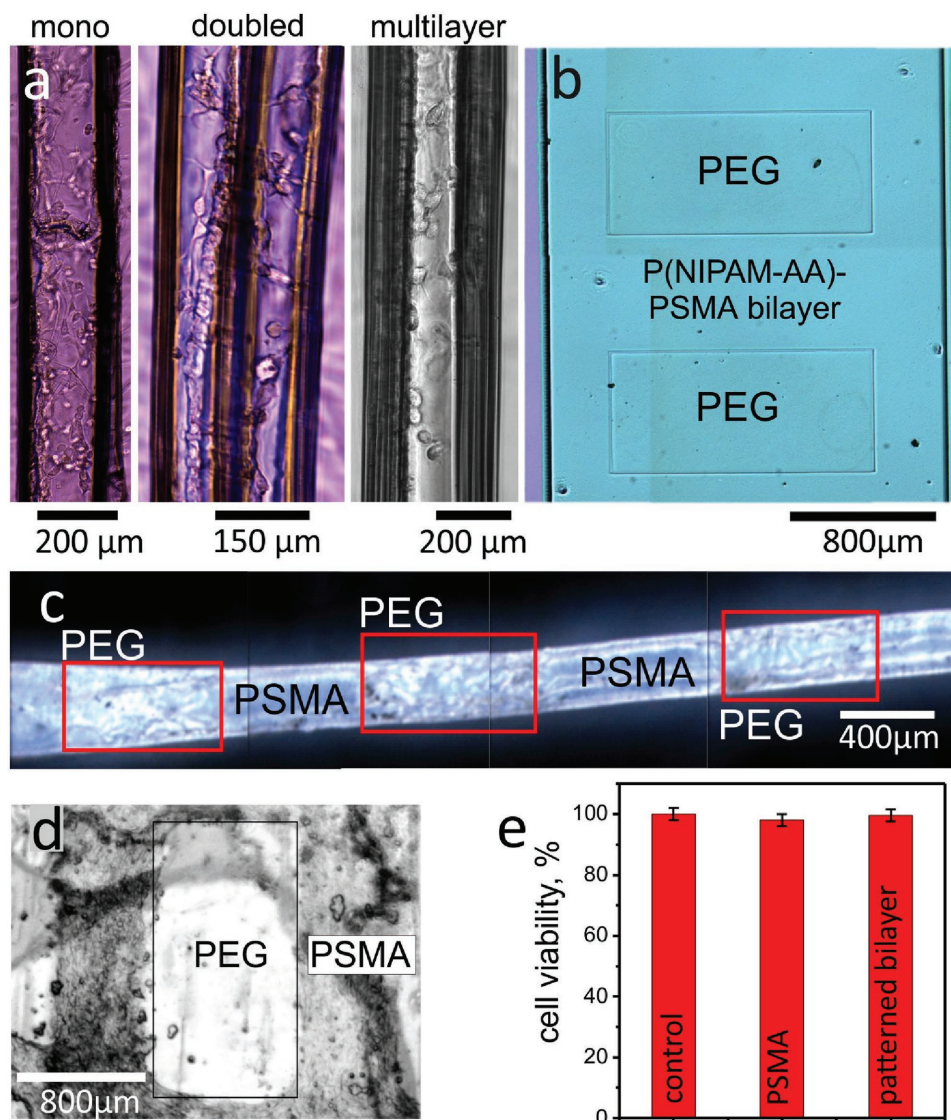


**Figure 4.** 3D cell patterning using shape-changing P(NIPAM-AA)–PSMA films: a) bright field microscopy snapshots of single, double, and multilayer P(NIPAM-AA)–PSMA tubes with encapsulated F3T3 cells inside; microscopy snapshots of P(NIPAM-AA)–PSMA bilayer with PEG pattern on it before b) (bright field) and after folding c) (dark field); d) bright field microscopy snapshots of F3T3 cells adhered on P(NIPAM-AA)–PSMA bilayer with patterned PEG; e) viability of cells on the top of control (on well plate as it is), PSMA films and PSMA films with PEG pattern.

photomask (size of the pattern was  $1600 \mu\text{m} \times 800 \mu\text{m}$ ). It was found that no F3T3 cells adhered to crosslinked PEG layer, while they readily adhere to native and oxidized PSMA (Figure S4, Supporting Information). This result must allow patterning of cells using patterned PEG layer on the top of shape-changing P(NIPAM-AA)–PSMA films.

To demonstrate this hypothesis, encapsulation of mammalian cells inside shape-changing bilayers with patterned PEG was validated. It is worth noticing that PEG on the top of the bilayer can influence the diameter of the tubes, since it adds to the thickness of the upper layer. To avoid change of the diameter, the thickness of PEG film was kept very thin (300 nm) that is much smaller than the thickness of PSMA layer (8 μm). It was observed that such a thin PEG layer did not affect the diameter of tubes. Bilayers were fabricated for cell encapsulation

experiments with patterned PEG film on them. These PEG-covered areas can be clearly seen using optical microscopy because swollen PEG and solid PSMA have a different refractive index (Figure 4b). Folding of a bilayer with PEG pattern resulted in the formation of a tube with PEG patterns located on the inner side of tubes (Figure 4c). To further improve the point that PEG-covered areas should protect PSMA surface from cell adhesion, an experiment was done where bovine serum albumin (BSA) was adsorbed on pure PSMA film by forming 1.5 nm thick layer as it was revealed by ellipsometry, while no adsorption of protein was observed on PEG-modified PSMA. As it was shown and discussed earlier, F3T3 cells adhered and spread on naked PSMA area and did not adhere to PEG-covered areas (Figure 4d). They demonstrated excellent viability on PSMA areas of patterned bilayer, which is comparable to that

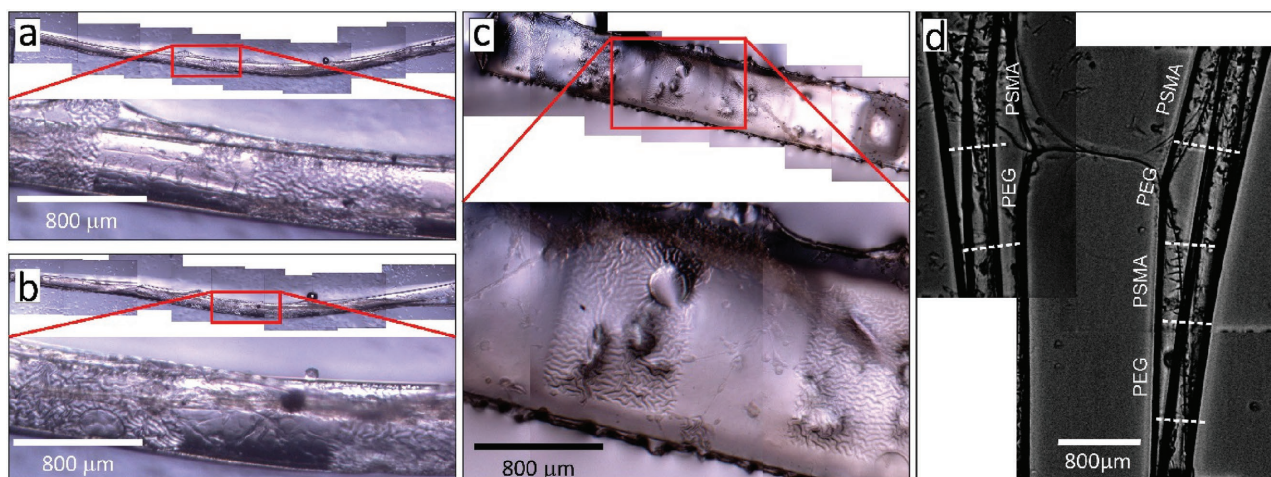


**Figure 5.** Examples of 3D cell patterning inside self-folded tube: a,b,d) bright field microscopy snapshots of F3T3 cells inside PNIPAM–PSMA tubes with PEG pattern; c) bright field microscopy snapshot of F3T3 cells on the unfolded PNIPAM–PSMA film with PEG pattern. It is clearly seen that cells are only in the areas not occupied by PEG.

on not patterned PSMA surface (Figure 4e). This supports the prediction that cells will adhere and remain viable inside the tubes with patterned PEG. The same approach was used as when cells were encapsulated in pure bilayer: cell dispersion was put on top of shape-changing P(NIPAM-AA)–PSMA–PEG trilayers at room temperature. The system was kept at those conditions for 30 min to give cells time to precipitate and then the temperature was raised up to 37 °C. At that temperature, PSMA layer's stiffness decreased and films were able to fold while encapsulating cells inside (Figure 5). The major was that the cells adhered only on those areas which were not covered by PEG and all of that happened not on the flat surface as already mentioned but in a 3D space on a curved surface. This means that a 3D cell pattern was indeed achieved using shape-changing polymer films. The mechanical properties of substrate where cells are adhered are highly important and can influence behavior of cells. The advantage of our approach is that the mechanical properties of polymers can be precisely controlled by crosslinking density that opens possibilities to

### 3. Conclusions

In this work, we demonstrated a novel approach for biofabrication using shape-changing films with patterned surface—4D biofabrication. We developed a new thermoresponsive shape-changing system based on poly(*N*-isopropylacrylamide–acrylic acid) poly(NIPAM-AA) and poly(stearylmethacrylate) (PSMA) bilayer. PSMA has a melting point of 34 °C and acts as a thermoresponsive component of the system, while poly(NIPAM-AA) swells in water and exerts bending force. It has been shown that by making films with different thicknesses of components, one can control the resulting radius of curvature of the folded structure. The bilayer was shown to be nontoxic for mammalian cells in addition to allowing their adhesion and growth on the polymeric surface.

These newly developed shape-changing films were used as a base for a more complex task—to develop a shape-changing

system for cell encapsulation with site-selective control where specific cells would adhere to the surfaces of films and inside folded structures. To achieve this, thin polyethylene oxide films were site-selectively deposited on top of the shape-changing bilayer and cells were not allowed to adhere there due to high hydrophilicity of such areas. As a result, tubes with patterned cell-covered areas were produced. Such system shows great potential in the field of tissue engineering and bioscaffolds fabrication for drug screening as well as for fundamental understanding of behavior of cells in 3D environment.

### 4. Experimental Section

**Synthesis of Polymers:** P(NIPAM-AA) copolymer was synthesized using free radical copolymerization. First, a mixture of *N*-isopropylacrylamide NIPAM (13.74 g), acrylic acid (0.57 g), benzophenone acrylate (0.67 g), and 2,2'-azobis(2-methylpropionitrile) (AIBN) (0.043 g) as initiator was prepared. The mixture then was dissolved in 50 mL of 1,4-dioxane. Oxygen was removed from the reaction mixture by a continuous flow of nitrogen through the solution for 20 min. The copolymerization reaction itself took place when the mixture was kept at 71 °C for 5 h. The resulting polymer was obtained by precipitation in diethyl ether and drying under vacuum overnight.

**Synthesis of PSMA:** Reaction mixture contained 10 g of stearylmethacrylate, 0.15 g of benzophenone acrylate, and 0.01 g of AIBN as the initiator of radical polymerization. 30 mL of toluene was used as solvent, and flow of nitrogen was used to remove oxygen from the reaction mixture. Polymerization was held at 71 °C for 24 h. The polymer was precipitated in methanol and dried under vacuum overnight at 60 °C.

**Preparation of Bilayer Samples:** Bilayers were prepared by sequential dipcoating of a cleaned silicon wafer into solutions of P(NIPAM-AA) in ethanol and PSMA in toluene. Thicknesses of polymer layers were regulated by the concentration of polymer solutions. Afterward, deposition samples were left at room temperature for 20 min to let PSMA layer to crystallize and solidify. The resulting bilayer was irradiated with 254 nm UV light through a photomask and then washed with dichloromethane to remove un-crosslinked polymer and obtain a rectangular pattern. The thickness of the polymer layer was determined by AFM scratch tests.

**Preparation of UV-Crosslinkable Polyethyleneglycol (PEG):** One gram of PEG (*M*<sub>w</sub> = 200 kDa) was dissolved in a mixture of 95 mL

of ethanol and 5 mL of water yielding a 1% solution. Then, 50 mg of 4-hydroxybenzophenone was added to the PEO solution. A PEO film obtained from such solution would crosslink upon UV irradiation.

**Preparation of Trilayer Samples:** P(NIPAM-AA)–PSMA bilayers were immersed in a mixture of sulfuric acid and hydrogen peroxide at room temperature to hydrophilize its surface. The oxidizing mixture contained 25 vol% of 30% aqueous hydrogen peroxide solution and 75 vol% of concentrated sulfuric acid. Immersion time was 90 s. Then the sample was washed in deionized water at 0 °C. After oxidizing treatment, a thin layer of PEO was dipcoated on top of the hydrophilized P(NIPAM-AA)–PSMA bilayer. The resulting trilayer film was irradiated by UV light (254 nm) through the first photomask, and the topmost patterned PEG layer was obtained by developing in water (Figure 1). After that, the second photomask was aligned on the sample so that PEG squares would occur on top of shape-changing rectangles of P(NIPAM-AA)–PSMA bilayer (Figure 1). The resulting sample was irradiated with 254 nm UV light and then washed with dichloromethane. Through this two-step photolithography, we obtained a sample which had patterned layer of PEG on top of patterned P(NIPAM-AA)–PSMA bilayer. The thickness of the polymer layers was determined by AFM scratch tests.

**DSC:** Differential Scanning Calorimetry was performed on a Mettler Toledo DSC821 measuring module. Samples were prepared by loading 5–10 mg of finely cut polymer pieces in a closed aluminum crucible. The polymers were scanned in three steps: heating from 0 to 180 °C, then cooling down to 0 °C, and then heating to 180 °C again. The heating/cooling rate was 10 K min<sup>-1</sup> for all samples and all steps.

**X-Ray Scattering Investigations:** X-ray scattering experiments were executed by means of the XRD 3003 Θ/Θ (GE Sensing & Inspection Technologies, Ahrensburg, Germany) at 40 kV, 30 mA, Cu-Kα radiation (monochromatization by primary multilayer system).

**Folding Experiments and Measurement of Tube's Diameters:** Prepared bi- or trilayer patterned samples were put into PBS buffer solution at room temperature. Then the temperature was increased up to 37 °C and films folded into tubes. Images of tubes were taken and their diameters were measured.

**In Vitro Cell Behavior Study:** Standard cell culture assay was conducted in accordance with the ISO 10993 standard to demonstrate the cell viability response of 3T3 mouse fibroblast cell line (ATCC-1658) toward PSMA (surface area = 0.8 cm<sup>2</sup>). All protocols pertaining to the use of mammalian cells were approved by the University of Georgia.

**Cell Culture:** Mouse fibroblast cells under sterile conditions were incubated at 37 °C in a humidified atmosphere with 5% CO<sub>2</sub> in 75 cm<sup>2</sup> T-flask containing complete DMEM medium (with 1% penicillin–streptomycin antibiotic solution and 10% fetal bovine serum (FBS)). The medium was changed every second day to revive the cells unless the confluency reached 80–90%. Thereafter, the mammalian cells were enzymatically detached from the flask surface using trypsin (0.18% trypsin and 5 × 10<sup>-3</sup> M EDTA). Cells were counted in a hemocytometer using the trypan blue dye (dye exclusion method).

**Quantitative Cell Viability Assay:** Pure PSMA films and shape-changing trilayers (surface area = 0.8 cm<sup>2</sup>) were incubated at 37 °C for 24 h in 10 mL of DMEM medium by following the ISO standards (ISO 10993-5:2009 test). Finally using a 96-well plate, 5000 cells mL<sup>-1</sup> were seeded in each of the wells (*n* = 7 for each sample type) by transferring 100 μL of cell culture in each well. Then, 10 μL of the polymeric extracts (if any) were introduced to the cells and incubated for another 24 h. After 24 h, 10 μL of a water-soluble tetrazolium salt, WST-8 [2-(2-methoxy-4-nitrophenyl)-3-(4-nitrophenyl)-5-(2,4-disulphophenyl)-2H-tetrazolium monosodium salt], based Cell Counting Kit-8 (CCK-8) solution was added to the resulting solution. The cells were incubated with a CCK-8 solution for 3 h to allow reduction of WST-8 dye to an orange-colored product, formazan, via the enzymatic activity of dehydrogenases in live cells that can be detected at 450 nm. Thus, the amount of formazan generated is an indication of the amount of viable mammalian cells in the solution. To normalize the background, plane DMEM medium without any cells was used as a reference. After 3 h, the cells were observed under a spectrophotometer at a wavelength of 450 nm. Percentage cell viability was calculated (relative

to the wells without any leachate exposure) using the following formula (Equation (2))

$$\% \text{Cell viability} = \frac{\text{Absorbance of the test samples}}{\text{Absorbance of the positive control samples}} \times 100 \quad (2)$$

**Qualitative Cell Growth Test:** Under sterile conditions, fibroblast cells were seeded in a 24-well plate (5000 cells mL<sup>-1</sup>) in presence of a polymeric film which was sterilized earlier under the UV light in a Biosafety Cabinet (ThermoFischer 1300 Series A2). Cells were allowed to settle on the polymeric surface by first keeping the films at room temperature for 20 min and then incubating the 24-well plate at 37 °C for 24 h. The polymer responded to the thermal stimulus and folded into cylinder shapes while encapsulating the cells inside it. The qualitative images of the cells were taken using the Olympus BX51 microscope at 5× magnification by random selection of wells with seeded cells.

## Supporting Information

Supporting Information is available from the Wiley Online Library or from the author.

## Acknowledgements

V.S. and J.P. contributed equally to this work. L.I. acknowledges German Research Foundation (DFG IO 68/1-1 and IO 68/1-3) for providing financial support to this study.

## Conflict of Interest

The authors declare no conflict of interest.

## Keywords

actuators, folding, hydrogels, thermoresponsive polymers

Received: October 27, 2017

Published online:

- [1] a) A. Khademhosseini, J. P. Vacanti, R. Langer, *Sci. Am.* **2009**, *300*, 64; b) S. Levenberg, R. Langer, in *Current Topics in Developmental Biology*, Vol. 61, Elsevier Academic Press Inc, San Diego **2004**, p. 113; c) H. Tekin, J. G. Sanchez, C. Landeros, K. Dubbin, R. Langer, A. Khademhosseini, *Adv. Mater.* **2012**, *24*, 5543; d) J. Malda, J. Visser, F. P. Melchels, T. Jüngst, W. E. Hennink, W. J. A. Dhert, J. Groll, D. W. Hutmacher, *Adv. Mater.* **2013**, *25*, 5011; e) N. A. Peppas, J. Z. Hilt, A. Khademhosseini, R. Langer, *Adv. Mater.* **2006**, *18*, 1345; f) H. Shin, S. Jo, A. G. Mikos, *Biomaterials* **2003**, *24*, 4353; g) J. L. Drury, D. J. Mooney, *Biomaterials* **2003**, *24*, 4337.
- [2] a) Y. Guo, R. T. Tran, D. Xie, Y. Wang, D. Y. Nguyen, E. Gerhard, J. Guo, J. Tang, Z. Zhang, X. Bai, J. Yang, *J. Biomed. Mater. Res., Part A* **2015**, *103*, 772; b) Q. Yao, J. G. L. Cosme, T. Xu, J. M. Miszuk, P. H. S. Picciani, H. Fong, H. Sun, *Biomaterials* **2017**, *115*, 115; c) W. Yang, F. Yang, Y. Wang, S. K. Both, J. A. Jansen, *Acta Biomater.* **2013**, *9*, 4505; d) N. L'Heureux, S. Paquet, R. Labbe, L. Germain, F. A. Auger, *FASEB J.* **1998**, *12*, 47.
- [3] B. P. Chan, K. W. Leong, *Eur. Spine J.* **2008**, *17*, 467.
- [4] a) E. L. S. Fong, S.-E. Lamhamedi-Cherradi, E. Burdett, V. Ramamoorthy, A. J. Lazar, F. K. Kasper, M. C. Farach-Carson,

- D. Vishwamitra, E. G. Demicco, B. A. Menegaz, H. M. Amin, A. G. Mikos, J. A. Ludwig, *Proc. Natl. Acad. Sci. USA* **2013**, *110*, 6500; b) F. Pampaloni, E. G. Reynaud, E. H. K. Stelzer, *Nat. Rev. Mol. Cell Biol.* **2007**, *8*, 839; c) A. Hansen, A. Eder, M. Bonstrup, M. Flato, M. Mewe, S. Schaaf, B. Aksehirlioglu, A. P. Schwoerer, J. Uebeler, T. Eschenhagen, *Circ. Res.* **2010**, *107*, 35.
- [5] M. J. Webber, E. A. Appel, E. W. Meijer, R. Langer, *Nat. Mater.* **2016**, *15*, 13.
- [6] K. Malachowski, M. Jamal, Q. Jin, B. Polat, C. J. Morris, D. H. Gracias, *Nano Lett.* **2014**, *14*, 4164.
- [7] a) J. L. Silverberg, J.-H. Na, A. A. Evans, B. Liu, T. C. Hull, C. D. Santangelo, R. J. Lang, R. C. Hayward, I. Cohen, *Nat. Mater.* **2015**, *14*, 389; b) H. Thérien-Aubin, Z. L. Wu, Z. Nie, E. Kumacheva, *J. Am. Chem. Soc.* **2013**, *135*, 4834; c) G. Stoychev, S. Turcaud, J. W. C. Dunlop, L. Ionov, *Adv. Funct. Mater.* **2013**, *23*, 2295.
- [8] S. Zakharchenko, N. Pureskiy, G. Stoychev, C. Waurisch, S. G. Hickey, A. Eychmuller, J.-U. Sommer, L. Ionov, *J. Mater. Chem. B* **2013**, *1*, 1786.
- [9] a) M. Chau, M. Abolhasani, H. Thérien-Aubin, Y. Li, Y. Wang, D. Velasco, E. Tumarkin, A. Ramachandran, E. Kumacheva, *Biomacromolecules* **2014**, *15*, 2419; b) D. H. Gracias, *Curr. Opin. Chem. Eng.* **2013**, *2*, 112; c) Y. Liu, J. K. Boyles, J. Genzer, M. D. Dickey, *Soft Matter* **2012**, *8*, 1764; d) J.-H. Na, A. A. Evans, J. Bae, M. C. Chiappelli, C. D. Santangelo, R. J. Lang, T. C. Hull, R. C. Hayward, *Adv. Mater.* **2015**, *27*, 79.
- [10] a) Y. Wang, Y. Li, H. Thérien-Aubin, J. Ma, P. W. Zandstra, E. Kumacheva, *Biomicrofluidics* **2016**, *10*, 014110; b) C. L. Randall, E. Gultepe, D. H. Gracias, *Trends Biotechnol.* **2012**, *30*, 138.
- [11] E. Gultepe, J. S. Randhawa, S. Kadam, S. Yamanaka, F. M. Selaru, E. J. Shin, A. N. Kallou, D. H. Gracias, *Adv. Mater.* **2012**, *25*, 514.
- [12] V. Stroganov, S. Zakharchenko, E. Sperling, A. K. Meyer, O. G. Schmidt, L. Ionov, *Adv. Funct. Mater.* **2014**, *24*, 4357.
- [13] J. V. Serbo, S. Kuo, S. Lewis, M. Lehmann, J. Li, D. H. Gracias, L. H. Romer, *Adv. Healthcare Mater.* **2016**, *5*, 146.
- [14] a) G. Stoychev, N. Pureskiy, L. Ionov, *Soft Matter* **2011**, *7*, 3277; b) S. Zakharchenko, E. Sperling, L. Ionov, *Biomacromolecules* **2011**, *12*, 2211.
- [15] G. Stoychev, S. Zakharchenko, S. Turcaud, J. W. C. Dunlop, L. Ionov, *ACS Nano* **2012**, *6*, 3925.
- [16] V. Stroganov, M. Al-Hussein, J.-U. Sommer, A. Janke, S. Zakharchenko, L. Ionov, *Nano Lett.* **2015**, *15*, 1786.
- [17] S. Pedron, S. van Lierop, P. Horstman, R. Penterman, D. J. Broer, E. Peeters, *Adv. Funct. Mater.* **2011**, *21*, 1624.
- [18] F. Liu, S. Jiang, L. Ionov, S. Agarwal, *Polym. Chem.* **2015**, *6*, 2769.
- [19] S. Timoshenko, *J. Opt. Soc. Am.* **1925**, *11*, 233.
- [20] R. Xiao, *Int. J. Appl. Mech.* **2016**, *08*, 1640004.
- [21] G. Stoychev, N. Pureskiy, L. Ionov, *Soft Matter* **2011**, *7*, 3277.
- [22] High molecular weight PEG is weakly soluble in pure ethanol.



## 6. Conclusions

Biofabrication is a rapidly developing field that aims to create artificial organs and tissues for transplantation. Vast multitude of approaches for bioscaffold fabrication have been developed but there are still problems to be solved. For example, it is still hard to control cell distribution inside scaffolds or achieve true vascularization. Additionally, most scaffolds are isotropic whilst natural tissues are anisotropic in their majority. To overcome these problems, scientists came up with the concept of self-folding materials which offer additional possibilities in bioscaffold fabrication. For example, unlike in conventional methods where cells were fixed in a continuous hydrogel matrix, self-folding systems provide certain degree of freedom for cell migration and proliferation. Additionally, nutrients and oxygen can easily diffuse inside self-folded tubes through open ends. The fact that cells can tolerate only limited variations of environmental conditions puts additional restrictions on potential systems for cell encapsulation. Most of the described systems weren't suitable for that purpose since most of the cells can't withstand considerable pH changes or high temperatures. Certain temperature-based systems have shown a potential towards successful cell encapsulation and scaffold production. However, there were several disadvantages that raised a need for an additional research. First, these systems were non-biodegradable. Second, at physiological temperature of 37°C these systems were unfolded meaning they can't be used for cell encapsulation and proper cell incubation. Third, cell distribution inside self-folded constructs could only be homogeneous which is not always desired.

The current thesis have focused to solve these problems and two major goals were developed:

- 1) The first goal was to develop a biocompatible and preferably biodegradable self-folding system which would be suitable for encapsulation of mammalian cells. The system had to stay unfolded at 20°C and fold at human body temperature. Such conditions were chosen due to practical reasons. Polymer film had to stay unfolded during cell seeding process while cells must survive long enough for this process to finish. 20°C is an ideal temperature to perform cell seeding. After cells have settled, the polymer film should fold in a controlled manner so that it keeps bended shape at human body conditions thus allowing proliferation of encapsulated cells.

- 2) The second main goal was to develop a way to control cell distribution inside self-folded tubes. This goal had addressed the common issue in tissue engineering when it is

difficult to control cell distribution inside scaffolds. It was decided to work out a “binary” way where some inner regions of self-folded structures were filled with cells and some weren't.

This chapter summarizes obtained results.

### **Biodegradable and biocompatible systems.**

The details of this part are shown in **Manuscript 1**.

The first developed self-folding system consisted of pure gelatine as hydrophilic polymer and polycaprolactone (PCL) as hydrophobic one. Both polymers were biodegradable and biocompatible. Gelatine had a sol-gel transition point at 36°C meaning it swelled and formed a gel in aqueous conditions at temperatures below that point while rapidly dissolved if the temperature was raised above that point. Bilayer films consisting of these polymers were able to fold at room temperature due to swelling of gelatine. When the temperature was raised above 36°C gelatine dissolved and the unfolded PCL film was left.

*Characteristics of the system:*

- Both polymers are biocompatible and biodegradable;
- Non-crosslinked system;
- Folding/unfolding occurred in PBS solution and in 20-37°C temperature range;
- Irreversible process. Gelatine dissolved leaving unfolded PCL film;
- Temperature is the trigger of unfolding;
- Folding within 1h.

The second system was photocrosslinkable and based on: 1) Gelatine as hydrophilic polymer. It was chemically modified with furfuryl isocyanate (Gelatine-F) and contained Rose Bengal as photoinitiator. 2) The hydrophobic polymer was a copolymer of 1,6-Hexanediol and fumaryl chloride (PHF); Camphoroquinone was added to it as photoinitiator. Both polymers were biodegradable and biocompatible. The system was irradiated by visible light with wavelength of 450nm through a photomask creating a crosslinked pattern. As in previous system, Gelatine-F swelled in water at room temperature while PHF is inert to water. Unlike in the previous system, the bilayers didn't fold because they were held by non-crosslinked Gelatine-F in between. After temperature increase above 36°C only the non-crosslinked Gelatine-F dissolved thus releasing self-folding bilayers.

*Characteristics of the system:*

- Both polymers are biocompatible and biodegradable;
- Presence of water soluble dye Rose Bengal. It was proven to be non-toxic for cell cultures;

- Crosslinked by visible light with  $\lambda = 450\text{nm}$ ;
- Folding occurred in PBS solution and in 20-37°C temperature range;
- Irreversible process. The film folded as soon as non-crosslinked Gelatine-F dissolved;
- Temperature is the trigger of the folding;
- Instant folding upon triggering.

The third system was based on pure Gelatine as hydrophilic polymer and Polycaprolactone (PCL) as hydrophobic one. PCL was mixed with 4-hydroxybenzophenone which served as photoinitiator. The system was crosslinked with UV light with 256nm wavelength. Photomask was used during irradiation to create a pattern. The folding principle of this system is the same as in the case of the second system (Gelatine-F + PHF). During contact with water at room temperature both crosslinked and non-crosslinked Gelatine areas swelled. Folding occurred when non-crosslinked Gelatine dissolved at temperature above 36°C.

*Characteristics of the system:*

- Both polymers are biocompatible and biodegradable;
- Crosslinked by UV light with  $\lambda = 256\text{nm}$ ;
- Folding occurred in PBS solution and in 20-37°C temperature range;
- Irreversible process. The film folded as soon as non-crosslinked Gelatine dissolved;
- Temperature is the trigger of the folding;
- Instant folding upon triggering.

The fourth system consisted of pure Gelatine as hydrophilic polymer and PHF-Q as hydrophobic one. Behaviour and properties of this system was very similar to the Gelatine-PCL one. Polymers were irradiated by UV light (256nm) through a photomask. This led to formation of crosslinked pattern with non-crosslinked areas around. Folding occurred upon immersion of the crosslinked bilayers into warm water.

*Characteristics of the system:*

- Gelatine is biocompatible and biodegradable. PHF is biocompatible and was expected to be biodegradable;
- Crosslinked by UV light with  $\lambda = 256\text{nm}$ ;
- Folding occurred in PBS solution and in 20-37°C temperature range;

- Irreversible process. The film folded as soon as non-crosslinked Gelatine dissolved;

- Temperature is the trigger of the folding;

- Instant folding upon triggering.

Folding behaviour of all developed systems was investigated as well as influence of polymer thicknesses on final tube's diameters. It was also demonstrated that PHF polymer is biocompatible and PHF-Gelatine system can be used for cell encapsulation. Unfortunately, it was found that degradation speed of Gelatine was too high and tubes couldn't hold their shapes longer than 6 hours.

#### **Investigation of reversible folding/unfolding of the Gelatine-PCL system.**

The details of this part are shown in **Manuscript 2**.

The UV-crosslinkable Gelatine-PCL system demonstrated a series of properties which led to some unexpected discoveries. It was found that if PCL is thick enough in comparison to Gelatine, the bilayer won't fold even at temperatures slightly above 36°C. Folding occurred only around 60°C. This temperature was known to be a melting point of PCL and folding took place due to melting and softening of crosslinked PCL. Consequent decrease of temperature led to unexpected unfolding. This observation was in disagreement with predictions. It was expected that PCL would crystallize in a folded shape upon cooling and no unfolding would occur.

Detailed investigations of this phenomenon showed that reversible folding/unfolding was demonstrated only by thin bilayers – PCL thickness was around 500 nm and gelatin was 1.6µm thick. Also, no unfolding was observed with non-crosslinked films. It was found that polymer chains of PCL were parallel to the substrate at the given film thickness and this orientation was saved even after melting and crystallization of the polymer. Crosslinked nature of the PCL layer played a major role in the retaining of parallel chains orientation. In other words, it was found that crosslinked Gelatine-PCL bilayers possessed shape-memory property which enabled usage of the system in reversible encapsulation and release of microobjects.

The possibility to use this system for controlled encapsulation and release was shown on the example of yeast cells. It was stated however that the system can't be directly used for encapsulation of mammalian cells due to high triggering temperature.

#### **Biocompatible and non-biodegradable system.**

The details of this part are shown **Manuscript 3**.

The new self-folding system was developed as a solution to the problems stated above: high degradability of gelatine and high folding temperature of PCL-Gelatine system. It was based on two polymers: 1) PNIPAM-AA – Copolymer of N-isopropylacrylamide and acrylic acid as hydrophilic polymer and 2) PSMA – Polystearylmethacrylate as hydrophobic one. Both polymers contained 2% of hydroxybenzophenone acrylate comonomer for photocrosslinking purposes. Crosslinked PNIPAM-AA swelled in PBS buffer solution in temperature range 20-37°C while non-crosslinked PNIPAM-AA dissolved. PSMA was a semicrystalline waxy polymer and was inert to water. It also had a melting point around 34°C which allowed to use it as a folding actuator in the same way PCL was used but in a much more suitable temperature range.

*Characteristics of the system:*

- Both polymers are biocompatible;
- Crosslinked by UV light with  $\lambda = 256\text{nm}$ ;
- Folding occurred in PBS solution and in 20-37°C temperature range;
- Irreversible process. The film folded upon melting of PSMA;
- Temperature is the trigger of the folding;
- Folding within 20min.

Influence of polymer thicknesses on tubes' diameters and folding behaviour was investigated. Obtained results were in qualitative agreement with theoretical predictions.

**Patterning of cells.**

The details of this part are shown **Manuscript 3**.

The PNIPAM-AA – PSMA system have shown a great potential for cell encapsulation. Self-folded tubes were shown to be stable in water medium for at least 3 months and actuation temperature of 34°C was suitable for cells. Cell patterning was achieved with the help of the third polymer - Polyethyleneoxide (PEO). Its purpose was to protect certain areas of PNIPAM-AA – PSMA bilayers from cell adhesion effectively creating a PNIPAM-AA – PSMA – PEO trilayers. PEO-covered areas were formed by photolithographical patterning.

3T3 mouse fibroblasts were used in cell viability and encapsulation experiments. It was shown that system components aren't toxic for the cells and PSMA surface is suitable for cell adherence. Optical observations of folded tubes demonstrated that cells were viable after 2 days of encapsulation and were adhered only to those areas inside tubes which weren't covered with PEO.

The results presented in this work demonstrated the proof-of-concept, proposing new self-folding systems for cell encapsulation and cell patterning which could be of great interest for various bioengineering applications. Desired cell density can be achieved by seeding cells on to self-folding polymer films before they fold. The proposed way of cell patterning can help achieving controlled non-homogeneous cell distribution. Diameters of individual tubes can be varied to obtain different degree of confinement. In perspective, such self-folded tubes could be used in guiding of neurons growth or mimicking of blood vessels. Studies of cell cultures behavior in a confined 3D space is among other possible applications.

However, cell patterning was achieved with the help of non-biodegradable materials. Even though, PSMA and PNIPAM-AA polymers were proved to be non-toxic and suitable for cell encapsulation, further investigations are required to find a way of cell patterning utilizing only biodegradable materials. One of the possible approaches may combine 3D bioprinting and self-folding principle to achieve even greater choice of materials and shape variety.

## 7. List of abbreviations

PCL	$\epsilon$ -polycaprolactone
PCL-B	Mixture of PCL (see above) and 4-hydroxybenzophenone
PHF	poly(1,6-hexanediol-co-fumaryl chloride)
PHF-Q	mixture of PHF (see above) and camphoroquinone
UV	ultraviolet light
IR	infrared light
PNIPAM-AA	poly(N-isopropylacrylamide-co-acrylic acid)
PSMA	polystearylmethacrylate
PEG	polyethylene glycol
PEO	polyethylene oxide
2D	2 dimensional
3D	3 dimensional
PDMS	polydimethylsiloxane
PBS	phosphate buffer saline
HUVEC	human umbilical vein endothelial cells
SMC	smooth muscle cells
VIC	leaflet interstitial cells
DBE	direct bioink extrusion
PNIPAM	poly(N-isopropylacrylamide)
NIPAM	N-isopropylacrylamide
PMMA	polymethylmethacrylate
p(HEMA-co-AA)	poly(2-hydroxyethyl methacrylate-co-acrylic acid)
NBA	<i>o</i> -nitrobenzaldehyde
Leibniz IPF	Leibniz Institut für Polymerforschung Dresden e.V.
TU Dresden	Technische Universität Dresden
USA	United States of America

## 8. Acknowledgments

First, I would like to acknowledge my direct supervisor **Professor Leonid Ionov** who gave me the opportunity to perform this work. Also, I express my gratitude to **Professor Manfred Stamm** for giving me the opportunity to start the research and being my supervisor during the first 3 years of the work.

Next, I'm grateful to my fellow colleagues for the help during my research: **Ivan Raguzin, Nikolay Puretskiy, Svetlana Zakharchenko, Indra Apsite, Alina Kirillova and Georgi Stoychev.**

Thanks to my collaborators who made it possible to conduct additional experiments and publish the obtained results: **Anne K. Meyer, Evgeni Sperling, Prof. Oliver G. Schmidt, Mahmoud Al-Hussein, Prof. Jens-Uwe Sommer, Andreas Janke, Dieter Jehnichen, Jitendra Pant, Prof. Hitesh Handa and Prof. Andreas Fery.**

I would like to say special thanks to **Dr. Alexander Ryabchun** for helping me to consider different doctorate programs and showing their advantages and disadvantages.

Thanks to my flatmate and friend **Martin Stammwitz** for helping me with various german official regulations.

Thanks to **Evgeni Karpov** – my colleague and friend who was indirectly responsible for my first meeting with my wife and to my wife **Maria** for continuous support in all spheres of life.

## **(Eidesstattliche) Versicherungen und Erklärungen**

(§ 9 Satz 2 Nr. 3 PromO BayNAT)

*Hiermit versichere ich eidesstattlich, dass ich die Arbeit selbständig verfasst und keine anderen als die von mir angegebenen Quellen und Hilfsmittel benutzt habe (vgl. Art. 64 Abs. 1 Satz 6 BayHSchG).*

(§ 9 Satz 2 Nr. 3 PromO BayNAT)

*Hiermit erkläre ich, dass ich die Dissertation nicht bereits zur Erlangung eines akademischen Grades eingereicht habe und dass ich nicht bereits diese oder eine gleichartige Doktorprüfung endgültig nicht bestanden habe.*

(§ 9 Satz 2 Nr. 4 PromO BayNAT)

*Hiermit erkläre ich, dass ich Hilfe von gewerblichen Promotionsberatern bzw. -vermittlern oder ähnlichen Dienstleistern weder bisher in Anspruch genommen habe noch künftig in Anspruch nehmen werde.*

(§ 9 Satz 2 Nr. 7 PromO BayNAT)

*Hiermit erkläre ich mein Einverständnis, dass die elektronische Fassung meiner Dissertation unter Wahrung meiner Urheberrechte und des Datenschutzes einer gesonderten Überprüfung unterzogen werden kann.*

(§ 9 Satz 2 Nr. 8 PromO BayNAT)

*Hiermit erkläre ich mein Einverständnis, dass bei Verdacht wissenschaftlichen Fehlverhaltens Ermittlungen durch universitätsinterne Organe der wissenschaftlichen Selbstkontrolle stattfinden können.*

.....  
Ort, Datum, Unterschrift